AFOSR-TR- 88-1002

(2)

FINAL REPORT-CT-85-10

Project Title:

HIGH PULSED POWER, SELF EXCITED MAGNETOHYDRODYNAMIC POWER GENERATION SYSTEMS

B.Zauderer,
E.Fleming,
J.Wang

Contract No: F49620-85-C-0025

Air Force Office of Scientific Research
Building 410
Bolling AFB,.DC 20332

Contractor: Coal Tech Corp.,P.O.Box 154,Merion,PA 19066

Period of Performance: November 1,1984-December 31,1985

December 27,1985

UNCLASSIFIED

SECURITY CLASSIFICATION OF THIS PAGE

REPORT DOCUMENTATION PAGE

1a. REPORT SECURITY CLASSIFICATION: Unclassified	1b. RESTRICTIVE MARKINGS
2a. SECURITY CLASSIFICATION AUTHORITY	3. DISTRIBUTION/AVAILABILITY OF REPORT: Approved for Public Release; Distribution Unlimited after 6/27/1986
2b. DECLASSIFICATION/DOWNGRADING SCHEDULE	
4. PERFORMING ORGANIZATION REPORT NUMBER(S): CT-85-10	5. MONITORING ORGANIZATION REPORT NUMBER(S): AFOSR-TR-86-1002
6a. NAME OF PERFORMING ORGANIZATION: Coal Tech Corp; 6b. OFFICE SYMBOL (If applicable):	7a. NAME OF MONITORING ORGANIZATION: AFOSR
6c. ADDRESS (City, State and ZIP Code): P.O.Box 154, Merion, Pa. 19066-0154	7b. ADDRESS (City, State and ZIP Code): BCA 410, Bolling AFB, D.C. 20332-6448
8a. NAME OF FUNDING/SPONSORING ORGANIZATION: Air Force Office of Scientific Res; 8b. OFFICE SYMBOL (If applicable): NP	9. PROCUREMENT INSTRUMENT IDENTIFICATION NUMBER: F49620-85-C-0025
8c. ADDRESS (City, State and ZIP Code): Building 410, Bolling AFB, D.C. 20332-6448	10. SOURCE OF FUNDING NOS.

PROGRAM ELEMENT NO.	PROJECT NO.	TASK NO.	WORK UNIT NO
61102F	2301	A7	N/A

11. TITLE (Include Security Classification): High Pulsed Power, Self-excited MHD Power Generation Systems

12. PERSONAL AUTHOR(S): B. Zauderer, E. Fleming(Consultant), J. Wang (Consultant)

13a. TYPE OF REPORT	13b. TIME COVERED	14. DATE OF REPORT (Yr., Mo., Day)	15 PAGE COUNT
Final	FROM 11/1/84 TO 10/31/85	12/27/85	139

16. SUPPLEMENTARY NOTATION

17. COSATI CODES			18. SUBJECT TERMS (Continue on reverse if necessary and identify by block number)
FIELD	GROUP	SUB. GR.	Magnetohydrodynamics (MHD) MHD Power, Metal Fuel Combustion Pulsed Power; Explosive MHD; Magnets
/	20.09		
/			

19. ABSTRACT (Continue on reverse if necessary and identify by block number)

The objective of this study was to examine the feasibility of achieving high power, high energy, repetitive pulses over a multi-second period, using a portable, self-excited, magnetohydrodynamic (MHD) generator system. To assure a compact, portable system, a room temperature MHD magnet, and operation without a supersonic diffuser was assumed. The approach selected was to use a cw, self-excited, MHD generator to provide the power for the magnetic field in a shaped explosive, argon plasma, MHD generator. The latter's output power pulses are converted in a pulse shaping network to the ultimate load. For the cw generator, a novel system consisting of a non-equilibrium MHD generator, with a noble gas working fluid, and heated directly with a high energy chemical fluid, was used. A novel, compact room temperature magnet was used with the cw MHD generator. This generator's system power output per unit volume and per unit total system weight is much higher than the values obtainable in high energy liquid or solid rocket fuel driven, combustion MHD generators. Among the barrier problems to the use of the shaped explosive, argon plasma MHD generator is survival of the all the compo- CONT

20. DISTRIBUTION/AVAILABILITY OF ABSTRACT	21. ABSTRACT SECURITY CLASSIFICATION
UNCLASSIFIED/UNLIMITED ☒ SAME AS RPT. ☑ DTIC USERS ☐	Unclassified

22a. NAME OF RESPONSIBLE INDIVIDUAL	22b. TELEPHONE NUMBER (Include Area Code)	22c. OFFICE SYMBOL
~~Major~~ Lt Col Bruce Smith	202-767-4908	AFOSR/NP

DD FORM 1473, 83 APR EDITION OF 1 JAN 73 IS OBSOLETE.

UNCLASSIFIED

SECURITY CLASSIFICATION OF THIS PAGE

nents for more that one pulse. It was found that the use of the novel cw MHD generator system directly with a pulsed forming network, and completely eliminating the explosive generator, resulted in a superior system performance compared to the best levels projected with advanced explosive and combustion MHD generators. Keywords: Explosive Magneto hydrodynamics; Metal Fuel Combustion. (jhd)

FINAL REPORT-CT-85-10

Project Title:

HIGH PULSED POWER, SELF EXCITED MAGNETOHYDRODYNAMIC POWER GENERATION SYSTEMS

B.Zauderer,
E.Fleming,
J.Wang

Contract No: F49620-85-C-0025

Air Force Office of Scientific Research
Building 410
Bolling AFB,.DC 20332

Contractor: Coal Tech Corp.,P.O.Box 154,Merion,PA 19066

Period of Performance: November 1,1984-December 31,1985

December 27,1985

TABLE OF CONTENTS

LIST OF TABLES

LIST OF FIGURES

ABSTRACT

The objective of this study was to examine the feasibility of achieving high power, high energy, repetitive pulses over a multi-second period, using a portable, self-excited, magnetohydrodynamic (MHD) generator system. To assure a compact,portable system, a room temperature MHD magnet,and operation without a supersonic diffuser was assumed. The approach selected was to use a cw, self-excited,MHD generator to provide the power for the magnetic field in a shaped explosive, argon plasma,MHD generator. The latter's output power pulses are converted in a pulse shaping network to the ultimate load. For the cw generator, a novel system consisting of a non-equilibrium MHD generator, with a noble gas working fluid, and heated directly with a high energy chemical fluid, was used. A novel,compact room temperature magnet was used with the cw MHD generator. This generator's system power output per unit volume and per unit total system weight is much higher than the values obtainable in high energy liquid or solid rocket fuel driven ,combustion MHD generators. Among the barrier problems to the use of the shaped explosive, argon plasma MHD generator is survival of the all the components for more that one pulse. It was found that the use of the novel cw MHD generator system directly with a pulsed forming network, and completely eliminating the explosive generator, resulted in a superior system performance compared to the best levels projected with advanced explosive and combustion MHD generators.

1. INTRODUCTION AND PROJECT OBJECTIVES

The primary objective of the present project was to examine the feasibility of achieving (a) **0.5 megajoule pulses** of (b) **10 microsecond duration** from a (c) **portable** (d) **self-excited** magnetohydrodynamic (MHD) generator system, at a (e) **10 pulse per second** repetition rate. In addition, the total operating time of (f) **100 pulses in a 10 second** time period was specified.

In implementing the project, the following major assumptions were made:

-A terrestrial application was assumed.

-The entire system must be portable, and have a reasonably long shelf life. This eliminated cryogenic storage of the oxidizer and the MHD generator working fluid, as well as superconducting or liquid nitrogen cooled magnets. It also means that the magnet must be self-excited by the MHD generator output, with a small initial magnetic field provided by a battery power source. The room temperature operation requirement is one of the primary barriers to the achievement of a light weight magnet. In this project, we discovered a solution to this problem.

-To eliminate the long supersonic-subsonic diffuser at the MHD generator exit, the generator exit static pressure must exceed 1 atmosphere.

-The design of the MHD generator was based on the actual range of operating conditions achieved in experimental MHD generators. It was found that in a number of other studies reviewed in the present project, that assumptions on generator performance were made which are considerable beyond the electrical or fluid mechanical performance limits attainable in realistic MHD generators.

-The analysis of the system was based as much as possible on the use of state-of -the-art concepts. In other words, we looked for pulsed power concepts that could be developed without requiring major technical breakthroughs. If a major advance was required, we tried to identify the technology. By way of example, we did not assume that if a component using current technology weighs 1 kg/kj, its weight could be reduced in the future to 0.1 kg/kj by unspecified means. Therefore, we believe that the pulsed power concept analyzed in the present study could be designed and fabricated for research testing purposes primarily using current technology.

A review of the literature of the past two decades on pulsed power MHD confirmed that there have been three identifiably different technical approaches to the generation of single power pulses. Researchers studying each of these

three approaches have claimed that they can be used to provide multiple pulses. However, to the author's knowledge repetitive pulsed MHD power at an energy level much lower than that of current interest, has not been experimentally demonstrated to date.

The three methods previously studied are:

One method used a very high explosive energy (1),that has apparently achieved four of the six objectives of the present project.This device has achieved 0.5 MJ power output pulses, although of 80 microsecond duration and without self-exultation of the magnet. Thus an additional pulse forming circuit is required to obtain a 10 microsecond pulse. However, we calculated that self-excitation of the magnetic field may be only possible up to a limited range of peak power output levels of about 0.5 MJ. However, repetitive pulsed operation will require a whole class of as yet undemonstrated breakthroughs. Based on the information given in the literature that was reviewed, there was no clearcut evidence that these problems can be resolved.

The second method uses a lower energy, plane wave, explosive MHD generator device (2-4) that can be designed to withstand repetitive power output pulses, but it requires relatively large MHD generator and magnet volumes to achieve the required power level of 0.5 MJ. Also, self excitation of the magnet is not simply to implement.

The third method uses a continuous (cw) multi-second , high energy, hydrocarbon based fuel, combustion MHD generator (2,5-7) whose continuous output must be converted to the required output pulse width by means of an appropriate pulse forming network (5,7). A minimum of 5 MW continuous electric power output is required to meet the present requirement of ten, (0.5 MJ) pulses per second. This approach can produce sufficient power to self excite the generator magnet. However the present requirement of a room temperature magnet coil results in the magnet weight which dominates the total system weight (6,7). It will be shown that nearly all the generators using this approach have similar specific power outputs per total system weight. The present study showed that the one exception (2) in which higher specific power levels were theoretically projected was based on generator performance assumptions beyond currently demonstrated limits.

The original approach considered in the present project was to combine method 3 and method 1, by using the combustion MHD generator to produce the magnetic field to drive the high energy explosive MHD generator. However, due to the above noted limitation it became apparent early in the study that this would most probably result in a higher weight system than one in which the cw MHD generator's output is connected directly to a pulse forming network. In addition, in a separate, parallel research effort, we invented a novel MHD generator concept that potentially offers superior performance for the present application. Most of the proposed effort was devoted to validating the suitability of this concept for its present application.

1.1. The Novel Chemical Fuel Fired, Noble Gas MHD Generator Concept Used in the Present Study:

This novel approach was developed as a result of an in-house independent research study at Coal Tech for the space based MHD power application. Space based MHD systems generally use a nuclear heat source to heat a noble gas, helium or argon, which is the MHD generator working fluid.

The high energy fuel,combustion MHD generators used in Method 3 above, are generally limited to relatively low heat to power generation conversion efficiencies, typically 10%,or less. Higher power conversions require extremely high pressure ratios in the combustion MHD generator.

On the other hand,noble gas,closed cycle MHD generators can attain very high conversion efficiencies at very low pressure ratios,due to their inherent high specific heat ratio. These generators operate with elevated,non-equilibrium,electron temperatures and electrical conductivities. 20%-24% conversion efficiencies have been measured in noble gas MHD generator experiments,(10,30).

However, historically the key barrier problem to the use of the noble gas generator for the present application, was the lack of a suitable heat source. With the exception of nuclear reactors, attainment of the minimum 2000^{o}K stagnation temperature requires bulky,and costly fossil fired regenerative heat exchangers.

In the process of further researching the technical background for the Coal Tech space based MHD power study,it occurred to us that to utilize the

high efficiency of the noble gas MHD generator, some means must be found to transfer the heat from a chemical fuel directly to the noble gas. This heat transfer medium could be a liquid or solid particle that is removed from the noble gas prior to the flow of the noble gas into the MHD generator. One method of accomplishing this is to use a metal fuel,which forms a solid/liquid oxide particle at the MHD generator inlet operating temperatures. Possible fuels are aluminum,zirconium,magnesium, or boron. The metal fuel burns in oxygen mixed with a noble gas in a cyclone combustor. The larger oxide particle products of combustion are centrifuged to the wall of the cyclone combustor. The smaller one micron size particles can flow through the MHD generator, with minimal impact on the generator performance.

The above combustor concept allows one to use the high performance potential of the noble gas MHD generator. Of even greater significance is that it allows one to use helium as the generator working fluid, which due to its low molecular weight, results in very high power densities in the MHD generator. Thus the approach we used was to replace the cw combustion generator with the metal fuel fired MHD generator. The metal fuel fired MHD generator is theoretically capable of reaching power output levels that are an order of 10 higher than the best performance that has been projected for combustion generator. Since this moved the operating envelope of the generator to beyond previous limits, a considerable portion of the present project was devoted to the study of the operating characteristics of this generator.

In addition, we recently invented a novel cooling method which enables one to obtain light weight,room temperature magnets. This was applied to the present project, and it resulted in major system weight reductions.

As a result of the cw generator effort,only a limited effort was expended on the problem of converting the cw noble gas MHD generator output to the required pulse shape. However, it was shown that only a pulsed magnet could be powered efficiently by the cw MHD generator to provide the magnetic field for the explosive MHD generator. A dc room temperature magnet requires too much power for operation at the 5 Tesla fields required by the explosive MHD generator. It was also found from the literature, that another method of producing a high energy pulse by using the cw MHD generator to produce a magnetic field through which a metallic projectile is driven to produce a high energy pulse is not very efficient. The low efficiency is due to the low velocity of the metal

projectile, and the need to limit the applied magnetic field to prevent buckling of the projectile.

It was tentatively concluded that the most effective method for converting the power output of the cw MHD generator to a 0.5 MW pulse is to use its output directly in a pulse forming circuit that produces a 10 microsecond output pulse.

In the present report, a critical evaluation of the four different MHD power generation methods, i.e. high energy explosive, plane wave explosive, cw combustion, and cw noble gas, will be given. Also, a brief discussion will be given on the problems of generating 0.5 MJ pulses by the use of the high energy explosive and the metal projectile. This will be followed by the discussion of the results of applying the metal fuel-noble gas MHD concept to the present application. The latter will include a discussion of the metal fuel combustor, the noble gas MHD generator, the novel light weight magnet used to self-excite the noble gas generator, and the analysis of the magnet requirements for operating the explosive MHD generator. The analysis of the combustor, generator, and magnet will also include a wall heat transfer analysis because this is one of the limiting parameters to the achievement of long duration operation of this generator at the upper end of its power output range. Finally, direction for future work in demonstrating the metal fuel-noble gas MHD generator, which we believe to be a major breakthrough in high power generation, will be discussed.

One final point should be made in connection with this project. The study of the generation of repetitive pulsed power from MHD generators has been the subject of numerous investigations in the past two decades. Therefore, an important aspect of the present study was to critically review these prior studies in the light of the present requirement in order to determine the applicability of the prior work and to eliminate any duplication of effort. Consequently, Section 2 of this Report deals with a review of the prior work. For economy in reporting, Section 2 also contains some of our analytical work which we performed in the evaluation of the first 3 pulse power methods, listed above. Section 3 contains the details of the novel concept that we are proposing to solve the project objectives.

2.DISCUSSION OF FOUR METHODS FOR THE GENERATION OF PULSED MHD POWER

2.1- The Very High Energy Explosive Method:

This method (1) uses a high energy explosively driven plasma source generator, as shown in figure 1. An argon working gas is placed in a cylindrical cavity which is surrounded by a very high energy explosive,Octol. A linear MHD generator channel is connected to the downstream end of a cylindrical tube,which is attached to the plasma generator (left hand side of figure 1). The explosive's detonation,progressively squeezes the plasma,as shown in figure 2, in the direction of the linear channel. After all the Octol is consumed, an aluminum plug is driven into the upstream end of the MHD channel duct to cap it, and prevent the Octol detonation products from mixing with the shock heated argon in the MHD channel.

The above method is being developed by Artec Associates (1,8,9). Its unique feature is the very high absolute level of the explosive charge. In the latest experiment reported with this device (8), about **0.5 megajoules** were delivered by the MHD generator to a resistive load, when **7.5 kilograms** of Octol (equal to 41.3 MJ) were used in the plasma source generator. Thus the overall conversion efficiency was **1.2%** . (This figure is based on the actual power delivered to the load. The analysis of this experiment in Ref.8 indicates that the theoretical efficiency was 2%). Although the electrical energy generated was 6.2 times the magnetic field energy stored in the MHD generator channel,the generator did not operate in a self excited mode.

The **primary inefficiency** in this device occurs in the conversion of the explosive energy to kinetic energy of the argon plasma. For the above cited experiment,this value was computed to be only 9%. On the other hand,the enthalpy extraction from the moving argon plasma to the MHD generator load was computed to be very high, namely 27%.

Ref.1 contains an analysis of the application of this pulsed MHD generator system to the objectives of the present project. The authors (1) state that to meet these objectives,the overall explosive to MHD power conversion efficiency, must be increased from the currently measured 2% (1.2% actual) to 12%. This requires **doubling** the MHD generator conversion efficiency from 27% to 50%, and, **tripling** the explosive to plasma kinetic energy conversion from 9% to 30%.

In our prior studies (10) of shock tube MHD generators, it was found that it is difficult to exceed 20-30% MHD generator efficiency in a quasi-steady, low magnetic Reynolds number,MHD generator. Reference 1 contains no information on how the 50% conversion is to be obtained.

However, it is believed that the more difficult barrier problem faced in the use of this device, is to increase the explosive to plasma kinetic energy conversion efficiency from 9% to 30%. Based on the very limited discussion of this problem in Refs.1 and 8, it is concluded that this is one of the **major barrier problems in this device**. Due to the complexity of the gas dynamic flow process in the plasma generator (figure 2) verification of this claim requires a very complex analysis. In Ref.8,use was made of a one dimensional, time dependent analysis for the flow and MHD processes in the device. The analysis is based on a Lagrangian formulation of the conservation equations of the plasma. However, in order to obtain agreement with experiment, it was necessary to assume that the Octol combustion products driver gas allowed the leakage of about 30% of the argon plasma through the driver-argon interface. While this may produce agreement with the experiment, it is too empirical a description of the gas dynamic processes that actually occur in the device. Therefore, extrapolation of these results to the much higher performance levels specified by the authors of Ref.1 is somewhat speculative.

The argon in the cylindrical container is compressed by the Octol detonation in a series of forward and reflecting shockwaves in the cylinder. This will produce an extremely high pressure and temperature at the downstream end of the cylinder. This hot argon will then expand by a complex non-steady process toward the central plasma channel,(Figure 2). At some point in the expansion process,the metal plug will cutoff the argon remaining in the downstream end of the original cylinder (see figure 2) from the hot argon that has already passed into the plasma channel.The argon in the MHD channel downstream of the plug, will be subjected to strong rarefaction waves, which will attenuate the expanding argon plasma. It is stated in reference 8,that an analytical model was used which describes the entire argon flow process. However, only overall performance results are given,. There is no description of the details of the flow process. It is thus not known how and if the cooling effect of this rarefaction wave system was included in the model.

There are several other barrier type problems that must be solved prior to

using this system in the present application. Reference 1 contains a number of very novel and ingenious solutions to all of them. Some are described in detail, while others are noted only briefly. A general conclusion that can be drawn from the material in reference 1,is that the major barriers to achieving the desired pulsed power outputs are not in the MHD generator part of the system, but in the explosive plasma generator. The primary barrier problem in the channel,namely its multi-pulse survivability,could be solved with the use of a disposable channel,if necessary. In the following ,the major elements of the repetitive pulsed power system proposed by Artec (1) will be listed from the point of view of identifying the barrier problems. The solutions proposed by Artec, and alternatives proposed by the present authors, will be presented:

a.Repetitive Pulse Operation in the Artec Explosive MHD Generator:

The most critical problem with this approach is that of repetitive power pulses. Due to the very high explosive loading ,the entire plasma generator (figure 1) as well as the MHD channel and magnet currently in use, are destroyed after each pulse.

For the MHD channel, a design is proposed (figure 3),which,it is claimed, will be able to withstand repetitive pulses. Its key feature is the use of stacked metal discs as structural supports for the channel and saddle coil magnet. In addition,to reduce transmission power losses, the transformer needed to convert the low voltage,80+ microsecond,generator output,to a 10 microsecond pulse,is incorporated into this structure. It is stated that this concept was used to design a channel capable of withstanding 3000 atm. pressure, delivering 120 kJ, and weighing 115 kg,i.e. 1 kJ/kg.

For the present application, it is stated in Ref.1 that a factor of 10 improvement in channel weight is required, i.e. a 600 kJ output will be obtained in a 60 kg structure, or 0.1 kJ/kg. This is to be accomplished with unspecified structural improvements. The assumption is made that the peak pressure in the channel will only be 4000 atm, compared to a 30,000 atm. (441,000 psi) plasma stagnation pressure. This implies a pressure recovery of only 13% in a low supersonic flow at a 50%! enthalpy extraction in the MHD generator. While this has not been verified by the present author, it appears to that the pressure recovery should be considerably higher.

In any case,in our subsequent analysis of this generator we used 4000 atm. as the peak pressure load in the channel, and we calculated that,theoretically, a multi-pulse channel could be fabricated from a high strength composite material. To indicate the scope of the forces acting on the channel walls ,one should note that 4000 atm. is equal to the pressure exerted by a 320,000 gauss magnetic field. In pulsed (microsecond duration) experiments on the generation of 100,000 gauss fields in single turn solenoid field coils, it was found (11) that ordinary metals were substantially deformed by the magnetic field forces. Our simplified thick wall cylindrical pressure analysis showed that the 2" I.D. MHD channel,used by Artec,would have a maximum stress of 100,000 psi with a 1" thick wall. This compares to the 150,000 psi ultimate strength in a metal reinforced composite wall. Nevertheless,the achievement of 100 pulse life with this channel clearly represents a major barrier problem.

For the repetitive plasma driver, Artec proposed the use of rapid fire gun technology in which the argon is pre-loaded in a cartridge containing the Octol explosive. The plasma cartridge is shown (Figure 4) inserted into a breech assembly in which voids and alternating shock mitigation layers are used to dissipate the explosive shock pressure. It is claimed that this design can be further improved to reduce the structural weight to 200 kg/kg of explosive. (Octol contains 5300 MJ/kg, and as noted,to generate 0.5 MJ, Artec used 7.2 kg of Octol.) To obtain 100 pulses, Artec proposes to use an automatic loading cartridge based on an unidentified proprietary design proposed by General Electric's Armaments Systems Division. Figure 5 shows graphically the firing rate of this "Explosive MHD Feed Concept" compared to other ordinance systems.

Assuming that the entire system as depicted in figure 4,or a variation thereof, combined with an autoloading cartridge could be developed, there are still other barrier problems to be overcome. The most important one is the need to improve the explosive to plasma conversion efficiency from 9% to 30%. In addition, ref. 1 has no discussion on how the "plasma source cartridge" (figure 4) is to be disengaged from the MHD channel, which is not disposable. For this reason, the present authors recommend that the use of a "disposable" MHD channel as an option that should be considered. In addition, there is no discussion on how the residual gases in the MHD generator are to be vented. In a lower energy,explosive MHD generator (3) it was shown that the residual gases in the generator can, under certain conditions such as the low repetition rate of several pulses per second, used in the present application,have an adverse

impact on the efficiency of the generator

b.Self Excited Magnetic Field in a High Magnetic Reynolds Number Flow:

The plasma produced by the Artec device has computed velocities in the 10-30,000 m/s range and electrical conductivities in the 10-40,000 mhos/m range. This results in magnetic Reynolds number of up to 35, based on a 5 cm. diameter MHD channel radius. Under these conditions, the magnetic field lines are very strongly displaced by the plasma in the MHD generator. This effect has been studied by Oliver and associates (12), where it was shown that the plasma flow is channeled in a manner similar to a constricting nozzle,(see figure 6).

Under these conditions it would be more effective to completely dispense with the orthogonal DC-MHD channel configuration used by Artec , and replace it with an inductively coupled AC-MHD generator. The saddle coil magnet would be replaced with a single turn solenoid, whose magnetic field is coaxial with the gas velocity vector, (instead of orthogonal as in the present configuration). The main advantage of this approach is that the efficiency of creating the magnetic field would be considerably greater. In the Artec experiment (9) with a 0.5 MJ MHD gross output; of the 230 kJ stored in the capacitor bank, 75 kJ was lost in transmission, 155 kJ was delivered to the magnet coil, and only 11.5 kJ,or 7.4% of the energy stored in the capacitor,was used for producing the 5.27 Tesla field inside the active MHD generator volume. In the self-excited MHD generator case, there is no capacitor bank, and the 75 kJ transmission loss would not exist. Therefore,the ratio of effective field in the channel to total generated magnetic field is 13.5,(Artec used a value of 12 by ignoring the resistive losses in the coil). The operation of the AC MHD generator with the Artec explosive generator will be discussed in Section 2.1.e.

c.Artec Magnet Coil Performance with External Capacitor Excitation:

Ref.1 states that closer coupling of the field and the channel reduces the required gross magnetic field energy to a value equal to 5 times that stored in the channel volume. Therefore, only 5*11.5 kJ, for a total of 58 kJ, would have to be stored in the magnet,versus the 155 kJ cited above. Since the minimum stored energy required to build up the magnetic field is a critical performance parameter in measuring the efficiency of this system, we performed several calculation to determine the validity of the claim that only

58 kJ of energy would be required. Based on the configuration of the MHD channel and magnet shown in figure 3 (taken from Ref.1) it appears that a saddle shaped coil,with a circular conductor winding cross-section in the axial channel direction is assumed. The magnet coil cross-section for this coil is shown in figure 5A. For this type of coil, the equation for the peak magnetic field is given by (13)

$$B=(2*\mu_o*j**p*r_i/\pi)*[(\alpha-1)\sin\theta] \qquad (2\text{-}1)$$

where j is the current density in the conductor, A/m^2; B is the field,assumed to be 5 Tesla in Ref.1; μ_o is the permeability of free space; p,the conductor packing factor,r_i the inside radius of the magnet winding cross-section in m.; α is the ratio of the external to internal conductor radii, and θ is the angle in the first quadrant subtended by the coil, as shown in figure 5A. It should be noted that there are three additional coil segments symmetrically placed about the origin, each of which contributes equally to the field in the center.

It is important to note that r_j is based on the external wall radius of the MHD generator channel. Only the internal dimensions of the MHD channel are specified in Ref.1, namely 5 cm internal diameter,65 cm.long. As noted above ,we estimated the wall thickness of the channel by assuming a composite matrix structure, having an ultimate strength of 150,000 psi, and using the isotropic,thick shell,cylinder stress equation. This equation provides only a crude stress estimate,since composite materials are non-isotropic. In any case,as noted above, a 1" generator wall results in a peak stress of 100,000 psi. Therefore, we used an r_j of 5 cm,which equals the outside diameter of the channel. For a repetitive,Artec MHD generator,this wall thickness may be too optimistic.

The outer radius of the magnet coal is equal to the skin depth. Since the test time in Ref.1 is 80 microseconds,we assumed that the field was externally powered , and that it is uniform during this time within 10%. This results in a sine wave time constant of 557 microseconds, and a skin depth,d, of 1.55 mm (14). The coil inductance,L, for a single turn rectangular coil,based on these dimensions is 0.22 microhenries (14). We assumed that the total coil current is confined between r_i and (r_i+d), and applied equation (2-1) to the Artec MHD channel with a 5 Tesla field. From this,we computed the stored energy

in the magnetic field,E,(which equals the product $L*I^2$, where I is the total current in the coil) to be about 100,000 joules or about double the minimum value of 58 kJ,assumed in Ref.1,(see above). Our computed value compares favorably with the 155 kJ measured in the Artec experiments with a non-optimized coil shape.

We also examined a coil which has a cosθ current distribution and which is supposedly more efficient in producing a transverse magnetic field in a circular channel (13). However, this resulted in about a 140 kJ stored energy. However,it not clear how such a current distribution could be generated in a single turn coil, which is required to obtain a low inductance in the magnet.

d. Self Excitation of the Artec Magnet Coil:

Refs. 1,2 and 9 state that the 0.5 MJ output MHD generator channel, whose internal dimensions are 5 cm D.* 65 cm.L, can be self excited. However, no computations are provided to backup this statement. We computed L/R risetime for this coil, using L=.22 microhenries, and the total resistance of the coil, internal plasma, and external load resistance for this generator. The latter two values were obtained from the references 1,2,and 9. The resultant magnetic field risetime was 193 microseconds versus a total 80 microseconds test time. Thus self excitation is not possible. However, ARTEC actually split the electrode region into two sections, one located downstream of each other in the channel. In this case L/R is 30 microseconds, which means that self-excitation is feasible for this case.

Thus with a 0.5 MJ gross output, and 0.1 MJ consumed in the magnet, the present ARTEC channel could approach the required 0.5 MJ net output, which is an objective of the present Project. However, it should be noted that an additional pulse forming circuit is required to convert the 80 microsecond generator output to 10 microseconds. Thus realistically the gross output of the generator should be increased considerable, probably to 1 MJ. In this case, self excitation becomes much more difficult because the inductance of the magnet increases with coil dimensions,while the explosive generator gas flow time does not. It may be possible to produce self excitation at the 1 MJ output level, possibly even higher, by using multiple channels, and this point warrants some further study. However, lacking the detailed data on the ARTEC MHD system, we believed that such an analysis would be too speculative at this time.

Before closing this Section, we should note that Swallom (5,6) has suggested an alternative solution to the self-excitation problem. He proposes to store the energy from the previous pulse for use in building up the magnetic field for the next pulse. This requires an external storage coil or capacitor, which greatly increases the magnet system weight. He provides no details on the implementation of this method, nor did we have time to study it, but it does appear to warrant closer examination.

e.AC Coupling of the Output the High Explosive MHD Generator:

An alternative approach to power extraction from this channel which was briefly explored, was the use to inductively extract the plasma energy by using a solenoid magnet,placed co-axially with the MHD generator channel. This eliminates the electrodes in the MHD generator and all its associated problems, e.g. electrode erosion, insulation breakdown. The output of the generator is inductively coupled to another coaxial solenoid placed either inside or immediately downstream of the primary field coil. This approach also eliminates the pulse transformer and circuit,used in the present in the Artec design (Figure 3).

To implement this AC coupled MHD generator,it is essential that the magnetic field lines be completely displaced by the plasma. A measure of this effect is the term M, which is equal to the product of the electromagnetic interaction parameter,S, and the magnetic Reynolds number,R, where

$$S=[B^2/2*\mu]/[.5*\rho*U^2], \qquad (2\text{-}2)$$

and

$$R=\mu_0*\sigma*U*D, \qquad (2\text{-}3)$$

B is the magnetic field strength; μ_0,the permeability of free space: ρ, σ, U are the plasma density,conductivity,and velocity;and D is the channel diameter. For the Artec experiment, S is only 0.016. Thus despite the high R of 35, M is only equal to 0.56.

To effectively use a coaxial solenoid, M should be considerably greater than 1. For a M value of 5, the B field would have to be increased to 15.7 Tesla. While this is considerably higher than the fields generated with the saddle coil magnets used in MHD generators, fields in this range have been obtained in pulsed solenoid coils (11). In addition, by increasing the field,the

length of the MHD generator is reduced, which in turn would reduce the pulse time. For example,for the above Artec experiment, increasing M from 0.56 to 5, reduces the required channel length from 0.64 m to 0.072 m. Therefore, if the same pulsed MHD output is obtained,the pulse time from the generator would be decreased from about 80 microseconds to 9 microseconds. Thus, it may be possible to completely eliminate the pulse forming circuit, since there would be no need to convert the 80 microsecond,low voltage MHD output to a high voltage,10 microsecond pulse,which is a requirement in the present application.

In the design of the 0.5 MJ net output, explosive MHD generator using a current fed pulse forming network, Artec computed that the MHD generation system,including the explosive plasma generator would weigh 1135 kg, while the pulse forming network would weigh 755 kg.Thus,the elimination of the latter with the AC coupled method would result in a considerable weight saving.

The AC coupled energy conversion technique of power extraction requires an external power source for the magnet. The provision for an external power source for the magnet was the basic approach used in the present study. However, there was insufficient time to investigate the design of a room temperature, pulsed solenoid magnet, operating at a 15. Tesla peak field, and interacting with the ARTEC plasma generator. Instead,we planned to study the interaction of a solid metal conductor moving at high velocity through the magnetic field in a solenoid.This problem is simpler to analyze, and it provides an insight into the energy exchange that can be developed with this concept. In discussing this problem with Dr.Sonju at the 23rd Symposium on MHD in June 1985, we learned that he and his colleagues (15) had studied the interaction of a high velocity, cylindrical metal conductor with the magnetic field in a solenoid.We will briefly summarize his findings, which suggest that inductive coupling may not an efficient method of energy conversion with a metal conductor, and probably also with plasma conductor. Before discussing the results of Sonju's analysis ,the performance of the pulsed system design of ARTEC will be summarized.

f.Summary of Artec's Proposed 100 Pulse Explosive MHD System

Artec considered four options to produce a repetitive 0.5 MJ pulse,namely, a single output MHD generator; five,series connected,MHD generators; ten,series connected,MHD generators; and one MHD generator,driving a pulse forming network

TABLE 1: SUMMARY OF 500 kJ NET OUTPUT CASES CONSIDERED BY ARTEC

Option	Weight-kg	Output-kJ	Output Voltage-kv
One 50 GW Generator	4000	3500	30
Five Generators	1950	1480	2.3
Ten generators	1440	1050	6.5
PFN generator	1890	500	220

(PFN). Of these, Artec selected the last one as the preferred approach. Table 1, summarizes, the weights and outputs of the four systems.

Of the 1890 kg total weight in the PFN system, 755 kg is due to the PFN. This provides considerable incentive to its elimination or at least simplification.

As will be discussed below,there is a considerable difference between the magnet weight estimated by Artec and the magnet weight estimated by Swallom (2) for a smaller, 50 kJ energy output, pulse system. Swallom's magnet is six times heavier than the Artec magnet. Based on our own calculations of the magnet required for the Artec channel we concluded that the Artec magnet weight estimate is too low, and a value near Swallom's estimate should be used.

In conclusion, it should be emphasized that the Artec results achieved to date are quite impressive in terms of the absolute pulsed power outputs achieved and in terms of the proposed designs for achieving these same output levels in a portable, repetitive, pulsed system. The comments made concerning the barrier problems, many of which are recognized by Artec, are meant to convey the complexity of the problem. Even if the system is only capable of achieving a single pulse, its current demonstrated performance represents a considerable advance in absolute power and energy output compared to results obtained in other explosive MHD generators. It should be noted that none of the papers that were reviewed contained any device capable of reaching the output levels reported by Artec.

2.2. Energy Extraction from a Metallic Projectile Generator:

As noted above, this problem was studied by Sonju and Teno (5). The method of inductively extracting the energy from a moving projectile is shown in

Figure 5B. A metal slug of diameter D_o, is driven at high velocity through a coaxial pair of solenoids, the outer one of inner diameter, D_2, provides the applied field, and the inner one, of inner diameter D_1, is excited by the flux distortions produced by the metal slug in the field lines. This flux distortion, as the field is penetrated by the metal slug is shown in figure 5C. The authors (5) performed an analysis of the conversion from the kinetic energy of the slug to electric energy in the pickup coil. To limit the slug weight a hollow beryllium cylinder, with a cylindrical and front face, wall thickness of about 1.7 cm, is used. The back face of the cylinder is open.

For a 20 kg slug, at 1000 m/sec velocity, the energy extraction from the slug increases, as expected, at approximately the square of the applied magnetic field. A 42 to 45 cm. diameter pickup coil is required to generate between 0.5 to 1 MJ output in a 100 microsecond pulse, as shown in figure 5D. The conversion efficiency increases with time, namely at a 500 microseconds pulse length, it is 50% higher that at 100 microseconds. If the weight of the slug is reduced by a factor of 10 to 2 kg, the coil diameter required is reduced by 50% and the energy output is reduced by over a factor of 10. Of greater significance is the relatively low kinetic to electric conversion efficiency, which is only 11% for the 20 kg slug, and 6.5% for the 2 kg slug. Since we are interested in a 0.5 MJ output, the slug weight would be about 10 kg, and for 100 pulses, the total slug weight would be 10,000 kg, plus an additional 10% for the explosive to drive the slugs. Thus the slugs alone are **2.5 times heavier than the total weight of the heaviest Artec system shown in Table 1.**

There are several points made by the authors of reference 5:

One, the drop in energy output with increasing D_1 in figures 5C and 5D is caused by the collapse of the hollow beryllium cylinder by the electromagnetic pressure. By the theory of elastic buckling of cylinders, this collapse is a function of the Young's modulus of elasticity. Its value is very high in beryllium, 40 mpsi. The authors (5) state that for this reason, increasing the velocity does not significantly improve the performance, as would be expected from the inductive coupling theory. They computed that if the velocity of the 2 kg slug were to be increased from 1000 to 3000 m/sec, the conversion would be only slightly higher. To achieve these velocities would require either electromagnetic acceleration of the slug, which has the appearance of a perpetual motion machine, or some other form of continuous acceleration, e.g. filling the projectile with a rocket fuel.

The present authors believe that increasing Young's modulus by using metal matrix composites is of considerable interest. For example ,in metals such as aluminum, the modulus is increased from 10 mpsi to 40 mpsi (17). PAN based carbon fibers have tensile moduli as high as 116 mpsi. This is three times the value in berryllium . This would allow an increase in the peak applied field to about 8.5 Tesla, and increase the conversion efficiency of the 1000 m/sec,20 kg slug to the 30% range, and the 2 kg slug to the 20% range. The advantage of this concept is that it may allow the frequency conversion of high energy pulses without opening high current carrying switches. However, a conversion efficiency in the 80-90% range is desirable, and above 50% is essential. Thus methods of increasing the buckling strength and slug velocity warrant additional study.However, such high efficiencies mean in effect that the slug is for all practical purposes stopped by the field. Whether this can be accomplished without having the slug deviate from its axial motion due to field non-uniformities, and strike the coil is highly uncertain.

This latter point is made by the authors of ref.5. To obviate this we would suggest placing the coil in a "gun" barrel formed from a nonconducting composite matrix. This will of course increase the magnet volume and considerably reduce the conversion efficiency.

Another point to be made on this concept is the large size of the slug, pickup coil, and magnet. The ID of the magnet in figures 5 C & D is 1 meter, and at room temperature operation, multi-MW's are required to power the magnet. Also,the pickup coil weighs 300 kg,if made from aluminum ,and 1000 kg with copper (5). However, the novel ammonia cooling method that we have invented (see Magnet Discussion below),will considerably reduce the magnet weights, at the expense of increased power consumption at room temperature operation. The power source for the primary coil is not discussed by the authors of reference 5. For efficient operation the primary coil should be pulsed. Therefore, a more compact configuration than that suggested by the dimensions given in figures 5B,C & D can be used.

In conclusion, the key barrier problems with this conversion scheme are the need to improve the buckling strength and to increase the velocity of the slug. The problem of magnet size and the problem of magnet destruction by the slug can be more readily solved. The investigation of advanced composites and rocket type acceleration of the slug warrants further study.Finally, it is

unlikely that this method can be used efficiently to produce 10 microsecond,0.5 MJ pulses,unless velocities in the 10,000 m/sec range are attainable. We have no suggestions on accomplishing this. Thus the metal slug approach will still require an additional pulse forming circuit to reach 10 microsecond pulses.

The application of the above approach to the ARTEC type plasma generator suggests that considerably higher efficiency should be possible ,if the magnetic fields are in the 15 Tesla range, as discussed in the previous section. In this case, the low velocity limitation of the metal slug, the large weight of the slug, the danger of the slug destroying the magnet are removed. Thus in the plasma device, one should be able to theoretically, greatly slow down the plasma velocity inside the magnet volume. Furthermore, a 10 microsecond, 0.5 MJ pulse can be directly generated in the plasma device. We had already reached this conclusion in the previous section. However, the details of the conversion analysis, beyond the infinite solid conductor approximation, were beyond the resources of this project.

We should note, off-setting these advantages, are the fact that the high wall thickness of the explosive channel means that less than 25% of the magnet field volume interacts with the plasma. Thus while the conversion efficiency from plasma kinetic to electric energy will be relatively high, the overall system conversion efficiency, which includes the conversion of the chemical energy to the applied magnet field energy will be very low with current performance levels. This can be seen as follows:

The noble gas dc MHD generator (see below) converts about 30% of the chemical energy to electric output. Assuming that this output is provided in pulsed form to the ARTEC type generator, one finds that for a 2" I.D. channel with a 1" wall thickness, only 25% of the field interacts with the plasma. Furthermore, at the present time ,only 9% of the explosive energy is converted to plasma kinetic energy. Thus even if we assume an 80% conversion efficiency between the plasma and the pickup coil in the inductively coupled solenoid, the net efficiency is only **0.54%**. If the efficiency of the explosive to kinetic energy conversion can be improved from 9 to 30%,as claimed by ARTEC (1), and if advanced metal matrix composite construction techniques are used to implant the magnet in the wall of the generator in order to increase the coupling between the plasma and applied magnetic field from 25% to 50%, then the net system efficiency would increase to **3.6%**. This is double that currently claimed by

Artec without self-excitation of the magnet. Since it may be slightly simpler to construct a repetitive 100 pulsed, AC MHD channel than a DC channel with internal electrodes, this approach warrants further study.

2.3- The Plane Wave Explosive Pulsed MHD Generator:

The other method of utilizing an explosive with an MHD generator has been in use since the early 1960's. A typical configuration is shown in figure 7, (19). A plane charge (Item 1) is located at the closed end of an MHD channel. Unlike the Artec system, the detonation products expand into the MHD generator,driving a linear shock wave into the ambient gas in the MHD duct. The gas can be either a noble gas or air. The detonation gas products generally have a low electrical conductivity. Therefore, most of the interaction with the magnetic field occurs in a thin conducting layer at the detonation shock front,which is usually seeded with an alkali salt. Figure 8 (Ref. 3) shows a simplified space (x)-time (t) diagram of the overall process. Region 2 in the figure represents the shock heated gas. Behind this region is a thin zone of highly conducting detonation products which are created by mixing the low ionization salt, e.g. cesium nitrate, with the front end of the explosive charge. The width of region 2 can be adjusted by changing the initial pressure of the gas in the channel,but in any case, the plasma slug length is generally considerably shorter than the MHD axial generator length. The MHD electromagnetic forces can only act on the conducting zone. Thus the MHD generator acts as a "brake" on the non-conducting,detonation products driver gas.

In the Artec device, the stagnation pressure,gas velocity, temperature, and electrical conductivity of the plasma are in the 10-20,000 atm, 10-30,000 m/s, 10-40,000 mhos/m, and 30-40,000°K range. In the plane detonation system, the corresponding values are in the 20-100 atm.; 4-8,000 m/s; 1-3000 mhos/m; 6-10,000°K range (3,19). This range can be extended somewhat (e.g. 15,800°K, 12,000 mhos/m,1000 atm.) by using lower initial argon pressures,or more explosive charge mass. However in the case of low pressure argon, the power output is less than with seeding the front face of the detonation products with a cesium salt. In addition, the magnetic Reynolds number in the plane wave system is generally less than 1, while in the Artec system it is much greater than 1.

The reported information to-date shows that these linear MHD generators have been operated with less than 1 Kg of explosive,(compared to 7.8 kg in the

Artec device) and the power output has been correspondingly lower.Typical power outputs have been 280 MW and 25 kJ (3) versus 10,500 MW and 500 kJ in the Artec device (1). **However, to date,the overall explosive to electric conversion efficiency in both systems is about the same, about 2% on average.**

Table 2 (adapted from Ref.20) shows a summary of the performance of several linear explosive MHD generators operated in the time period from 1963-1980. Here the authors of Ref.20 have used an interesting method of presenting the overall system efficiency,N (%). This term is divided into two products. One is ratio of the magnetic field energy stored in the active MHD generator volume, W_B, divided by the explosive energy, W_E. The other term is the ratio of the electric power output of the generator, P, divided by W_B,i.e.

$$N\ (\%) = [W_B/W_E],(\%) * [P/W_B] = A,(\%) * B \qquad (2\text{-}4)$$

The advantage of this formulation is that the second term shows the effectiveness of the transfer of energy between the magnetic field and plasma, while the first term is a measure of the effectiveness of the coupling between the explosive energy and the magnetic field. If,for example,the second term is very much less than unity, a large MHD generator volume is required for energy extraction. Similarly, if the first term on the R.H.S. of the equation is much less than unity, one can deduce indirectly that the conversion of explosive to plasma energy is low. These effects can be demonstrated by applying the equation to the evaluation of several linear explosive MHD systems, having a configuration similar to figure 7, as well as to the Artec configuration (Figure 1).

Table 2 shows several interesting results:

-Both the linear and the Artec generators produced about the same overall energy conversion efficiency of several percent, which is far less than the 12% objective for the Artec device. However, the reason for the low efficiency differs in the two systems.

-All the reported experiments with the linear generators used light charges (<1 kg of explosive),and relatively large MHD generators channels, while the Artec device used a heavy charge (7.8 kg) and a relatively small MHD channel.

TABLE 2: COMPARISON OF THE PERFORMANCE OF LINEAR EXPLOSIVE MHD GENERATORS & THE ARTEC MHD GENERATOR, USING EQUATION 2-4.

No.	Ref.	MHD Volume,c.c.	X,kg	P,MW	E,kJ	B Field,T	A,(%)	B	N,(%)
LINEAR EXPLOSIVE MHD GENERATORS									
1	21	2.5*2.5*46=288	.015	4.6	0.15	1.7	0.7	0.3	0.2
2	21	2.5*10*46=1150	.015	23	0.75	2.3	2.8	0.35	1.0
3	22	20*15*78=23400	.45	280	25	2.8	4.0	0.4	1.6
4	23	10*10*70= 7000	-	100	-	2.5	1.2	0.5	0.6
5	3	15.5D*165=31,100	.01	144	7.4	3.5	11.	0.27	2.8
6	20	5*10*100=5000	.04	43	7.4	5.3	26.	0.14	3.7
ARTEC EXPLOSIVE MHD GENERATOR									
7	8	5.1D*64=1300	7.8	10500	502	5.2	0.03	40.	1.2

-The linear devices achieved relatively high conversion of explosive energy to plasma kinetic energy,as evidenced in part by the term "A". In one linear experiments, namely No.6, this term reached a value of 26%, while in the Artec experiment, it was only 0.03%. The authors of reference 20 state that in the linear explosive generator experiments,the explosive to plasma kinetic energy conversion efficiency was in the 40-60% range, while the authors of the Artec generator (1), state that this conversion efficiency was only 9%.

-On the other hand ,due to the high magnetic Reynolds number of 35 in the Artec generator, the plasma to MHD generator conversion efficiency, as described by the term "B",is of the order of 100 times greater in the Artec generator than in the linear generators, where the magnetic Reynolds number is less than 1. It thus appears that the benefits of a more efficient MHD generator in the Artec system is offset by the much less efficient plasma generator.

-It should be noted that a plot of N versus A for the linear MHD generator results,shows that the overall efficiency N tends to an asymptotic limit of about 4% (see figure 9). The authors (20) of this figure claim that the overall efficiency limit of these devices is 4-6%, and it would appear that the Artec results may have an even lower limit.

-Implicit in this entire discussion is the assumption that the explanations given by the various experimenters, as to the description of the processes occurring in these devices, is correct. This point is not simple to verify because only limited measurements (such as shock front velocity) are made in these experiments. It is entirely possible that the Artec device,for example,

may have a higher initial efficiency of explosive to plasma conversion, and that the rarefaction wave discussed in the previous section is the cause of the low overall deduced efficiency. If this is the case, then a much shorter MHD channel (obtainable by using a much higher magnetic field) would result in an improved overall efficiency value of N. It is thus not clear why the linear and ARTEC explosive MHD generators, which are based on basically different design concepts should show similar low overall efficiency limits. Thus to achieve an overall N value of 12%, which the authors of ref.1 have identified as the goal for an efficient self excited 0.5 MJ output MHD generator using the ARTEC generator concept, will require experimental verification.

-Another extremely important point should be made in connection with the linear channels. Unlike the Artec channel which is destroyed after each test, it appears that the linear channels are capable of surviving multiple firings. In fact the channel used in Reference 3 was capable of multi firing operation. However, in its present configuration, a 500 kJ net output device based on the design in reference 3 would be far too heavy to meet the portability requirements. [Incidentally, this also means that the plane wave explosive generator is most probably not suitable for the inductive power extraction discussed in the previous sub-section.]

2.4.Comparison of a Repetitively Pulsed Plane Wave & Artec Generator

Swallom (2) has performed an analytical study of an explosively driven pulsed MHD generator,and a continuous (1-5 seconds) MHD generator,driving a pulse forming network. The application considered was less stringent that the current application in that only 50 kJ of power output of 25 microsecond duration,was required. The repetition rate was up to 20 pulses per second, with a lifetime of 600 pulses ,which is almost similar to the present requirement.

Swallom proposed using a linear explosive MHD generator based on the design concept of Ref.3, due to his belief that the Artec concept would not survive multiple firing. The specific conditions used by Swallom for the linear pulsed,explosive, MHD generator,are as follows:

RDX explosive-4 MJ/kg. Plasma pressure-1500 atm.; electrical conductivity-1000 mhos/m.; velocity- 20,000 m/s.; MHD generator- 5 cm.D * 50 cm.L; magnetic field-4 Tesla; pulse length- 25 microsecond; gross pulse energy output-250 kJ; net pulse energy output-50 kJ.

The difference between these output levels is used to charge the capacitor bank for the next pulse. In other words, the design is not based on direct self excited operation of the magnet. Instead, most of the gross output of the generator is used to charge a capacitor bank, which in turn powers the magnet for the next pulse. There is no information given on the weight of the capacitor bank. Also, it is noted that by (undefined) switching of the output pulses, this capacitor bank, generator, and magnet combination could be used to eliminate the pulse forming network at a saving of 500-600 kg. However, there are no details provided on how this is to be accomplished.

Table 3 shows a comparison of the component weights obtained by Swallom for the linear explosive,pulsed MHD generator with the estimated weights for the Artec case,using a current fed pulse forming network to convert the MHD generator output to a 10 microsecond pulse. Artec uses reactants for 100 pulses, with 9 MJ per pulse of explosive energy input, 850 kJ MHD power output to the PFN. With a 35% loss in the PFN, the net output is 500 kJ. Swallom uses reactants for 600 pulses, with 3.2 MJ per pulse of explosive energy input, a 250 kJ MHD gross output, and a 50 kJ net output.

The main difference between the two results is that the Artec system is projected to produces 10 times as much net energy output for about the same total system weight. A major cause for this difference is the very optimistic assumptions by Artec on the magnet power self-excitation and magnet weights

In addition, the following differences exists:

-For roughly the same channel dimensions (although undefined for this case by Artec, the channel dimensions are estimated to be several centimeters in diameter,and several 10's of cm. in length for the Artec channel; compared to dimensions of 5 cm.D*50 cm.L in Swallom's channel), and magnetic field strengths (5-6 Tesla for Artec and 4 Tesla for Swallom), the Artec magnet weighs a factor of six less than the Swallom magnet. Based on our calculations of the Artec magnet,we conclude that the weight estimate is much too low.

-The weights of the explosive plasma generator are much better defined in in the Artec report (1) than in Swallom's report (2). Based on the prior experience of the respective authors in the explosive research field, the Artec estimates have much greater credibility.

TABLE 3: COMPARISON OF EXPLOSIVE PULSED SYSTEMS WEIGHTS FROM REF.1 & REF.2

REF.1-Artec Output-500 kJ;100 pulses,10 m.s.		Ref.2-Swallom Output-50 kJ;600 pulses;25 m.s.	
Feed System			
-100 Empty Cartridges	80 kg		
-Magazine	125 kg		
-Autoloader	200 kg		
Feed System Subtotal	405 kg	Feed System	100 kg
Containment Vessel	335 kg	Containment Vessel	200 kg
MHD Channel & Magnet	105 kg	MHD Channel	50 kg
		Magnet	600 kg
Auxiliary Power Supply & PFN	822 kg	Aux.Power Supply & PFN	800 kg
Miscellaneous	53 kg	Misc.	200 kg
Total System Weight	1720 kg	Tot. Sys.Weight	1950 kg
Reactants-100 pulses-Octol	170 kg	Reactants-600 pulses-RDX-	480 kg
Explosive Energy Input/Pulse	9 MJ	Explosive Energy Input/Pulse	3.2 MJ
Gross Power Output/Pulse	.85 MJ	Gross Power Output/Pulse	.25 MJ
Net Power Output/Pulse	.50 MJ	Net Power Output/Pulse	.05 MJ
Gross Overall Efficiency	9.4%	Gross Overall Efficiency	7.8%
Net Overall Efficiency	6.1%	Net Overall Efficiency	1.6%

-The overall gross explosive to electric output conversion efficiency of 9.4% assumed by Artec,and 8%, assumed by Swallom, represents a major advance over current reported results. As discussed in the previous sub-section, the authors of ref.20 state that the linear explosive generator is limited to 4-6% gross efficiency from the MHD generator (See figure 9 & Table 2).

-In addition, Swallom computes that almost 80% of the gross output of the MHD generator is required for magnetic field excitation, using a method that allows elmination of the PFN. The net efficiency is,therefore, 1.6%. The Artec concept uses a 65% efficient PFN , which results in a net efficiency of 6.1%. However, Artec assumes a very low magnet energy requirement of about 50 kJ. Our own calculations show that the magnet energy requirement is at least 100 kJ, plus the resistive losses in the magnet. Also, for gross MHD output above 0.5 MJ, we estimate that self-excitation will be very difficult to achieve in 80 microseconds of generator operation. With self excitation, we compute a gross output for the Artec case of about 0.7 MJ, and a gross efficiency of 7.8%.

In concluding this section on explosive MHD generators, we note that the primary barrier problems faced by the linear system are:

A) Increasing the absolute net power output to 500 kJ, and

B) Improving the overall conversion efficiency to a level where a 500 kJ net output will result in a portable system.

On the other hand, the key barrier problems with the Artec system are:

A) MHD channel survivability for multiple pulse use, and

B) Improving the conversion efficiency of the explosive to plasma kinetic energy above the present 9% level. In view of the apparent limitation in overall conversion efficiency in the linear explosive generator to the 4%-6% range, it must be demonstrated experimentally that this limit in overall conversion efficiency does not apply to the Artec system or the Swallom system

The problem of achieving self excitation of the magnetic field, while difficult to solve ,is not as important a barrier problem. We noted that up to about 0.5 MJ gross output, self excitation may be possible within the 80 microsecond test time of the Artec generator, while the use of the "post pulse" output of the linear generator to charge a capacitor bank for the next pulse, as suggested by Swallom, may be suitable for both the plane wave and Artec generator. In addition, our approach of using a dc MHD generator to power the magnet for the explosive generator can be used for the Artec generator at acceptable overall system efficiencies, if the explosive to plasma kinetic energy is improved to the 30% goal set in Ref.1.

2.5 Pulsed Power From a CW Multi-Second Combustion MHD Generator

Swallom also analyzed {2} the theoretical performance of a solid rocket type fuel, self excited, cw MHD generator, to be used in place of the explosive MHD generator, to produce 50 kJ, 25 microsecond long pulses, with a 20 pulses per second rep rate, and a total of 600 pulses. Self excitation of the magnet is initiated with a battery produced field of 1 Tesla, which is amplified with the MHD generator output to 4 Tesla. The use of a heat sink MHD channel and magnet limited the total run time for the 600 pulses, to one second. Figure

10 shows a schematic diagram of this system.

Although a pulse forming network would be required for conversion of the dc power to the required pulse shape, this problem was not investigated (2).

Figure 11 shows the gross and net (after subtracting the power required for the 4 Tesla self-excited field) power output for the generator, for several magnetic field strengths. One notes that at a 4 Tesla field, the bulk (80%) of the gross power output is consumed in self excitation of the magnet. [The reason for this is that room temperature, heat sink magnets at fields above 2 Tesla have very high power consumption levels, especially at low MHD power outputs of several MW. Even the PAMIR MHD generator (7), with its 28 MW gross output, had a 50% magnet power consumption at 4 Tesla.] Also, the gap between the gross power output curves in Figure 11, narrow as the field increases to 4 Tesla, which indicates that much higher power outputs are best achieved by increasing the channel volume instead of the magnetic field.

Table 4 compares the cw MHD generator component weights with those of the linear explosive case. One notes that the two systems have nearly identical weights, with the major difference being the weight of the magnet. However, neither the performance nor the weight of the pulse forming network is included in this cw case. We estimate the chemical to gross MHD power conversion efficiency at 10%, and the net MHD efficiency at 2.5%, due to the 65% power requirement for the self excited magnet. In addition, if the PFN efficiency is 65%, as assumed by Artec (1), the net efficiency to the load for the cw system is about 1.6%, or, coincidentally, equal to the 1.6% for the explosive system.

The overall volume of this system is 1.45 m^3 compared to 1.58 m^3 for the 50 kJ explosive system. Thus both systems are fairly compact.

In Part 3 of this Report we compare the performance of these combustion generators with the new noble gas generator. However, several items will be noted here. We found that the generator analysis (2) contained assumptions which we consider to be far too optimistic.

In the first place, the exit to entrance area ratio of 13 to 1 is far greater than has been operated in any experimental channel. MHD channel's operate under adverse pressure gradients, and a very high area ratio will most like-

ly result in flow separation from the walls.The highest area ratio channel that has been operated to the best of our knowledge had a 6 to 1 area ratio (10).

In addition, the length of each sequence of pulses is only 1 second, compared to our requirement of 10 seconds. Our analysis of the room temperature, heat sink, saddle coil,MHD magnet used by Swallom, using the method of ref.13, showed that he assumed a very high coil current density of about $7*10^7$ A/m^2 which results in a 20% resistance change in the 1 sec. operating time. This enables him to achieve a 4 Tesla field. For longer operating times, the field is limited to 2 Tesla, as was the case in a recently operated (6) self-excited combustion MHD generator. We thus consider the Swallom generator as too optimistic a design for a cw MHD power source. However, it is useful as a basis for comparison with other concepts and experimental generators.

Applying Swallom's analysis to the present requirement of 500 kJ pulses, of 10 microsecond duration,and 10 pulses per second, and assuming Artec's 65% conversion efficiency in the pulse forming circuit, one finds that the net power output of the generator, excluding the magnet power requirements, will be 7.7 MWe,or 7.7 times greater than the system analyzed by Swallom. Since there are other inefficiencies in the system, the gross cw MHD power required will be somewhat higher. Our analysis in Section 3 is for 10-20 MWe gross output from the MHD generator.

Multi MW levels of net MHD generator output have been obtained by several Russian researchers with solid rocket type fuel fired, self-excited,generators operating for several seconds. The application was earthquake research (7,24-26). Figure 12 shows a photograph of such a generator, which produced up to 28.8 MWe gross power in a pair of parallel MHD generators, enclosed in a self-excited room temperature magnet. One generator was used to power the 4 Tesla magnet, and the other one delivered 15 MWe MHD power to a load (26). Each generator was 1 m. long, and had an area ratio of only 1.6. The gas pressure and mass flow rates for this experimental generator,were 50 atm. and 30 kg/sec, respectively, compared to 70 atm. and 3 kg/sec. for Swallom's theoretical 1 MWe generator.The overall dimensions of the MHD generator system deduced from this photograph (by comparison with the truck [ERS-67] in the background) appear to be several 100 m^3, (compared to Swallom's result of 1.45 m^3 at 1 MWe). The bulk of the volume is taken up by the magnet,which suggests that for the present application, the PAMIR type MHD generator is not portable

Recently a self-excited, combustion generator, designed for a power output in the range of Swallom's design, has been operated (6). The magnetic field was 2 Tesla, and the enthalpy extraction achieved was 3%, for a gross power output of 4.8 MW, of which 1/2 was consumed by the magnet.

An alternative approach to the use of a combustion MHD generator is to use a superconducting magnet. While this eliminates the advantages of long shelf life inherent in the solid fuel, self excited MHD generator, it sharply reduces the size of the cw MHD generator system. Figures 13 and 14 (Ref.29) show the schematic and dimensions of a several minute operating time, 25 MWe net power output MHD generator, using a 4 Tesla superconducting magnet. Both liquid and solid fuel versions were considered (29). The channel is actively cooled. However, it can only operate for short time periods, in the range of 1-200 seconds on-time, and 2-300 seconds off-time, with a total life of 1-16 operating cycles, and a total life of 0.5 to 2 minutes on-time. An analysis (29) of a 10 MWe net output MHD generator based on this design, operating in 21 sec. bursts, with 30 sec. off-time between bursts, and a total life of 63 sec, resulted in a total system weight of about 1920 kg and a volume of 3 m^3, which is almost identical with the 1 MWe self excited, cw MHD generator results computed by Swallom, (2).

Based on the above evaluation, one concludes that for multi- megawatt net power output, the magnet size and weight required for self excited operation is the limiting factor in MHD power supply portability. Therefore, if portability and system size are primary considerations, use of a cw MHD power supply in the multi-megawatt range requires either a superconducting, or cryogenic magnet, or possibly our novel ammonia cooled, room temperature magnet.

In concluding this Section, we note that our original project plan had been to use the above combustion MHD generator to power the magnet for the Artec type explosive MHD generator. However, after our discovery of the advantages of the noble gas generator, we performed no further work on the combustion generator. The noble gas generator, as will be shown, far exceeds the performance potential of the combustion generator.

Finally, we note that all the above systems have chemical to pulsed power conversion efficiencies in the range of several percent. The 12% level projected by Artec requires the solution to major barrier problems.

TABLE 4: COMPARISON OF CW & LINEAR EXPLOSIVE PULSED SYSTEM WEIGHTS FROM REF.2

CW MHD GENERATOR		EXPLOSIVE LINEAR MHD GENERATOR	
Output-1 MWe,30 sec.,20 pulses/sec.		Output-50 kJ;600 pulses;25 m.s.	
Feed System	60 kg	Feed System	100 kg
Gas Generator	150 kg	Containment Vessel	200 kg
MHD Channel	50 kg	MHD Channel	50 kg
Magnet	1800 kg	Magnet	600 kg
Aux.Power Supply,w/o PFN	150 kg	Aux.Power Supply & PFN	800 kg
Miscellaneous	100 kg	Misc.	200 kg
Total System Weight,w/o PFN	2310 kg	Tot. Sys.Weight,with PFN	1950 kg
Reactants-30 sec.,100% reser.	180 kg	Reactants-600 pulses-RDX-	480 kg
Est.Gross Overall Efficiency*	10%	Est.Gross Overall Efficiency	7.8%
Estimated Overall Efficiency	1.6%	Est.Overall Efficiency to load	1.6%

NOTE:1) Since the pulse forming network (PFN) was not included in the cw MHD generator case, the system weight must be increased by at least 600 kg, and the net efficiency must be reduced by at least 35% [as assumed by Artec (1)], to produce the 50 kJ, 25 microsecond pulses with the cw MHD generator.

2)-*-The Gross Overall Efficiency for the cw case is the chemical energy to total MHD output conversion. Since 75% of the gross output is used to self excite the magnet, the Net MHD Output Efficiency is 2.5%. This must be further reduced by the loss in the PFN. Assuming it is 65%, one obtains a value of 1.6%.

2.6.Non-equilibrium,Closed Cycle,Noble Gas,MHD Generators:

This generator was originally developed in the 1960's for use with high temperature gas cooled reactors with solid fuel cores, at temperatures up to 2000°K. Both terrestrial power plant and space power plant applications were considered. The electrical conductivity in alkali seeded gases at these temperatures is negligible. However, it was postulated that the induced magnetic field in the generator could be used to produce an electron plasma, whose temperature exceeds the stagnation gas temperature in an amount determined by the generator configuration.For the linear Faraday generator,the degree of electron heating is given by (27)

$$[T_e/T_o] = [1+\gamma*(1-K)^2M^2\beta^2/3*\delta] \qquad (2\text{-}5)$$

where the subscript e,o apply to the electrons and gas stagnation conditions,γ is the ratio of specific heats, β is the Hall parameter,or ratio of electron cyclotron to collision frequency, and δ is an electron loss parameter that depends on the type and concentration of molecular impurities. It can be seen that for this ratio to exceed unity, the Hall parameter should be greater than unity and the loss parameter should be near unity. This means that non-equilibrium ionization requires the use of noble gases,with molecular gas impurities concentrations in the ppm range.

Due to the great expense of building high temperature,inert gas heat sources, most experimental efforts at demonstrating this mode of power generation in the 1960's were limited to systems with thermal power levels of under 1 MW, and MHD channels with 10's of cm^2 cross-sections.As a result,wall losses dominated these devices.In addition,it was discovered that non-equilibrium plasmas are subject to plasma instabilities which reduce the effective Hall parameter to a level of 1 to 2,which further inhibits non-equilibrium ionization.

To overcome the thermal input limitation,a number of investigators (including the present author),used shock tubes as a heat source,where neither the stagnation temperature nor the thermal input are as restricted as in steady state devices.In a series of experimental programs,sponsored primarily by the Office of Naval Research in the time period of 1962 to 1975, we demonstrated in 1964 (28) the existence of the phenomena of non-equilibrium ionization in a small MHD channel (5x5x30 cm^3).By using a shock tunnel and supersonic MHD

Channels,with volumes of 0.02 and 0.04 m^3,and 3/1 and 6/1 area ratios, [labelled ST-20 &40],respectively; input thermal power level of 3-10 MWt were obtained, {Ref. 10},{see figure 15}. At a stagnation temperature of 3520°K, a non-equilibrium power level of 1.8 MWe, equal to 19.3% enthalpy extraction, was attained {See Table 5}. At T_o of 2580°K,a power output of 0.63 MWe, equal to 16.5% enthalpy extraction, was measured. In the latter case,the electron temperature in the generator exceeded the gas stagnation temperature. These results were obtained with plasma instabilities in the generator which limited the effective Hall parameter to the 1 to 2 range.The power output densities were about 40-50 MWe/m^3.

Other shock tube non-equilibrium MHD experiments also produced high enthalpy extractions, {30} {See Table 5}. Researchers at Eindhoven University using a 1 to 2.8,generator entrance to exit area ratio,channel obtained 24% enthalpy extraction at T_o of 3300°K, while researchers at Tokyo University measured 9% enthalpy extraction at T_o of 2800°K in a disc type generator. More recently {31},this group has obtained 20% enthalpy extraction at only 2200°K, in a disc type generator. In addition,researchers showed that molecular contamination levels below 1% in diatomic species (N_2), and 0.1% in triatomic species (CO_2,H_2O), would not significantly degrade generator performance {32}.

Thus the scientific basis for the closed cycle non-equilibrium MHD generator had been established by the mid-1970's. The next step was to demonstrate high generator "turbine" efficiency, which must be in the 70% range,{including diffuser losses},to obtain an efficient Brayton cycle with this generator. To meet this goal, it was necessary to reduce electrode losses by operating the generator with emitting electrodes, which required multi- second operation in a blowdown mode. It was calculated {33} that a 50 MW thermal input generator would achieve 30% enthalpy extraction in a 3 m.long channel,with a 15 MWe output and a 69% generator isentropic efficiency. The computed power output density was a modest 30 MWe/m^3,i.e. the scale up was based on the ST-40 shock tunnel generator discussed above. A blowdown facility design was implemented under EPRI sponsorship {33} and figure 16 shows a drawing of this facility design. The project was not implemented,primarily as a result of system studies for utility scale central station power plants {34}, which showed that such systems were more costly than the open cycle MHD or gas turbine fired systems.

Table 5 -*Power Density and Enthalpy Extraction of Various Generators* -(From Ref.30)

Group	Gas + seed	P_{th} MW	$\dot{m}$ kg/sec	P_{stagn} bar	T_{stagn} K	B T	$M_{entrance}$	Area ratio	P_e MW/m^3	η_{enth} percent	Comments
Frascati	He + 0.26% Cs	0.71	0.077	1.75	1,770	3.5	0.81	1.1	10.5 (max 14)	0.65	Preionization, 20 A.
Tokyo	He + 0.1% K	.35	.046	1	2,800	1.13	2	1	50	9	
Eindhoven, 3-1	Ar + 0.05% Cs	4.2	2.3	7.9	3,585	2.94	1.8	1.4	83	5.3	
Eindhoven, 10-1	Ar + 0.05% Cs	5.9	3.4	7.2	3,322	3.57	1.6	2.8	140	24	
General Electric, ST 20	Ne + 1.2% Cs	5.2	2.5	2.2	2,150	1.3	1.6	3	23	6.5	
General Electric, ST 20	Ne + 1.7% Cs	11.3	4.5	4.4	2,620	1.3	1.6	3	55	9.5	
General Electric, ST 40	Ne + 1.0% Cs	9.45	2.75	5.39	3,520	2.7	1.5	5.8	46	19.3	
General Electric, ST 40	Ne + 1.0% Cs	3.84	1.53	2.56	2,580	2.52	1.5	5.8	16	16.5	12 el., 30 A/el. preionization.

In the late 1970's, a group at the University of Eindhoven tested a closed cycle MHD blowdown generator at the 5MW thermal level. This generator has produced 0.36 MWe,equal to 7.3% enthalpy extraction at T_o of 1910°K. In addition, researchers in Tokyo are constructing a similar size closed cycle blowdown experiment for use with a disc type generator (31). This more recent work has provided further confirmation of the higher performance potential of the closed cycle generator, provided a low cost heat source can be developed.

It should also be noted that considerable work has been done on the theoretical analyses of closed cycle MHD generators at central station,MHD power plant sizes, using the above experimental results. The focus of the generator analyses in all these cases,was on both high enthalpy extraction and very high generator isentropic efficiency, which results in low power densities (under 100 MWe/m^3),(e.g.Ref.35). For example,figure 17 (from Ref.10) shows the theoretical enthalpy extraction of a 2000 MW (thermal) generator as a function of generator area ratio. A high generator isentropic efficiency also requires a high efficiency (i.e. high pressure recovery) in the diffuser,located at the exit of the generator. This in turn results in very long diffusers, as is shown for the 50 MW blowdown generator in figure 16.

For the pulsed power application, high isentropic generator efficiency is much less important than high enthalpy extraction and high power density. Since there was no heat source suitable for a practical application of non-equilibrium pulsed MHD power, this topic received almost no attention to date. In reviewing the present author's prior work in non-equilibrium MHD only one unpublished item of relevance to pulse power was found. This analysis is shown in figure 18 (from Ref.36),where a calculation was performed for a 40 MWe output, high performance closed cycle MHD generator operated at a electric load ratio of 0.5-0.55, which results in a low generator efficiency. In this case the power density is 200 MWe/m^3,which is about the same as in high performance open cycle MHD generators. It should also be noted that in all these calculations a very high plasma turbulence model, which results in reduced performance of the generator, was used. However, there exists considerable experimental evidence that by using very low fractions of ionizable seed,which allows full ionization of the seed, this turbulence can be suppressed and the performance of the generator improves dramatically (31). In the present project, the generator analysis was performed with the assumption that plasma turbulence is suppressed

2.6.a.Fossil Fuel Fired, Regenerative Ceramic Heat Exchangers for Closed Cycle MHD:

By the late sixties,it became clear that a 2000°K gas cooled nuclear reactor would not be developed in the foreseeable future. Therefore, closed cycle MHD research was directed toward the development of a 2000°K (3100°F) fossil fuel fired-heat exchanger. For this purpose a regenerative ceramic storage heat exchanger,(similar to those used in the steel industry) was developed. In this device,the combustion gases and the MHD system working fluid, i.e. the noble gas, are alternately cycled through the same passages in the heat exchanger

One such heat exchanger, rated at 1 MMBTU/hr is shown in Figure 19 (37). The heat source for the heat exchanger was a novel 1 MMBTU/hr air cooled,cyclone coal combustor (figure 20), capable of removing almost all the liquid coal slag, which could plug the narrow (1/4 inch diameter) heat exchanger passages. It was demonstrated (37) that this heat exchanger could be used to heat argon to 2000°K,with molecular contamination levels below 100 ppm.

Our purpose in describing this heat exchanger system at some length is to point out the barrier problem presented by the heat exchanger in the closed cycle system, non-equilibrium MHD system. Even in the present pulsed power application, the heat exchanger represents a major weight penalty. For example, using the 1 MWe net output combustion MHD generator of Ref.2 as a basis for comparison; assuming a 30% enthalpy extraction in the non-equilibrium MHD generator, a 2000°K peak stagnation temperature, and a 10 second operating time , one finds that one must store 1.26 million BTU in the ceramic bricks of the heat exchanger. (For proper operation of the heat exchanger, the heat storage in the ceramic is about 10 times the heat extraction per pulse. Using alumina ceramic bricks, one calculates the weight of the ceramics to be 950 kg. This is equal to 50% of the entire weight of the combustion generator in Table 4 of the previous sub-section. In addition,using a 50% void fraction in the heat exchanger for gas passages, one computes a total volume of 0.73 m^3, which is equal to 50% of the total system volume of the 1 MWe combustion generator of Ref.2. Thus this heat exchanger approach is clearly not suitable for the present application, unless a means is found to **directly transfer the heat from the combustion products to the noble gas generator working fluid. This is the central aspect of our invention**, which will be discussed in the next Section.

3. HIGH ENERGY CHEMICAL FUEL FIRED, NOBLE GAS MHD GENERATOR

3.1. Factors Limiting the Power Output/Unit Volume and Enthalpy Extraction from MHD Generators

The power output per unit volume in a MHD generator is given by

$$P=\sigma*U^2*B^2*K*(1-K) \qquad (3-1)$$

where σ is the electrical conductivity of the gas in mhos/m; U the gas velocity in m/sec; B the magnetic field in Tesla, and K is the load factor, which equals E/UB, where E is the electric field due to the load resistance. In an equilibrium plasma, maximum power is obtained at K=0.5, while in an non-equilibrium plasma, where σ is a function of the generator current, K is a maximum at about 0.3.

The high power output, pulsed combustion MHD generators discussed in Section 2.5 {Ref.2,6,7} used solid rocket type fuels,with a high aluminum solid fuel content. The combustion products, whose molecular weight is in the range of about 30, reach stagnation temperatures of 4000°K, and electrical conductivities somewhat above 100 mhos/m. Fields of 4 Tesla are about near the maximum achievable in room temperature heat sink magnets. The ratio of specific heats for these gases is about 1.1. Thus they can be expanded to a high Mach number, {e.g.2}, and a high local velocity of 2000 m/s,while maintaining a high static gas temperature {3300°K}, and a high electrical conductivity. Thus from equation 3-1,the maximum power output/volume at the combustion generator entrance is in the range of 1600 MW/m^3. This power decreases rapidly in the downstream direction so that the average over the generator volume is considerably less. The highest measured value to date is about 500 MW/m^3,{Ref.7}.

The above power output could be increased to possibly an average of 1000 MW/m^3 by the use of cyanogen,C_2N_2, or tetracyanoethylene,C_6N_4m which can reach combustion temperatures of 5100°K at 100 atm.

On the other hand, in noble gases,the high ratio of specific heat,1.67, sharply lowers the static gas temperature at high Mach numbers.However, non-equilibrium ionization results in conductivities of 100 mhos/m at static gas temperatures in the generator below 2000°K, even in the presence of plasma

instabilities. In prior MHD generator experiments , achievement of these conductivities has required the use of argon or neon,with their low electron scattering cross-sections, rather than helium, which has a very high cross-section. However, the high molecular weight of argon lowers its velocity in the generator and offsets its high conductivity, when high power output is required. When added to the temperature limitation of 2000°K in fossil fuel heat exchangers, one finds that the power output densities in argon are in the range of 100's MW/m^3. In the generator calculation shown in figure 18, the power density is only 200 MW/m^3 with argon at very high stagnation pressures. At lower argon pressures, plasma instabilities due to the Hall effect, lower the effective conductivity, so that in the experimental shock tube-MHD generators,power densities were between 16 and 140 MW/m_3 were obtained, as shown in Table 5.

If helium could be heated to 4000°K stagnation temperatures, then conductivities as low as 50 mhos/m, Mach numbers of 2, magnetic fields of 4 Tesla, and a load factor,K,of 0.3; would result in a power output of 4000 MW/m^3. Thus it is clear that the main barrier to the use of the non-equilibrium MHD generator for the present application is the development of a chemical fuel heat source that will allow heating helium to the 3000-4000°K temperature range. **The invention of the metal fuel combustor by the present authors has the potential for achieving this objective.**

Enthalpy Extraction in the Generator:

The power that can be extracted from an MHD generator is also limited by the enthalpy extraction from the gas. This is determined by the gas properties and flow dynamics. One factor limiting power output is gas flow deceleration. It was stated (38) that for flow deceleration greater than 22%, choking of the flow takes place. Flow deceleration is essential for power conversion because at constant velocity, the channel cross section increases too rapidly (39). For example in the analysis of the combustion generator in reference 2, the area ratio was assumed to be 13 to 1, which is about twice the maximum value at which a generator has been operated to date (10).

The best combustion generator performance reported to date (7) achieved an enthalpy extraction of only 12%. The primary reason for the low enthalpy extraction in combustion gases is the low ratio of specific heats, which for hydrocarbon combustion products at the 3000-4000°K is about 1.1. The ratio of

generator outlet to inlet enthalpy, H_o/H_i, in a MHD generator is given by the following,(27)

$$H_o/H_i = [P_o/P_i]^{N*(\gamma-1)/\gamma} \qquad (3\text{-}2)$$

where P_o/P_i is the pressure ratio across the generator and N is the generator polytropic efficiency, given by (12)

$$N= K/[1+(\gamma-1)*M^2*(1-K)/2] \qquad (3\text{-}3)$$

here K is the electric loading parameter in a Faraday generator and M the Mach number. As noted above, for maximum power,in an equilibrium plasma, K=0.5.

We applied equation 3-2 to three gases, with specific heat ratios of 1.1 (representative of hydrocarbon combustion products), 1.2 (representative of ultra high temperature (4000^oK) diatomic gas species (such as CO,N_2),obtained from the combustion of cyanogen type fuels), and 1.67 for monatomic gases, and with K=0.5, and M=2.The resulting pressure ratios and enthalpy extraction are shown in Table 6.

TABLE 6:ENTHALPY EXTRACTION VS PRESSURE RATIO,AS A FUNCTION OF γ

γ	=1.1	=1.2	=1.67
N	=0.45	=0.42	=0.30
and P_o/P_i=0.1; one obtains			
H_o/H_i	=0.91	=0.85	=0.76
alternatively, for H_o/H_i=0.80, one obtains			
P_o/P_i	=.005	=0.04	=0.16
or P_i/P_o	=200.	=25.	=6.3

One notes that at a pressure ratio of 10/1, the hydrocarbon fuels have an enthalpy extraction limit of 9%, while the monatomic gases have a limit of 24%. Alternatively, to obtain a 20% enthalpy extraction in the former requires an unrealistically high pressure ratio. While these equations oversimplify the problem,they do point out the desirability of operating with noble gases, or at

least with non-dissociating diatomic gases. [It should be noted that in the metallic solid fuels used in the above noted high conductivity experiments (6,7), the presence of hydrogen-oxygen compounds lowered the specific heat ratio to 1.15].

3.2. The Chemical Fuel Heat Source for the Pulsed Helium MHD Generator:

As was explained above, the primary barrier to applying the technical results achieved with the closed cycle MHD generator, is the problem of heating the noble gases from the 2000°K ceiling attainable with fossil fuel fired, heat exchangers, to the 3000-4000°K required for high pulsed power output levels in helium. In a Coal Tech sponsored study on the problem of achieving high power levels for space power plants, we invented the concept of using a high energy fuel in modest concentrations, relative to the generator working fluid, as a high temperature heat source for helium. The central element in the use of this heat source is to assure that the fuel's products of combustion do not adversely affect the equilibrium or non-equilibrium electrical conductivity of the generator working gas.

The background for this invention has been Coal Tech's work during the past several years on the development of a cyclone coal combustor. The concepts involved in the combustion of coal particles in this combustor have been adapted to metal fuel particle combustors by using the metal oxide products of combustion to directly heat a noble gas. This is possible because the oxides condense at a temperature greater than that of the generator operating temperature. Therefore, it should be possible to remove the oxide particles upstream of the generator by using the swirling flow field of a cyclone combustor. This method is used to remove liquid coal ash particles in a cyclone combustor. One such combustor operating in a two stage configuration is shown in figure 21. The metal is burned with preheated oxygen in the first stage. The peak temperature attainable in metal fuels is either equal to the boiling point of the oxide or the dissociating temperature of the oxide. Part of the helium used in the MHD generator is mixed with the oxide combustion products in the first stage. The metal oxide combustion products then exhaust into the second stage where they are mixed with the balance of the helium. Other inert gases, including the low molecular weight gas hydrogen, can be used. It is necessary to centrifuge to the walls most of the metal oxides inside the combustor in order to maintain a high flow velocity in the generator. Since the combustor operates at

very high temperatures, the walls can be readily covered with a liquid oxide or metal layer to which the oxide combustion product particles will adhere.

Table 7 shows the adiabatic flame temperatures at 100 atm. for several metal fuels. We also show that only a very low mol fraction of fuel is needed to heat a noble gas from either 298°K, or 1366°K to 2000°K. 1366°K was selected as the peak temperature to which a noble gas can be heated in a recuperative shell and tube heat exchanger which is much more compact than the ceramic brick regenerative heat exchanger discussed previously.In the following section,a more detailed analysis of the combustion processes relevant to the present pulsed power application will be given.

For the present,we note that the peak stagnation temperature to which a noble gas can be heated is primarily determined by the gas stagnation pressure at which the noble gas generator operates. For example,the vapor pressure of ZrO_2 is about 50 atm. at 6000°K (40). At this temperature the noble gas pressure should be several 100 atm. to maintain a low ratio of molecular oxide vapor pressure to noble gas partial pressure. As the gas expands in the supersonic nozzle to the MHD generator, the oxide vapor will condense, and depending on the size of the condensed particles they will either deposit on the walls of the combustor,nozzle,generator,or be transported with the noble gas through the MHD generator. If the ratio of vapor pressure of the oxide relative to the noble gas is too high, then the particle drag of the condensed oxide will decelerate the flow and the benefit of a low molecular weight noble gas on high generator performance will be reduced. This can be corrected by reducing the peak operating temperature,i.e. the ratio of oxide to noble gas partial pressure. For example, at 5000°K, the ZrO_2 vapor pressure is only 5 atm., and a noble gas pressure of several 100 atm. should assure a high gas velocity in the generator.

Similarly, if aluminum is used as the fuel, the vapor pressure is about 5 atm. at 4000°K, and about 0.03 atm. at 3000°K. Thus operation at noble gas pressures in the 50 to 100 atm. range should allow the use of aluminum in this temperature range, and most of the calculations of generator performance in this study were made in this temperature range, using aluminum.

TABLE 7:METAL OXIDE PROPELLANT COMBUSTION AND HEATING OF NOBLE GASES

REACTION	ADIABATIC FLAME TEMP. @ 100 atm.,(°K)	MIXTURE COMPOSITION (MOL%) HEATED TO 2000°K FROM 298°K,1366°K		
		Ar	O_2	FUEL
$Al_s+3/4O_2=$				
$.5Al_2O_3$	4700-(fr.298K)	92.2	3.3	4.4- (298K)
		97.0	1.7	1.3-(1366K)
$B+3/4O_2=$				
$0.5B_2O_3$	5027-(fr.298K)	89.3	4.6	6.1- (298K)
		95.7	1.8	2.4-(1366K)
$Zr+O_2=ZO_2$	6250-(Based on boiling point limit)			

3.3. Aluminum Combustion as A Thermal Energy Source for Non-Equilibrium MHD Generators

3.3.1. General Requirements of the First Stage

In the first combustor stage, (See figure 21), aluminum powder is burnt with oxygen in the presence of helium to provide an exit gas temperature in excess of 4000K. Since the flame temperature is limited by the boiling point of the liquid Al_2O_3 product which is pressure dependent (40), combustion should be carried out at total pressures greater than the 5 atm partial pressure of Al_2O_3 at $4000^{\circ}K$.

At the combustion temperature, the combustor product stream should contain no free oxygen while the Al_2O_3 should exist essentially in the liquid state. i.e. the vaporization or decomposition of Al_2O_3 , which occurs at the boiling point, must be minimized. Elimination of free oxygen requires operation at aluminum levels in excess of the stoichiometric amount while the vaporization/decomposition of Al_2O_3 at the boiling point is prevented by introducing sufficient inert gas, in this case helium, to serve as a heat sink and hold the temperature at, or below, the boiling point of the oxide.

To limit the size of the combustor in relation to the MHD generator, the time available for aluminum ignition and burnup is around 2-3 ms. This requires that the Al particles be small (<10 diameter) and that ideally, the combustion proceed at near adiabatic condition as possible, i.e. with minimum radiative and conductive heat losses to the environment. For most cases of interest this latter condition is satisfied because the entrained particle density in the combustor is high enough to result in black body radiation from the combustion volume.

The following discussion develops the appropriate reaction stoichiometry to meet first stage combustor requirements. We then describe the combustion model employed, as well as the evaluation of experimental data necessary to predict particle combustion times as a function of operating conditions.

3.3.2. Reaction Stoichiometry

With 10% excess Al, aluminum suboxide (Al_2O) is an expected combustion product (51) via:

$$Al_g + 0.5*Al_2O_{3(l)} \Rightarrow 0.75\ Al_2O_{(g)} \qquad (3\text{-}4)$$

The overall reaction stoichiometry is then:

$$1.1*Al_s + 0.75*O_2 + x*He \Rightarrow 0.475*Al_2O_{3(l)} + 0.075*Al_2O_{(g)} + x*He; \quad (3\text{-}5)$$

The enthalpy of the reaction is -180 Kcal/(1.1mole Al), based on thermochemical data in Reference 52. The mol coefficient for He,"x" depends on the flame temperature (boiling point) which is a function of pressure, i.e."x" is the amount of He needed to "soak up" the reaction enthalpy which otherwise would go into vaporization/decomposition of Al_2O_3 at the boiling point.Table 8 presents results of adiabatic calculations at several pressures.

The calculations show that high levels of He must be injected to "soak up" combustion heat above that required to raise the products just to the boiling point with no vaporization/decomposition. Without He, about 63% of the Al_2O_3 liquid would be vaporized/decomposed at 1 atm (53,54). As noted, these calculations are for an adiabatic system. In an actual combustor there would be some heat losses (about 10%),and the amount of He required to limit the temperature would be reduced. However, the mol fraction amount of He that can be added is still high. For example, at 10 atm,a 30% heat loss would only reduce the required He content in the reactant gas (balance O_2) from 88% to 79%.

3.3.3.Aluminum Combustion Model

In general, individual metal particles can burn in either a vapor phase or by surface reaction,depending primarily on the physical properties of the metal and its oxide (55). Of importance in defining the reaction mode are the relative boiling points (BP's) of the metal and the oxide, viz. if the BP of the oxide is greater than the BP of the metal, vapor phase reaction between the metal and oxidant is expected, otherwise there is a heterogeneous, surface oxidation reaction. Since the BP of Al (2773^{o}K,Ref.56) is less than that of Al_2O_3 (3800K, Ref.56) we have vapor phase combustion. Other metals burning in the vapor phase according to the BP rule include Mg, Be, Na, K, Ca and Li while surface burning is predicted for B ,Si and Zr (Reference 40).

The overall combustion of Al particles appears to occur in three stages

Table 8. RESULTS OF STOICHIOMETRY CALCULATIONS FOR THE ADIABATIC REACTIONS OF ALUMINUM PLUS OXYGEN DILUTED BY HELIUM (10% Excess Al)

"x"= mols ot He "X"=mol fraction,i.e. partial pressure of reactant

"F"=moi fraction,i.e. partial pressure of products

CASE 1. P=1 atm;	x=6.77;	T_f=3800K[a]	
Reactant Gases		Products	
$X(O_2)$= 0.10		$F(Al_2O)$	=.010
X(He)= 0.90		F(He)	=.925
$X(O_2)$= 0.05[b]		$F(Al_2O_3)$	=.065
CASE 2: P=10 atm;	x=5.41;	T_f=4333K	
$X(O_2)$= 0.12		$F(Al_2O)$	=.013
X(He)= 0.88		F(He)	=.908
$X(O_2)$= 0.06[b]		$F(Al_2O_3)$	=.080
CASE 3: P=100 atm;	x=4.15;	T_f=5000K	
$X(O_2)$= 0.15		$F(Al_2O)$	=.016
X(He)= 0.85		F(He)	=.883
$X(O_2)$= 0.075[b]		$F(Al_2O_3)$	=.101

a) Flame temperature = boiling point (Reference 40)

b) Average $X(O_2)$ for overall reaction

(53). In the first stage, the particle is heated from ambient to its ignition temperature (T_{ig}), accompanied by particle melting and formation of a thin solid oxide skin. Also, as the particle heats up, the oxide skin is fractured, to expose new metal surface, due to a favorable ratio of thermal expansion coefficients for Al and its oxide (55). The second stage involves the transition from ignition to quasi-steady-state burning. Here the droplet temperature rises from T_{ig} to some steady-state value near or below the metal melting point (54). In addition, the droplet becomes surrounded by a continuous liquid oxide layer.

In the third stage, there is continuous vapor phase combustion with metal vapor evaporating and diffusing toward a relatively narrow reaction zone where oxygen is present by diffusion from the bulk gas stream. This reaction zone lies very close to the droplet surface for Al, and its temperature is appx. equal to Al_2O_3 BP (Ref.54). Vapor phase combustion rates are controlled by the metal vapor and oxygen diffusion process since diffusion is slower than evaporation, or the inherent chemical reaction rate. However, if the amount of oxygen is too low and/or heat losses to the environment are too high, the vapor phase reaction mechanism collapses with reversion to a slower surface oxidation mechanism; this is especially a problem for large, single particles (54,56).

Two important distinctions must be made. In an evaluation of experimental data and theoretical models: First, the total combustion time for a particle is the sum of the ignition and burning times; and second, the mode of particle heat-up to ignition differs in bulk flame or multi-particle combustion, compared to single-particle cases.

With the above distinctions in mind, a qualitative description of multi-particle Al combustion can be made. After combustion initiation by some external source, e.g. a pilot, hydrocarbon fuel flame, the flow of powdered Al plus O_2 and He, (adjusted for desired heat release rate and stoichiometry), are mixed in the combustor with self-propagation of the flame. In single particle ignition, slow surface oxidation supplies the requisite thermal energy (51). On the other hand, in bulk flame combustion, incoming particles are heated to T_{ig} largely by radiation from the main flame. As the particles heat up they undergo the vapor changes associated with the three stages conceptual reaction described above. The following sections quantify the important aspects of the present descriptive model by dealing with total combustion time as the sum of ignition and burning times.

3.3.4. Calculation of Aluminum Particle Combustion Times.

As previously noted, the time required to completely burn an Al particle is equal to the heatup time of the particle to T_{ig} and the time to burn the particle. This approach assumes that the transition time from actual ignition to steady-state burning is negligible.

3.3.4.1. Ignition Time

Ignition temperatures T_{ig} for metal particles are dependent on the relative physical properties of the metal and its oxide (55) but in the case of Al its T_{ig} is near to the melting point (933K, Ref.56). The onset of ignition is associated with the breakdown of oxide skins and sufficiently vigorous reactions to promote a progressive temperature rise (55). Experimentally determined values of T_{ig} for Al particles have been reported: viz. 918°K (56), and 1000°K (51). In the latter study, which was for single-particles, it was also found that T_{ig} depends somewhat on particle size and oxygen content in the ambient gas.

Since conduction is relatively fast for small particles, they are assumed to be heated iso-thermally. Thus, the calculations of heat-up to ignition time, (t_{ig}),assumes that the heat requirement,(H),is the amount needed to raise a solid spherical Al particle of some given diameter,(d_o) from ambient temperature (298°K) to T_{ig} (assumed to be 1000K,from Reference 51):.

$$H = (\pi d_o^3/6)*(\rho)*[c(T_{ig}-T_o) + \Delta H_{fus}] \qquad (3\text{-}6)$$

where H = required particle ignition heat in kcal,or (Btu); d_o = original particle diameter in micrometers,or (ft); ρ = density of Al in g/cm^3, or (lb/ft^3); c = specific heat in kcal/g-K, or (Btu/lb-F); T_{ig} = ignition temperature in °K,(°F); T_o= ambient temperature; and ΔH_{fus} = latent heat of fusion in kcal/g, or (Btu/lb).

Since the specific heat (c) is fairly constant for solid and liquid Al (0.25 and 0.26 Btu/lb/F respectively, (57)), no distinction between phases is made in equation (3-6).

The radiative heating rate,(q_r),of the particle is given by:

$$q_r=(\pi d_o^2)*\bar{\varepsilon}*\sigma* k*(T_f^4 - T_s^4) \qquad (3\text{-}7)$$

where q_r= radiant heat to particle in kcal/millisec.,or (Btu/m.s.); $\bar{\varepsilon}$ = average emissivity of the particle surface; σ = Stefan-Boltzman constant; T_f = bulk flame temperature in ^oK, or (^oR); T_s= average particle surface temperature = (1000 + 298)/2,^oK; and k= 2.78 x 10-7 , a factor to convert hours to milliseconds. The values of the various parameters used in equations (3-6) and (3-7) are given in Table 10.

Applying Equations (3-6) and (3-7) to various initial conditions, one obtains ignition times (t_{ig}) from equation (3-8)

$$t_{ig}= H/q_r \ ; \qquad (3\text{-}8)$$

Results are shown in Table 9

TABLE 9. RESULTS OF IGNITION TIME CALCULATIONS BASED ON RADIATIVE HEATING OF PARTICLES BY BULK FLAME

PRESSURE atm	T_f ^oR	d_o[a] microns	H BTU	q_r BTU/m.s.	t_{ig} m.sec.
1	6841	10	$1.51*10^{-9}$	$1.77*10^{-9}$	0.85
1	6841	50	$1.90*10^{-7}$	$4.42*10^{-8}$	4.3
1	6841	100	$1.52*10^{-6}$	$1.77*10^{-7}$	8.5
10	7800	10	$1.51*10^{-9}$	$2.99*10^{-9}$	0.51
10	7800	50	$1.90*10^{-7}$	$7.48*10^{-8}$	2.6
10	7800	100	$1.52*10^{-6}$	$2.19*10^{-7}$	5.1
100	9001	10	$1.52*10^{-9}$	$5.3*10^{-9}$	0.29
100	9001	50	$1.90*10^{-7}$	$1.32*10^{-7}$	1.5
100	9001	100	$1.52*10^{-6}$	$5.30*10^{-7}$	29.

a) 1 micron = 3.29 x 10^{-6} ft b) General formula (for T_{ig} constant) ; $t_{ig}=(1.88*10^{14})*d_o/[T_f^4 - 1161^4]$;where d_o in microns,T_f in ^oR.

TABLE 10. PARAMETER VALUES USED IN CALCULATIONS OF REQUIRED HEAT AND HEATING RATE OF ALUMINUM PARTICLES

PARAMETER	VALUES	COMMENT
d_o	10,50,100 microns	---
ρ-density	167 lb/ft^3, (Ref.57)	---
c-specific heat	0.25 BTU/lb-^{o}F,(Ref 57)	Fairly constant for solid-liquid Al
T_{ig}-ignition temperature	1000^o,(1341^{o}F),(Ref.51)	----
T_o-ambient Temp.	298^{o}K	----
$\bar{\epsilon}$-particle emissivity	0.5,(Ref.57,60)	Est.value for solid Al_2O_3 skin on Al particle at T_s=700^{o}F
T_f-bulk flame temperature	3800^{o}K @ 1atm; 4333^{o}K @ 10 atm; 5000^{o}K @ 100 atm.(Ref.40)	Flame temp.assumed equal to pressure dependent BP of Al_2O_3
T_s-Ave.particle surface temp.at heatup	700^{o}F	Ave.of T_{ig},1000^{o}K & T_o-300^{o}K
ΔH_{fus}-latent heat of fusion of Al	169 BTU/lb,(Ref.57)	

The calculated ignition times on Table 9 indicate that ignition times decrease with decreasing particle size and increasing pressure. The results at 1 atm are in general agreement with measured values of 1-3 ms for multi-particle systems, viz. powdered metal torches (53) and may therefore be taken as validating the radiative particle heating model.

3.3.5. Burning Time

Once the Al particles ignite, they enter the region of quasi-steady-state, vapor phase combustion described previously. Here, particle burnout time depends on particle size, mole fraction of oxygen in the unreacted, ambient gas, and total pressure (54,55). Although an empirical correlation (55) found measured burning time proportional to the 1.8 power of the particle diameter, theoretical and other experimental considerations of diffusion controlled processes indicated a diameter-square dependence (54,55). The correlation of Reference 55 showed that burning time was also dependent on oxygen mole fraction, as $X_{O2}^{-0.9}$. This is in qualitative agreement with dependences given in Reference 54. Finally, Reference 58 gives detailed modeling of the Al particle burning time (with H_2O) and shows a dramatic drop in burning time as pressure increases from 1 to 20 atm followed by a small rise up to 100 atm. The results agreed with experiments. Theoretical evaluation of this pressure dependence of burning time ascribed the effects to changes in mean-free-path for reactants diffusing to the reaction zone.

Although Reference 55 provides an empirical formula which allows calculation of Al particle burning times at 1 atm, it is believed that results obtained from this source would not be suitable for the present analysis. The reason for this is that the data employed in the formulation are from combustion of composite fuels, where Al particles are embedded in a hydrocarbon matrix. Also the possibility exists that the measured burning times are not completely free of heat-up or ignition time effects.

For the present application, the most useful experimental data for Al + O_2 burning times are found in Reference 59. Here, single Al particles (300-450 microns in diameter) were reacted at 1 atm in 20% O_2/80% Argon mixtures, and in air. Since the particles were heated to ignition temperature by a Xenon flash discharge, the measured burning times are most probable not affected by the heat-up period. Fitting burning time data from Reference 59 to a diameter-square equation resulted in excellent linearity with the line passing through the origin as required. Folding in the other operational dependences discussed above we have:

For pressures, P, of 1 to 20 atm

$$t_{burn} = (1.0284 - 0.0284*P)*(6.6*10^{-4}*d_o^{\,2})*(X_{O2})^{-.9} \qquad (3\text{-}9a)$$

and for P of 20 to 100atm

$$t_{burn} = (0.44 + .001*P)*(6.5*10^{-4}*d_o^{\,2})*(X_{O2})^{-.9} \qquad (3\text{-}9b)$$

where t_{burn} is the burning time in m.sec.; P, is the pressure in atm, d_o = particle diameter in microns; and X_{O2} is the mole fraction of oxygen in unreacted gas stream.

It should be noted that since the burning time data from Reference 59 are based on single-particle tests, it is necessary to ascertain whether they were carried out in sufficient oxygen to off-set radiative losses to the environment. From Reference 54, the "minimum" oxygen mole fraction (X_{O2}) is estimated to be 0.26 to 0.33 for 300 to 450 micron Al particles. Since the tests in Ref.59 were carried out at X_{O2} = 0.2, the measured burning rates may be somewhat longer than those of a multi-particle system but are considered adequate for a conservative estimate.

The results of burning times, using Equations 3-9, are shown in Table 11.

TABLE 11. CALCULATED ALUMINUM PARTICLE BURNING TIMES AS A FUNCTION OF OPERATING CONDITIONS.

PRESSURE atm	d_o microns	X_o^{2},[a] -	BURNING TIME milliseconds
1	10	0.05	0.98, {6.1},[b]; {0.26},[c]
1	50	0.05	25.0, {102.},[b]
1	100	0.05	98.0, {342},[b]; {26.},[c]
10	10	0.06	0.62
10	50	0.06	16.0
10	100	0.06	62.0
100	10	0.075	0.37, {0.14},[c]
100	50	0.075	9.2
100	100	0.075	37.0, {14.},[c]

a) Since $X_{O2} \rightarrow 0$, during combustion, an average value from Table 8 is used

b) Measured, as per the empirical correlation in Reference 55.

g) Calculated for Al + H_2O in Reference 58.

Calculated values of burning time in Table 11 suggest that overall combustion times of 2-3 ms are possible only with small particles (<10u) at pressures up to 100 atm. In order to achieve the desired temperature and product state in the first combustor stage, one finds that the required level of O_2 is quite low. Therefore, this results in longer burning times,for a given particle size, than would be measured in single-particle or propellant testing,where significant excess oxygen is present.

For comparison the burning times calculated from empirical fit to Al-Hydrocarbon composite fuel combustion (55) at 1 atm are significantly higher than those calculated from equations 3-9. This supports our conclusion that those results (55) were not applicable to pure metal combustion. Calculated (58) burning times for Al + H_2O are 3-4 times smaller than those calculated for Al + O_2 from equations 3-9. The reason for the discrepancy is not clear; it may be due to the different oxidizers or be an artifact of the model used in the Al + H_2O case, or it could reflect the effects of heat losses on the single-particle tests,upon which equations 3-9 is based. In any case, it appears that the burning times calculated in the present analysis are reasonable and, indeed, may be upper limits to actual burning times.

3.3.6.Total Combustion Time.

The total combustion time for Al particles has been defined as the sum of ignition and burning times i.e.

$$t_{comb} = t_{ig} + t_{burn} \qquad (3\text{-}10)$$

By combining the results on Tables 9 and 11, the total combustion times thus determined are obtained. They are given in Table 12.

As can be seen from Table 12, minimum combustion times occurs with small particles, and at elevated pressures. In addition, burning time appears to contribute to the overall combustion time more than heat-up or ignition time, especially for large particles.

TABLE 12. TOTAL COMBUSTION TIME OF ALUMINUM PARTICLES AS A FUNCTION OF OPERATING CONDITIONS

PRESSURE atm	d_o microns	TOTAL COMBUSTION TIME, EQ.3-10 milliseconds
1	10	1.8, (47/53)
1	50	29, (15/85)
1	100	107, (8/92)
10	10	1.1, (46/54)
10	50	18., (14/86)
10	100	67., (8/92)
100	10	0.7, (41/59)
100	50	11., (14/86)
100	100	40., (7/93)

a) Numbers in parentheses are percent of total combustion time due to ignition and burning, respectively.

3.3.7. Products of Combustion.

Of interest in the present analysis is the composition of the combustor product stream as well as the size distribution [and vapor pressure] of the liquid Al_2O_3. The product mole fractions have already been given in Table 8 with 90% He and <10% Al_2O_3. In the reaction zone itself droplets of Al_2O_3 initially form in the 0.05 - 0.5 micron range (58). With Al combustion in air, a bimodal distribution of liquid Al_2O_3 arises with <2u droplets, or "smoke", forming in the reaction zone, and 5 to 50 microns agglomerates appearing as residue or "lobes" on the metal droplet surface (55). However, if the oxidizing gas contains a true inert such as Ar (or He) there is no product accumulation on the burning metal droplet (59) and only the smaller Al_2O_3 droplets are expected. This would be the case in the present analysis. If so, particle capture of the products of combustion will be more difficult inside the first and second combustion stages (Fig.21), and it may be necessary to add an inert particle agglomeration stream, such as a refractory oxide, e.g. ZrO_2, to capture the oxide combustion products in the combustor.

3.4. Analytical Model for the Non-Equilibrium MHD Generator.

In this Section, the description and assumptions used in modeling the generator performance will be given. The point of view taken was to base the performance as much as possible on actual experimental data. The objective of the analysis was to match a range of metal fuel combustor output conditions to a wide range of generator operating conditions.

The rigorous analytical solution of the performance of this generator is complex since it requires the simultaneous solution of the electron and gas conservation equations, Ohm s law for the generator, and the computation of the electron and gas kinetic properties. Due to the strong Hall effect in MHD generators, especially with noble gas working fluids, the conductivity is a tensor quantity.

For our present high power application, we found that the linear MHD generator connected in the Faraday mode, is preferred because the Hall parameter (β) is generally low, and the use of helium results in very high transverse Faraday, output voltage which is sufficient to self-excite the magnet. We arbitrarily placed a maximum value 4 for the Hall parameter in the present analysis

3.4.1. Ohm's Law for the Linear, Segmented Electrode, Faraday Generator:

Fig.22 shows a generator schematic, whose current and voltages are given by (27)

$$j_y = \sigma_{eff}[E_y - U_x B_z] \qquad (3\text{-}11)$$

$$E_x = \beta_{eff}[E_y - U_x B_z] \qquad (3\text{-}12)$$

where, j_y is the transverse, Faraday current in A/m^2, E_y is the sum of the transverse Faraday electric field due to the external load and due to the anode and cathode electrode voltage losses in V/m. [Based on experimental experience, this loss has been assumed at 50-200 Volts (10)]. U_x is the local gas velocity in m/s, B_z is the transverse magnetic field in Tesla, and E_x is the axial Hall field due to the Hall effect, which is a function of the effective Hall parameter, β_{eff}. Similarly, σ_{eff} is the effective electrical conductivity of the plasma, which is lower than the scalar electrical conductivity due to plasma non-uniformities and due to the effect of finite electrode width. The latter phenomena causes a crowding of the current flow lines into

the edges of the electrodes which have a finite width in the axial direction. This effect occurs in all Faraday generators, but it is more pronounced in non-equilibrium devices due to their operation at higher Hall parameters. The reduction in the scalar values of . and . due to finite electrodes is given by (41)

$$\sigma_{eff};\ \beta_{eff} = \sigma;\ \beta\ /[1+p*(\beta-0.4)] \qquad (3\text{-}13)$$

where p is the electrode segmentation ratio, which equals the sum of the axial electrode and insulator widths divided by the anode to cathode separation. For β of 4, the maximum value used in our analysis, and p of 0.1 ,the finite segmentation effect reduces σ and β by 40%. Even for β of 10, the reduction is only 49%. For most of the present calculations, β was less than one in the first half of the channel, and the finite segmentation effect was small. This allows the use of a coarser segmentation ratio, than the p=0.1 assumed, which considerably reduces the number of load circuits.

3.4.2.Plasma Non-Uniformities: The non-equilibrium MHD generator is subject to two types of plasma non-uniformities that can sharply reduce σ and β . One type is due to instabilities *in the bulk of the plasma* resulting from the coupling of the electron heating and ionization equations with the current flow. This "plasma turbulence" effect decreases σ and β to an assymptotic value dependent on a "plasma turbulence parameter",PTP, which varies from 0 to 1. In experimental generators (e.g.10), we found that a value of PTP in the range from 0.5 to 1 provided good correlation with the data. For large Hall parameters, the σ_{eff} and β_{eff} are given by

$$\sigma_{eff} = 2*\sigma/\beta \qquad \text{and} \quad 1<\beta_{eff}<2. \qquad (3\text{-}14\text{-a,b})$$

For our application, where as noted β is at most 4 at the exit of the generator, σ and β are each is reduced by about 50%. However, for β of 10, which is representative of conditions in generators operating at 2000°K stagnation temperatures with argon, seeded with less than 1% cesium or potassium, the effective conductivity is reduced by a factor of 5.

The second type of plasma non-uniformity is a sub-set of the first type. It results from current concentrations at the electrodes due to the finite electrode segments (27). This concentration enhances the non-equilibrium conductivity at the electrodes. Depending on the wall temperature and the scale of the

axial inter-electrode separation, the enhanced conductivity can be transported in the downstream direction to the point where a high conductivity layer forms along the entire electrode wall. This layer internally short circuits the generator, and for all practical purposes results in negligible output.The experimental evidence on the existence of this effect is in our opinion inconclusive because those generator that exhibited this effect (e.g.42) also had other design or operating characteristics, such as very narrow inter electrode spacing, poor pressure recovery in the diffuser, and possibly conducting wall layers due to cesium deposition on the channel wall, all of which can severely degrade the generator performance in small channels.

To avoid the effect of both plasma non-uniformity problems in the present analysis, we assumed that the generator would operate under conditions of complete ionization of the cesium seed. Both theoretical and experimental evidence strongly supports the hypothesis that under these conditions, almost full Hall voltage recovery is achieved in the generator.Figure 23 (Ref.43), shows experimental results in a MHD generator at full ionization of the seed. At this condition, nearly complete Hall voltage recovery is measured,which indicates that the instabilities have been suppressed.

At the start of the analysis , we had planned to focus on "traditional" non-equilibrium generator operation, namely stagnation temperatures in the 2000-2500^{o}K range, where strong non-equilibrium effects, (which in turn implies high Hall parameters), are required. The computer code was written to seek solutions for the generator performance equations that would result in full ionization of the seed. However, as the study progressed, it became clear that much better combustor-generator performances would result by operating at very high stagnation pressures and stagnation temperatures in the 3000-4000^{o} range, and higher. Under these conditions, the importance of non-equilibrium plasma phenomena decreases, and the Hall parameter also decreases to average values between 1 and 2. Therefore,many of the cases were analyzed at conditions of partial ionization of the seed, where the higher cesium concentration results in higher scalar conductivities, and higher power output. There was insufficient time to revise the code to allow selection of optimum cesium seed concentration.

3.4.3.Wall Heat Transfer and Friction Losses: Two methods have been used to treat these wall losses. The first, and preferred method is to solve the inviscid core flow simultaneously with the boundary layer equations, using the

flat plate assumption (38). The wall heat transfer and friction losses are confined within the boundary layer displacement thickness, and the axial variation of the channel cross-section is obtained by adding or subtracting the displacement thickness to the core flow cross-sectional area.

The other method is to use a complete one-dimensional formulation of the gas dynamic conservation equations along the lines suggested by Shapiro (45). In this method a friction term is added to the momentum equation and a wall heat transfer term is added to the energy equation. The wall friction loss results in a stagnation pressure loss. The latter set of equations for the linear MHD generator are given by Rosa (27). For the present power application, the wall friction pressure loss is of minor importance, since it can be compensated by increasing the initial gas storage pressure to offset this pressure loss.

In the present analysis, we used a simplified approach based on the first method. We included the boundary layer friction effect only insofar as to specify the maximum allowable flow deceleration between the entrance and exit of the generator, which was taken as 22% (38). The wall heat transfer loss was calculated separately after obtaining the inviscid core flow solution, and it was used to determine the design requirements for the MHD channel wall. The heat loss was at most 10% of the thermal input to the generator. This loss can also be compensated by a slight increase in the stagnation temperature. Therefore, the results presented are optimistic to the extend that the stagnation temperatures and pressures must be increased slightly to compensate for wall friction and heat transfer losses.

3.4.4. Molecular Contaminants: The non-equilibrium electron heating equation, (Equation 2.5) has a term δ in the denominator which accounts for the loss of electron energy due to inelastic collisions with molecules. Non-equilibrium ionization can be readily maintained with (32) with molecular contaminant levels below 0.01 to 1%,with the lower limit applying to triatomic molecules, and the higher level applying to diatomic molecules. In our metal fuel combustor concept, we plan to burn with excess metal fuel to "getter" all oxygen in the combustor. The primary product of metal fuel combustion is a solid or liquid metal oxide particle, and there is no evidence that a small amount of these particles passing through the generator will have any significant effect on the electron concentration. There is a small concentration of gaseous metal oxide species (about 1% of Al_2O),which is a gas at the combustor stagnation

temperatures of present interest. However, it is anticipated that this low concentration will be further reduced by condensation as the gas cools in the nozzle and generator.

3.4.5. Generator Model Used: The complete solution of all the core flow equations described above, even under the assumption of suppression of plasma turbulence, involves a lengthy computer analysis. However, Dellinger (44) discovered a relatively simple method for analyzing the core flow MHD generator. For the non-equilibrium generator, it leads to a major simplification. He showed that by manipulating the conservation equations, the current density , j_y, could be related to a conductivity term, a magnetic field dependent term, an area, and a velocity dependent term, as follows:

$$\left[\frac{1}{\sigma\rho^2 u}\left(\frac{\partial\rho}{\partial h}\right)_p\right] j_y^2 + \left[\frac{B}{\rho a^2}\right] j_y + \left[\frac{1}{A}\frac{dA}{dx} + \frac{(1-M^2)}{u}\frac{du}{dx}\right] = 0 \qquad (3\text{-}15)$$

where a= speed of sound; A=channel cross-section; h=enthalpy; M=Mach #; u= axial velocity; x= axial distance; ρ=gas density; σ=conductivity.

Dellinger found that in a non-equilibrium plasma and at moderate current density, the first term can be neglected, and j_y can be expressed as

$$j_y = \frac{-\rho a^2}{B}\left[\frac{1}{A}\frac{dA}{dx} + \frac{(1-M^2)}{u}\frac{du}{dx}\right] \qquad (3\text{-}16)$$

For the Faraday generator, the power density of the generator is given by

$$j_y * E_y = j_y^2/\sigma + j_y * u * B \qquad (3\text{-}17)$$

For $K = E_y/uB > 0.8$, the quadratic term can be neglected, and equation 3-17 substituted into 3-16. The resulting equation shows that high power output from the generator requires rapid area change, steep velocity gradient; high speed of sound; and high velocity, (Mach #). In the pulsed power generator one is not concerned with a high isentropic generator efficiency, and thus K will be selected at a value of 0.5, or slightly less, to further increase the power density. In this case, the quadratic term in 3-17 cannot be neglected and one must use equation 3-16 to solve for the generator performance.

To use equation 3-16, one must specify the inlet stagnation pressure and temperature, the inlet static pressure, temperature, the generator pressure

ratio, the load factor,K, and the exit Mach number. In this case, the area and velocity ratios are also fixed, and one must manipulate polynomial expressions for the area and velocity profiles to obtain optimum generator performance. However, Dellinger found that a more efficient generator could be obtained if an exponential form of the area and velocity ratio are specified.Specifically, for a channel of length,L,

$$[1/A]*[dA/dx]= \text{Constant, or} \qquad A/A_o=\exp[B(x/L)] \qquad \langle 3\text{-}18\rangle$$

where $B=\ln(A_r)$, and A_r is the overall area ratio of the generator. Similarly,

$$u/u_o = \exp[\ln(u_r)*(x/L)] \qquad \langle 3\text{-}19\rangle$$

where u_r is the overall velocity ratio.

Based on theory and experiments in high power,supersonic,combustion generators {38}, it was determined that u_r cannot be less than 0.78 without flow separation. In a non-equilibrium supersonic generator {10}, we found that u_r could be as low as 0.70 without producing observable flow separation. However, for the present analysis,we used a value of 0.78. Based on these same non-equilibrium MHD generator experiments {10}, and prior experiments, and considering the discussion of Section 3.1, we used a range of A_r between 3 and 6 in our analysis. Also, the inter electrode width was maintained at 1.5 times the channel height in the field direction,similar to the value used in the shock tube channel in Ref.10.

Since at the channel inlet the conductivity is very low, one must specify a very low value of K {typically 0.05 to 0.1} to ignite the plasma and achieve non-equilibrium ionization. Once all the terms on the L.H.S. of equation 3-16 have been specified at x=0 {the channel inlet},one obtains j_y. j_y is then substituted into a combined electron energy and electron continuity equation to find the electron temperature and electrical conductivity of the plasma at x=0.

Using a stepwise axial integration one solves for the change in plasma properties,using the gas continuity and energy equations to obtain the input quantities for the next interval,for substitution into equation 3-16, etc.

3.5.Non-Equilibrium MHD Generator Results;

The above procedure was used to obtain the performance of a series of generators,using argon or helium, seeded with cesium . Initial Mach numbers of 0.5, 0.8,1.5,2,2.5. and 3.5 were specified. A stagnation temperature range of 2000-4000°K, and stagnation pressures from 10 to several 100 atm. were used. In the initial series of calculations,B was kept constant over the entire generator length, with a range of values of 1 to 6 Tesla. However, to reduce potential plasma turbulence effects, it was specified that the B field should be reduced to maintain the Hall parameter below 4. It was found that in most cases B remained constant because β was less than 4 in the plasma.

It will be recalled that the objective of this analysis was to map out the expected range of performance of a non-equilibrium MHD generator,used in combination with the metal fuel fired combustor,for application as a magnet power supply to the Artec type ,explosive, pulsed MHD generator. The complete elimination of the Artec generator would result in a requirement of 7.7 MWe net power output from the noble gas MHD generator,to deliver 0.5 MJ/pulse at 10 pulses per second to a load,[i.e. (0.5 MJ/0.65)*10 pps=7.7 MW, where 0.65 is the efficiency of the pulse forming network; See Section 2.5] In addition,power is required to self excite the noble gas generator magnet. For this reason most of the cases were analyzed in the 10-20 MWe gross output range. In addition, to exhibit the performance potential of the noble gas generator,we ran a number of cases up to the 100's MWe gross output levels. Finally, with our own resources,we ran cases up to the 30,000 MWe gross output level.These cases are not included in this Report, but are available from Coal Tech on request.

3.5.1. Summary of the Results and Comparison with Combustion MHD & Fossil Fuel,Heat Exchanger- Noble Gas MHD: Table 13 shows an overview of the type of performance attainable with the metal fuel fired, noble gas MHD generator for a range of power output levels. Also shown are the power requirements for heat sink magnets, and for our novel,ammonia cooled,room temperature,magnet concept. We also show for comparison,experimental and theoretical high energy fuel, combustion MHD generator results, which were discussed in Section 2.5. We also show the major advantage of applying the metal fuel combustor to the noble gas MHD generator, by comparing the present results with the performance of a non equilibrium MHD generator,using 2000°K argon,which was designed (33) to produce 15 MWe. This generator design was based on the experimental results in the 2 MWe output shock tunnel driven MHD generator of Ref.10.

TABLE 13. OVERVIEW OF THE PERFORMANCE OF PULSED MHD POWER SYSTEMS

	MHD GENERATOR										MHD MAGNET		
ASE	L. (m)	A.R.	TIME (sec)	FIELD (Tesla)	TEMP. (^{o}K)	G.P. (MW)	E.E. (%)	PD (MW/m^3)	ED (MJ/kg)	SP (kW/kg)	TEMP. (^{o}K)	WGT. (kg)	M.P. (MW)
OAL TECH CHEMICAL FUEL FIRED-NOBLE GAS MHD GENERATOR													
G-2A	.6	4	10	2	4000	**17.3**	19	**1730**	**3.9**	**9.5**	300	200	7.2
G-2B	.6	4	10	2	4000	**17.3**	19	**1730**	**3.9**	**2.9**	300	2200	2.1
M-4	.35	6	10	4	4000	**15.8**	25	**5700**	**5.2**	**5.6**	300	325	9.4
N-1	1.2	6	10	4	4000	**52.0**	33	**1375**	**7.0**	**9.2**	300	830	25.0
N23	2.4	6	10	5	4000	**226.0**	33	**1500**	**6.9**	**20.0**	300	1670	56.0
OMPARISON WITH OTHER EXPERIMENTAL PULSED MHD POWER SYSTEMS													
ef.6	1.3	2.3	5	2	4000	4.8	3	**82**	**0.2**	**0.8**	300	3000	2.4
ef.7	1.	1.6	3	4	4000	**28.8**	12	**500**	**0.6**	**0.8**	300	3500	13.8
OMPARISON WITH OTHER THEORETICAL PULSED MHD POWER SYSTEMS													
IRECT COMBUSTION HEAT SOURCE													
ef.2	1.2	**13**	1	4	4000	**4.0**	8	**186**	**1.3**	**0.4**	300	1190	3.0
Ref.29	2.3	**10**	21	4	3420	**25.0**	10	**200**	**1.0**	**6.5**	4	1030	0.0
HEAT EXCHANGER HEAT SOURCE													
ef.33	3.0	**6**	60	4	2000	**14.0**	28	**33**	**0.3**	**0.1**	77	17000	9.6

EE NOTES ON NEXT PAGE

NOTES FOR TABLE 13:

-L=MHD GENERATOR LENGTH A.R.=GENERATOR AREA EXPANSION RATIO

-TIME=CONTINUOUS ON TIME -FIELD= MAGNETIC FIELD

-TEMP.=GAS STAGNATION TEMPERATURE -G.P.=GROSS GENERATOR OUTPUT

-E.E.=GROSS GENERATOR ENTHALPY EXTRACTION=G.P./GAS HEAT INPUT

-PD= POWER DENSITY/INTERNAL GENERATOR VOLUME

-ED= ENERGY DENSITY=G.P./GAS MASS FLOW RATE

-SP= SPECIFIC POWER=[(G.P.-MAGNET POWER)/(TOTAL WEIGHT OF SYSTEM). The Ref.33 case includes the weight of the ceramic heat exchanger in total system weight.

-TEMP.=INITIAL MAGNET COIL TEMPERATURE-Coal Tech Case #G-2B,Refs. 6,7,2, and 33 use heat sink copper magnets. Other Coal Tech cases use novel cooling concept. Ref.29 case uses a superconducting magnet. Ref.33 case magnet is precooled to LN_2 temperature.

-WGT.=COPPER COIL WEIGHT-without support structure.Support structure appx. doubles this weight.

-M.P.=MAGNET POWER for specified operating time.

Details of the runs are as follows:[The magnet and system weight results will be discussed in more detail in later sections of the Report]

-Case #G-2A is the base case for this Project, using the NH_3 cooled magnet. The gross MHD generator output is 17.3 MW. After subtracting the magnet power of 7.2 MW, one obtains a net output [SP in the Table] of about 9.5 kW/kg of total system weight. This is over 10 times the specific power level experimentally observed or projected for room temperature magnets using high energy hydrocarbon fuels, as shown in the cases from references 2,6, & 7 in the Table.

Similarly the power density per unit channel volume [PD] and the energy density per gas mass flow rate in the channel [ED] is 3 to over 10 times that obtained in the hydrocarbon systems. Although a superconducting magnet (Ref.29) allows the hydrocarbon based systems to approach the present system performance in terms of specific power [SP]; the power density [PD] and energy density [ED] in the former are considerably lower. The use in our Case #N-23 of a super-

conducting magnet of the size used in Ref.29 (i.e. with a 2.3 m.long generator) would result in a SP that is 4 times higher than in the Ref.29 case.

Case #G-2B shows the benefit of active NH_3 cooling in reducing magnet weight.The heat sink copper coil weight in this Case is over 10 times that of the NH_3 cooled case,yet the magnet power reduction is only a factor of 3.5.

Case #M-4 shows that doubling the magnetic field to a level of 4 Tesla which is achievable in a heat sink magnet for only 2 to 3 seconds or with active cooling, results in a very high power density for the same gross generator output as in Case G-2A. Case #M-4 is for a NH_3 cooled magnet. The higher magnet power results in a net reduction in the specific power output.

Increasing the channel dimensions to the 1.2 to 2.4 m. range used in the hydrocarbon based generators of references 2,6,7, & 29, results in a major increase in power output in our system. Cases #N-1 and N-23 use NH_3 cooled magnets, and generators the size of a long desk.The gross output is 52 and 226 MW, respectively. With the 300°K magnets, the specific power approaches 20 kW/kg. With a 6 Tesla superconducting magnet, the net power output in Case #N23 is 540 MW.

By way of comparison with prior noble gas generators, Table 13 also shows the predicted performance of an MHD generator with an argon working fluid, heated by a gas fired ceramic heat exchanger (33), as discussed in Section 2.6 (See figure 16). It was designed for high thermodynamic cycle efficiency operation not pulsed power operation. This result shows that this type of device is not suitable for high pulsed power operation. For this reason research on achieving high power densities in noble gases at that time focussed on shock tubes and explosive drivers (such as the Artec system).

In conclusion, Table 13 shows that the Chemical Fuel Fired-Noble Gas MHD Generator can achieve extremely high output power densities which are about 10 times greater than that obtainable with hydrocarbon based, high energy fuels,as the generator working fluid. The high performance is obtained with moderate magnetic field strengths and with assumptions that are based primarily on prior experimental data.

3.5.2. Variation of Parameters in the Non-Equilibrium MHD Generator:

Table 14 shows the variation of parameters in the generator for a high power density case [Case # M4] that meets the present project objectives.

TABLE 14-HIGH POWER DENSITY-CASE #M4:

P_o=103 atm., T_o=4000°K, L=35 cm., A_{in}=25 cm^2, A_i/A_o=6. [P.D.(x)= Local Power Density]; Subscripts: s-Static Gas; e-Electron Temperatures.

X	B	HALL#	P_s	T_s	T_e	U	M #	J_y	K	σ	G.P.	P.D.(x)
m	T	-	atm.	°K	°K	m/s	-	A/cm^2	-	mho/m	MW	MW/m^3
0	4	0.63	6.2	1297	3464	5243	2.5	226	.05	117	0	2744
.15	4	1.13	3.7	1480	3379	4730	2.1	117	.47	125	5.3	10373
.35	4	2.8	1.2	1189	3109	4096	2.0	37	.73	106	15.8	4490

-The static pressure, P_s, at the exit is greater than 1 atm., thus allowing operation without a long diffuser.

-The average ionization of the cesium seed was 20%. However, the average Hall parameter is only 1 so that plasma turbulence effects should be small.

-As noted, K is specified at near short circuit at the generator entrance to ignite the plasma. The specified area and velocity variation result in a nearly constant Mach number, M, along the channel length, and a gradually increasing K toward open circuit at the exit.

-J_y is based on the combined electrode-insulator area. Therefore, for equal conductor and insulator areas on the electrode walls, the current density at the first electrode is 450 A/cm^2. This value is near the theoretical value obtained from Dushman's equation (46) for thermionic emission with tungsten heated to its melting point of 3683°K, where the emission is 385 A/cm^2. Due to the high heat flux to the channel wall, a tungsten electrode thickness of about 1/8" can reach this temperature in several seconds, as will be shown in the Heat Transfer Section. Alternatively, arc conduction can produce this current density. Also, electrode emission can result from the deposition of cesium on a tungsten electrode (46). In the present case, the cesium concentration of $2.3*10^{16}$/cc is too low to produce more than 10 A/cm^2 emission at the cathode by the deposition process. However, it may be possible to impregnate the electrode with cesium to increase its emission limit. Incidentally, to utilize the cesium emission effect requires tungsten electrode temperatures in the 1400-

2000°K range.Due to the extremely high wall heat flux,{See Section 3.9.2},maintenance of this low temperature will require extensive cooling of the electrode.

-The average power density in this channel is 5700 MW/m^3, or 10 times that in the highest power combustion generator,operated to date {7}.

TABLE 15-PERFORMANCE VS AXIAL DISTANCE:BASE CASE #G2:

P_o=49 atm.,T_o=4000°K,L=60 cm.,A_{in}=75 cm,A_i/A_o=4.

X	B	HALL#	P_s	T_s	T_e	U	M #	J_y	K	σ	G.P.	P.D.(x)
m	T	-	atm.	°K	°K	m/s	-	A/cm^2	-	mho/m	MW	MW/m^3
0	2	0.62	3.0	1297	3316	5237	2.5	111	.10	120	0	1240
.30	2	1.03	2.0	1545	3246	4625	2.0	60	.46	127	5.8	2540
.60	2	1.83	1.0	1427	3086	4085	1.9	29	.65	115	17.3	1540

Table 15 shows the results for the Base Case, which was selected to be compatible with a magnetic field that is readily achieved with room temperature magnet operation. By reducing the area ratio to 4/1 from 6/1, tripling the entrance area, and doubling the channel length, one obtains basically the same performance as in Case #M4.In the present case, the current densities are cut in half, and the current is well within the limits of thermionic emission with tungsten.

All the analyses were performed for an electrode pitch of 0.1, which in this case requires about 40 electrode pairs. The low Hall parameter enables one to reduce the number of electrodes. However, due to the increase in the transverse voltage from channel entrance to exit of 120 V. to 1100 V., it is not possible to use a single electrode pair, which would be normally possible with the low Hall parameter.

Finally, the power output is about 2.3 times the level required to produce the 0.5 MJ pulses directly through a pulse forming circuit,without the explosive generator. This allows considerable flexibility in the selection of the magnet design,(as shown in Table 13),and in the selection of the pulse circuit.

3.5.2.1. Effect of Magnetic Field on Performance & Self-Excitation

TABLE 16-EFFECT OF THE MAGNETIC FIELD ON PERFORMANCE

CASES#F1,F2,F5,& M4; T_o=4000°K, L=35 cm., A_{in}=25 cm^2; A_i/A_o=6. Degree of Ionization of Cs=20%. Stagnation P_o, T_o at X=0. All other results apply to the generator exit, X=35 cm. M_i=2.5; M_e=2; K at inlet=0.05.

CASE	B T	HALL# -	P_o atm.	P_s atm.	T_e °K	U m/s	Cs/He %	J_y A/cm^2	E.E. %	σ mho/m	G.P. MW	P.D. MW/m^3
F5	1	1.72	14	.17	3085	3892	.40	21	21	224	1.7	600
F3	2	2.30	42	.50	3108	4035	.16	31	21	168	5.4	1930
F1	3	2.65	72	.90	3111	4077	.09	35	24	130	10.4	3710
M4	4	2.80	82	1.22	3109	4096	.07	37	25	106	15.8	5640

Table 16 shows the effect of magnetic field strength on performance of a channel. The stagnation pressure is adjusted to allow generator ignition at the entrance with K=0.05, i.e. nearly short circuited. This set of calculations was performed to study the methods suitable for self-exciting the generator. Unlike the combustion generator, where a high equilibrium conductivity is available at the entrance of the generator to start substantial current flow, in the present non-equilibrium MHD generator, plasma non-equilibrium must be first established. Only then can the self excitation process begin.

In all four cases, an electrode voltage loss of 100V, was subtracted from the gross power output to yield the power output values shown in the Table. Also, the calculation at the generator entrance began with K=0.05, although we could have applied an external field for the low B field case to assist the plasma ignition. The first case, F5, applies to the start of self excitation where an external battery powered applied field of 1 Tesla is provided. To assist the ignition process we provided a high cesium seed concentration, which means a low degree of ionization of the seed.

One interesting result of the calculation is the nearly identical enthalpy extraction (21%-24%) in the four cases. This result is due to the specification of a uniform rate of change of area and velocity in equation 3-16 for the four cases.

Another very interesting result is that the stagnation pressure must be decreased with decreasing B field. Therefore, the exit static pressure is significantly below 1 atm. for fields slightly greater than 3 Tesla, which means that a long supersonic-sub-sonic diffuser is required for the generator. Thus this method of self-excitation is not suitable for the present application, where a 1 atm. static exit pressure is required to eliminate the diffuser. Also, one notes that this generator operates at fields of about 3 Tesla without benefit of a supersonic diffuser. We found that we could lower the field further, and still eliminate the diffuser, by increasing the channel length and entrance area. Therefore, we selected the 60 cm. long channel (Case G2) rather than the 35 cm. long channel,for the present Base Case because it allows a high performance output above 10 MW with only a 2 Tesla field.

In combustion MHD generators the self-excitation current is drawn from the upstream electrodes in a Faraday connection (47), or from the total output voltage in diagonally connected generators (6),or from a separate generator, as in the PAMIR unit (7). For the non-equilibrium MHD generator, it occurred to us that this could be accomplished by using the downstream electrodes in the Faraday connection to power the magnet coil. In this way the higher induced voltages and lower initial pressures at the downstream end of the generator could be used to ignite the plasma. The result of such a calculation is shown in Table 17, for two cases, # N4 and # N4A. In both cases the channel length is 1.2 m. However, in the first case the first upstream electrode (@ X=0) and M=1.5, was connected to the load,i.e. K=0.1, while in the second case , the first electrode connected to a load was located at X=0.4 m, where M=2.5 and K=0.05.

TABLE 17-EFFECT OF LOCATION OF FIRST APPLICATION OF A LOAD ON THE PERFORMANCE -CASES #N4, N4A; T_o=4000°K, L=120 cm.,A_{in}=100 cm^2,A_i/A_o=6.
Degree of Ionization of Cs=90% for case N4, and 80% for Case N4A.
Stagnation P_o,T_o at X=0.All other results apply to the generator exit.
1st Load Applied at :X=0 for Case #N4; and @ X=40 cm. for Case # N4A

CASE	B	HALL#	P_o	P_s	T_e	U	Cs/He	J_y	E.E.	σ	G.P.	P.D.
	T	-	atm.	atm.	°K	m/s	%	A/cm^2	%	mho/m	MW	MW/m^3
N4	1.5	3.75	12.6	.47	3354	3282	.01	8.7	27	95	15.7	413
N4A	1.5	1.40	41.	1.2	3096	4225	.06	27	16	111	28.9	963

One notes in Table 17 that by initially igniting the generator downstream from its entrance region, one can maintain a very initial high stagnation pressure. This results in a static pressure greater than 1 atm. at the generator exit, and it eliminates the diffuser. We reach the important conclusion that self-excitation in a non-equilibrium MHD generator requires initial plasma ignition at the downstream electrodes,with a battery powered starting field in the range of 1 to 1.5 Tesla.

3.5.3.Effect of Initial Mach Number on Performance:

TABLE 18-EFFECT OF THE MACH NUMBER ON PERFORMANCE

CASES#C1, C2, & 25;T_o=4000°K,L=2.2 m.,A_{in}=200 cm^2;A_i/A_o=5.15
B= 6 Tesla,(See Text); M_i= Mach # and β_i=Hall parameter @ X=0.
Stagnation P_o,T_o at X=0.All other results are for generator exit,X=2.2 m.
Degree of Ionization of Cs=12% (Case #C1),15% (Case #25); 20% (Case #C2)
K at inlet=0.5 (Case #C1); 0.16 (Case #25); 0.24 (Case #C2).

CASE	M_i	β_i	P_o	P_s	T_e	U	Cs/He	J_y	E.E.	σ	G.P.	P.D.
	-	-	atm.	atm.	°K	m/s	%	A/cm^2	%	mho/m	MW	MW/m^3
C1	0.5	0.97	26	1.3	2704	2266	.02	5	45	29	92	750
25	1.5	1.40	89	3.9	2760	3353	.02	9	29	19	238	1930
C2	2.5	2.65	170	2.0	2764	4220	.006	6	30	14	248	2010

The three cases shown in Table 18 were selected to exhibit the effect of initial Mach number on the channel performance. The specific channel geometry chosen is somewhat smaller in size than the non-equilibrium blowdown design using a 2000°K gas fired heat exchanger (Figure 16), whose computed output with argon seeded with Cs was 15 MWe (33).

The only reason for selecting a high B field was to obtain high power output in the subsonic case # C1. In all our calculations,we specified that the axial magnetic field profile was to decrease in the downstream direction in order to maintain the Hall parameter below 4. In the Cases #25 & #C2, the peak Hall parameter of 2.75 and 3.5 respectively was reached at the exit of the channel, so that B remained at 6 Tesla.However,for the subsonic case #C1, the Hall parameter reached 4 at X=1.6, and B was decreased to 3.4 Tesla at X=2.2 to maintain the Hall parameter at 4.

The channel choked at X=2.2 m for the subsonic case, so the calculation was terminated at this point for all three cases. The key result from this calculation is that subsonic operation is of no interest in the present application. The performance is much lower than for the supersonic cases, and an extremely high magnetic field is required to obtain good performance. On the other hand in this high field case there is little benefit in very high supersonic Mach number operation. This is not the case at lower field, where Mach 2.5 provides higher output due to the lower static pressure and the higher mass flow rate in the channel.

3.5.4. Effect of Generator Length & Entrance Area on Performance:

All the calculations were performed for generator length to mean diameter ratio in the range of 4 to 10. Combustion generators have been designed and operated with L/D ratios at the upper end of this range. (e.g. Ref.2 used a value of 8). A lower range of L/D is justified in the non-equilibrium generator because the conductivity upstream and downstream of the generator is low, which reduces the power losses due to end effects.

From the above Tables one can deduce that the main effect of increasing the channel length and entrance area, for the above range of L/D, is to increase the stagnation input enthalpy. Since the area ratio and velocity decrease in the supersonic generators was specified to be in the same general range for all cases, the relative performance of the generator, as predicted by equation 3-16, was proportional to the input enthalpy. Thus the required power output of the generator can be used to specify the dimensions of the machine. For example, the present 10-20 MW output range can be attained in a 35 to 60 cm. long generator with a 25 to 50 cm^2 entrance area, and a 4 to 6 area ratio, at fields of 2 to 4 Tesla, and stagnation temperatures of 3000-4000^{o}K.

3.5.5. Effect of Stagnation Temperature on Performance:

The four Cases in Table 19 were selected to exhibit the effect of stagnation temperature on the performance of a specific size channel. One notes that as T_o is increased, the allowable stagnation pressure increases, so that the thermal input power increases. As noted previously, since the channel is designed using equation 3-16, the relative performance is very similar as long as the area ratio and velocity change remain the same.

One interesting result is that the power output increases as the square of the stagnation temperature ratio, instead of a linear relationship. This is due to the increase in conductivity with temperature, despite the fact that the electron temperature at the channel exit decreases by 1100°K for Cases V1 to N1. One notes that even at 2000°K, the performance is excellent with 26% enthalpy extraction. However, the static exit pressure is only above 1 atm at 4000°K, suggesting that for this set of conditions only this case can operate without a diffuser.

Another point to be made is that due to the placement of a limit of 4 on the Hall parameter, the magnetic field had to decrease near the exit, from the 4 Tesla value at the upstream end of the generator. In all the cases, the Hall parameter reached a limit of 4 at an axial location, which increased with distance from the channel entrance, and with increasing stagnation temperature.

<u>One concludes that the generator will operate satisfactorily in the entire temperature range. However, the upper temperature range provides greater operational flexibility</u>.

TABLE 19-EFFECT OF THE STAGNATION TEMPERATURE ON PERFORMANCE

CASES #V1,#V3,#E1,& #N1;L=1.2 m.,A_{in}=100 cm^2;A_i/A_o=6
B_i= 4 Tesla; M_i=1.5,M_e=1.33; 1.37; 1.39; 1.44 for 4 Cases, respectively.
Stagnation P_o,T_o at X=0.All other results are for generator exit,X=1.2 m.
Ionization of Cs=90% @ X=0, and 100%; 98%; 92%; 78% @ X=1.2 m. for the four cases, respectively;K=0.1 @ X=0

CASE	T_o °K	B_e T	P_o atm.	P_s atm.	T_{el} °K	U m/s	Cs/He %*10^3	J_y A/cm^2	E.E. %	σ mho/m	G.P. MW	P.D. MW/m^3
V1	2000	2.4	12	.47	4487	2327	2.2	5.3	26	22	9.7	255
V3	2500	2.6	16	.63	3880	2602	2.8	6.7	29	30	16.9	445
E1	3000	3.0	22	.84	3577	2849	3.5	8.	30	35	26.7	700
N1	4000	3.4	34	1.19	3377	3290	5.2	10	34	43	52.1	1375

NOTE:Subscript "e" applies to the channel exit,"el" to the electron temperature

3.5.6. Effect of Degree of Ionization of Cesium on Performance:

TABLE 20-EFFECT OF THE IONIZATION ON PERFORMANCE

CASES #21,#22,#23; T_o=4000°K; L=2.4 m., A_{in}=200 cm^2; A_i/A_o=6

B_i=5 Tesla; K=0.15 @ X=0

M_i=1.5, M_e=1.44; 1.43; 1.41; @ X=2.4 m. for the 3 Cases, respectively.

The location of all other results are marked as Xi for X=0, and Xe for X=2.4 m.

CASE	Ne/Cs % (Xi)	Ne/Cs % (Xe)	Cs/He % (Xe)	B T (Xe)	P_o atm. (Xi)	J_y A/cm^2 (Xi/Xe)	E.E. % (Xe)	σ mho/m (Xi/Xe)	G.P. MW (Xe)	P.D. MW/m^3 (Xe)
21	90	76	.0021	4.3	47	34/5	35	21/19	149	990
22	50	35	.0046	4.95	60	44/6	34	26/20	187	1250
23	15	10	.0177	5.0	74	54/8	33	31/22	226	1510

This Table shows several very interesting results:

Most important is the major increase in power output with decreasing degree of ionization. In other words, the penalty for suppression of plasma turbulence by using full ionization of the seed, is achieved at the cost of requiring operation of the generator at extremely low seed concentrations. In Case 21, the seed concentration is only **21 parts per million.** A similar result was obtained in almost all the cases analyzed in this study. Since the conductivity is proportional to the electron concentration in this electron concentration range, a cesium concentration of 21 ppm is too low to provide any appreciable conductivity. The electron concentration at the channel entrance is 2 times greater in Case 23 than Case 21.

Unfortunately, the computer code was written to find the cesium seed concentration at which a specified degree of ionization would be obtained. This was necessary for the full ionization cases which were of primary interest for the suppression of plasma turbulence. However, the was no time to change the computer code to find solutions for optimum performance at low degrees of ionization, after it became apparent that this would result in better performance at high stagnation temperatures, where the low Hall parameters limit the plasma turbulence losses. For example, the Cases in Table 20 show that the Hall parameter is relatively low at the high values of magnetic field (5 Tesla) used, and it decreases with increasing cesium concentration. In Case 21, the

Hall parameter increased to our limit of 4 inside the channel, and B was slightly reduced to maintain this limit. In Case 22, the limit of 4 was reached at the exit, while in #23, the peak Hall parameter was only 3.1.

Table 20 also shows that the degree of ionization,seed fraction,and conductivity are reasonably constant along the entire generator length. The current density decreases in the downstream direction because the generator is forced toward open circuit by the selected channel geometry and velocity distribution.

Also, the attainable power density increases significantly as the cesium concentration is increased and the degree of ionization is decreased. We should note that even in the low stagnation temperature,non-equilibrium MHD generator experiments (10) we always obtained significantly higher power output at high cesium concentrations,(i.e. low degrees of ionization). We had attributed (10) this primarily to improved electrode conduction. However, the present study leads us to conclude that at higher stagnation pressures,a high cesium concentrations is more important for high power than suppression of plasma turbulence .This is especially the case in helium, where a high electron scattering cross section results in a lower conductivity and Hall parameter, relative to argon.

One final point is of interest. Table 20 shows that the power output attainable with the present approach is over 15 times that projected for a larger non-equilibrium generator,with argon, at 4 Tesla, and 2000^{o}K (33).

3.5.7.Effect of Channel Area Ratio on Performance:

Calculations were performed primarily with area ratios of 1 to 6, in some cases the area ratio was 1 to 4,and finally in a few other cases it was 1 to 10. Comparison of performance as a function of area ratio is not simple to exhibit. In general,the higher area ratio results in a higher enthalpy extraction. To achieve extremely high values (in the 40% range),requires area ratios of 1 to 10. However, as noted previously in this Report, it is doubtful that the flow will remain attached to the channel wall in this case. On the other hand, there is some benefit in using a lower area ratio,(e.g 1 to 4). This results in a more uniform cross section magnet, which is more efficient and simpler to construct. It also allows pressure recovery to one atm. at lower stagnation pressure, although at the cost of lower enthalpy extraction. Based on our prior experimental experience (10), we prefer a 1 top 6 area ratio.

3.5.8. Comparison of Helium vs Argon Generator Performance:

TABLE 21-EFFECT OF GAS ON GENERATOR PERFORMANCE

-CASES #E1,#V1-(Helium),#E2,#L4-(Argon);L=1.2 m.,A_{in}=100 cm^2;A_i/A_o=6. B_i=4 Tesla; M_i=1.5; M_e=1.4 for 3000°K Cases; 1.3 for 2000°K Cases. Degree of Ionization of Cs=90% @ X=0. K at inlet=0.10. Electrode Loss=100 V. Stagnation P_o,T_o at X=0. All other results apply at generator exit,X=1.2 m.

CASE/ GAS	T_o °K	B_e T	P_o atm.	P_s atm.	T_{el} °K	U m/s	Cs/He %	J_y A/cm^2	E.E. %	σ mho/m	G.P. MW	P.D. MW/m^3
E1/He	3000	3.0	22	0.8	3577	2849	.0035	8	30	35	26.7	700
E2/Ar	3000	2.9	43	1.6	4255	902	.0109	15	24	214	13.0	340
V1/He	2000	2.4	12	0.5	4487	2327	.002	5	26	22	9.7	255
L1/Ar	2000	2.6	23	1.0	5431	367	.006	10	14	103	3.4	89

The four cases in Table 21 were selected to clearly demonstrate that despite argon's much higher conductivity, the power output in argon is much less than in helium. At 2000°K, the primary cause for the low performance in argon is the large effect of the electrode voltage loss. Using experimental data from shock tunnel driven MHD experiments {10}, an electrode loss of 100 to 200 Volts was assumed in the present analysis. For argon this reduced the enthalpy extraction in Case #L1 from 27% to the 14% value tabulated, and the gross power output from 6.3 MW to 3.4 MW. In the helium Case #V1, the corresponding values were 30% to 26%, and 11.2 MW to 9.7 MW.

The relative importance of electrode losses decreases with increasing T_o, B and channel size. Nevertheless for the channels under present consideration, i.e. 0.35 m > L > 1.2 m, the electrode loss effect is substantial in argon. In the argon Case #E2, it reduces E.E from 34% to the 24% , and the power from 18 MW to the 13 MW shown in Table 21. For helium, the values are 33% to 30% and 29 MW to 27 MW.

ALthough the argon results show static exit pressures above 1 atm, while the helium results are less than 1 atm.,we have already shown previously that the helium generator performance can be adjusted to obtain a static exit pressure above 1 atm.

The present results clearly show that in a high performance generator, helium is the superior working fluid. Since most prior multi-second non- equilibrium MHD generator experiments have been performed in facilities with at most several MW thermal input and at temperatures of 2000°K, the advantage of using helium was not readily apparent. In fact even by ignoring electrode losses, the present analysis shows that the power and enthalpy extraction obtained with helium is 50% higher than in argon.

3.5.9. General Conclusion on the Performance of the Non-Equilibrium Generator

The MHD results selected were designed to show the operating range accessible with the use of the novel metal fuel combustor. Using helium seeded with cesium, it is possible to exceed the prior projected performance levels in non-equilibrium noble gas generators, by over a factor of 10; and in high performance combustion generators, by a factor of 5 to 10. The present analysis was of limited scope, and we have not fully explored the potential of the generator.

Based on the results to date, a 35 to 60 cm long generator operating at 2 to 4 Tesla and 3000-4000°K, and using helium seeded with cesium, will produce power outputs of the order of 10 MW. Higher temperatures can be used to reduce the magnetic field strength.

By staying well within the size range of prior experimental generators, the present concept can produce power output levels in the 100's and 1000's of MW. In fact about 30,000 MW was obtained in a calculation performed outside the scope of this project, in a channel of a size equal to that of the largest combustion generators operated to date.

3.6. The Magnet for the MHD Generator

Two problems related to magnet use in MHD generators were investigated in this project. One of these is the analysis of the self excited magnet coil for the cw non-equilibrium MHD generator discussed in Section 3.5. The other was the analysis of the magnet suitable for the explosive Artec type MHD generator, powered by the net output of the cw MHD generator. As part of this effort,we applied our recent discovery of a novel method for cooling room temperature magnets which potentially could reduce the magnet weight by a factor of 10 below that of heat sink magnets.

3.6.1. Self Excited Magnet for cw MHD Generator

It was noted in the review of the self excited cw combustion MHD generators that the weight of the room temperature heat sink magnets used in these generators represented about 50 to 75% of the total system weight. In the present application of 10 second total operation, the component's weight is much greater than the consumable's weight. Therefore, there is considerable incentive to reduce the weight of the magnet. One way of accomplishing this is to use a cryogenic,actively cooled,or a heat sink magnet. Table 13 summarizes the magnet weights for several of the combustion MHD systems, including a 25 MW MHD generator powered by a superconducting magnet (29). One notes that the total weight of this SC magnet is 1030 KG. This is less than 1/3 the weight of the coils only,in the 300^{o}K heat sink magnet used in the 28 MW PAMIR self-excited,combustion generator (7).

The long term storage requirement in the present application eliminated the consideration of cryogenics. We therefore considered active cooling and heat sink operation of a 300^{o}K magnet.

3.6.1.1. Heat Sink Magnet: The analysis of heat sink magnet operation is relatively straightforward. One determines the maximum allowable change in conductor resistance during the total operating time,(i.e. 10 sec.). This change is given by $R=R_{o}*(1 + A*T)$, where "A" is the resistance-temperature coefficient. Surprisingly, there is a considerable divergence in the literature on the value of "A", probably due to the variation in the copper properties. We used a value of "A" @ 20^{o}C, of 0.0068/^{o}C for Cu,and 0.0043/^{o}C for Al (48). Since the allowable coil resistance change is usually taken to be 10%, it limits the temperature change to only 14.7^{o}C in Cu,and 23.2^{o}C in Al.

From the allowable resistance change,the maximum allowable current density in the magnet is obtained,by balancing the ohmic dissipation with the heating of the copper. Figure 24 from ref.4, plots the allowable current density in a wire as a function of pulse length and allowable resistance change, with an coil temperature of 77°K. The authors state that these curves also approximately apply to room temperature conditions. We computed that the stated current of $2*10^7$ A/m^2 for a 10% resistance change and 10 sec. on-time, will result in a 20°C temperature increase at 300°K, vs the 14.7°C allowed for a 10% resistance change.This means that the allowable current density must be reduced by 16%.

For the magnet analysis,we used Case G-2 as the Base Case. Its 17.2 MW output (Table 15) was representative of the upper end of the range of required power output for the self excited cw MHD generator for the present application,namely, producing 0.5 MJ pulses for 10 sec., through the use of an Artec type explosive MHD generator,or a pulse forming network. For simplicity, we assumed that the magnet was a saddle coil of square cross-section equal to the mean diameter of the outer generator wall in the plane perpendicular to the magnetic field vector. This resulted in an internal coil volume of $0.23*0.23*0.87$ m^3, where 0.87 m is the axial coil length between the two "saddles" of the magnet. This is length is usually specified as 20% longer than the axial electrode length in the generator (0.6 m for Case G-2),to assure field uniformity. We selected a value 45% longer than this in order to match the tabulated values for the minimum volume saddle coil magnets, as given in Ref.13,Table 2.1. The magnet coil height in the B field direction was selected at twice the outer channel diameter to assure a uniform field inside the channel cross-section.

Using the current density of $2*10^7$ A/m^2 for the heat sink case, a conductor packing factor of 0.9, and a 2 Tesla field, we estimated the copper coil weight for Case G-2 as 2200 kg. This number should be doubled to account for the structural elements in the coil. As will be shown in the next Section, the magnet weighs **six** times the weight of the rest of the cw MHD system. For this case, substitution of aluminum does not significantly reduce the coil weights because 2 Tesla is about the limit for efficient field generation with a heat sink copper coil. Thus the use of the higher resistance aluminum results in such a large coil cross-section that inefficient use is made of the conductor. It is thus clear that active cooling is essential if significant weight reductions are to be achieved, even for operating times of only 10 sec.

3.6.1.2. NH_3 Cooled Room Temperature Magnet: The only way to sharply decrease the magnet weight is to increase the current density, which occurs at the expense of increased power consumption in the magnet. Due to the extremely high power output density of the present generator, this magnet power vs weight tradeoff is very attractive. Weight reduction is almost inversely proportional to the current density in the coil, or equivalently to the power consumed in the coil. Thus from a system point of view one must consider the effect of increasing the weight of the power supply to the magnet vs the weight reduction in the coil. As will be shown ,with ammonia cooling of the magnet and the metal fuel MHD generator, this tradeoff favors magnet cooling.

Based on our review of literature on cryogenic pulsed coils (e.g. 4),it was clear that to benefit from magnet cooling ,boiling heat transfer must be used. The reason for this is that in nucleate boiling the heat transfer from a surface is proportional to the latent heat of vaporization, which allows a much higher heat transfer rate than conventional convective cooling with a liquid. It is stated in ref.4, that cryogenic conductors can be cooled at the rate of 10 w/cm^2. To correlate this to a room temperature coil we used an empirical correlation for the peak nucleate heat transfer rate, given by (49)

$$q/a = 143*(\rho_v * h_{fg})*[(\rho_l - \rho_v)/\rho_v] \qquad (3\text{-}20)$$

where q/a is the peak boiling heat flux, $BTU/hr\text{-}ft^2$; the subscript applies to the liquid and vapor state of the coolant of density ρ in lb/ft^3. h_{fg} is the latent heat of vaporization. Equation 3-20 shows the benefit of a high h_{fg} fluid. Of the room temperature refrigerants only ammonia has a very high h_{fg}. At 68^oF and saturated conditions, i.e. 124.3 psi,its value is 510.5 BTU/lb, which is one half that of water. By contrast Freon 12 has a value of only 62.2 BTU/lb at 68^oF and 82 psi. Water of course is unsuitable because of its very low vapor pressure at R.T. Liquid nitrogen also has a low h_{fg} of 85.4 BTU/lb at 1 atm. and -320^oF, decreasing to zero at the critical point of 500 psi and -233^oF.

Substituting saturated liquids of NH_3 and N_2 at 124.3 psi and 14.7 psi into equation 3-21, one finds a peak heat flux of 457,000 $BTU/hr\text{-}ft^2$,(144 W/cm^2),and 76,500 $BTU/hr\text{-}ft^2$,(24 W/cm^2), for the two fluids, respectively. The allowable 10 W/cm^2 cooling rate given in ref.4 for LN_2 is equal to 40% of the value obtained from equation 3-20. Applying the ratio of peak heat

flux from equation 3-20 for NH_3/LN_2 to the allowable cooling rate, one finds that if this rate is 10 W/cm^2 in LN_2, then it should be 60 W/cm^2 in NH_3. We used the latter value as a limit in the analysis of a NH_3 cooled magnet.

To apply this result to coil design, one selects a time period for a 10% increase in the conductor resistance. One validates that this time is longer than the risetime to the peak current in the self excited magnet coil. As we will discuss below, the L/R risetime of the coil for the present case is less than 0.1 seconds. We therefore selected arbitrarily a 0.5 sec. time period for the 10% resistance increase. By balancing the ohmic dissipation with the heating of the conductor, one obtains the allowable peak current. This is then used to obtain the minimum conductor cross section that can be cooled with the assumed 60 W/cm^2 cooling rate. Using the 50% conductor void fraction that is used in cryogenic pulsed coils {4}, we computed that the peak current allowed in Cu was $1.26*10^8$ A/m^2 {or 6.3 times the value in a heat sink magnet}. In Al, the peak current was $8*10^7$ A/m^2. By contrast, the peak allowable current in a LN_2 cooled magnet is only $4*10^7$ A/m^2. Thus if the magnet power can be efficiently supplied with a lightweight power supply, a NH_3 cooled 300°K magnet could be lighter than a LN_2 cooled magnet. This is a very unexpected and surprising result. The above analysis is by no means optimized, since we could adjust the allowable resistance value and time interval changes in any direction that will minimize the coil weight. Also it should be emphasized that this concept is feasible only with a lightweight magnet power supply

---

TABLE 22. PERFORMANCE OF MAGNETS IN THE NON-EQUILIBRIUM CW MHD GENERATOR

CASE	r_j (m)	FIELD (Tesla)	J_{COIL} A/M^2	MAG.TEMP (°K)	WGT. (kg)	MHD PWR. (MW)	MAG.PWR. (MW)	NET PWR (MW)	COOL.
COPPER COILS									
#G-2A	.13	2	$1.26*10^8$	300	200	17.3	7.2	10.1	NH_3
#G-2B	.13	2	$2.0*10^7$	300	2200	17.3	2.1	15.2	NONE
#G-2C	.23	2	$1.26*10^8$	300	335	17.3	10.2	7.1	NH_3
#G-2D	.23	2	$2.0*10^7$	300	3465	17.3	1.9	15.4	NONE
#G-2E	.23	2	$5.0*10^7$	77	1210	17.3	1.3	16.0	LN_2
ALUMINUM COIL									
#G-2F	.23	2	$8.0*10^7$	300	200	17.3	12.5	4.8	NH_3

Table 22 lists the performance of the magnets for the Base Case #G-2. r_j is one-half the distance between the inner walls of the long sides of the saddle coil. r_j was assumed to be one-half the outside diameter of the channel at a point equal to the average inter-electrode spacing. Also, it should be noted that the weights in the Table apply to the conductor coils only. The total magnet weight also includes the support structure, which we have assumed to be equal to the coil weights in computing the total specific power of the system in Table 13.

Cases G-2A & B apply to the MHD generator Base Case. One notes that only a factor of three increase in magnet power, decreases the magnet weight by a factor of 10. We also show three cases ,#G-2C,2D, & 2E, where the separation of the inner walls of the coils was nearly doubled to 2*.23 m. In this case the NH_3 coil is four times lighter than the LN_2 cooled coil. Case #G-2E is for LN_2 cooling. Although in this case, the power is almost 8 times less than with NH_3 cooling, it is not not sufficient to make the LN_2 magnet attractive for the present application in terms of total system weight.

Case G-2F shows that the NH_3 cooled, aluminum coil is 60% of the weight of the copper coil (Case #G-2C), and its power requirement is only 20% greater than for copper. It is thus an attractive alternate material for the magnet.

There are several major technical problems that must be addressed before this NH_3 cooled magnet can be used.

One, ammonia is toxic in large concentrations. However it is used extensively in industrial refrigeration systems.

Two, ammonia is not used with copper in the refrigeration industry because it rapidly attacks copper. Ammonia is used with aluminum and Case #G-2F shows that the lower weight of aluminum nearly compensates for its higher resistivity and power requirement.

Three, after investigating the corrosion problem and discussing it with a consultant from the ammonia refrigeration industry, we found that dry ammonia liquid reduces the CuO on the surface of the copper by the reaction

$$3\ CuO + 2\ NH_3 \Rightarrow 3\ H_2O + 3\ Cu + N_2 \qquad (3\text{-}22)$$

This reaction does not cause any problems in the present application. However, in long term use, it is very difficult to keep water out of an ammonia system. It is this reaction that produces the familiar blue color of ammonia attack. The reaction results in the formation of $Cu(NH_3)_4^{++}$, which scales and removes the copper. However, if one stores the ammonia in a steel vessel until ready for use, then in a pulsed power application, there need not be any water in the NH_3, and even if there is there will not be sufficient time to attack the copper in 10 seconds of operation.

Four, a more serious problem is the fact that only in pool boiling does one achieve continuous nucleate boiling. In a hollow tube conductor, it is very likely that the liquid will rapidly boil and the entire passage will fill with ammonia vapor where the heat transfer rate will be sharply lower. Thus a design must be found to rapidly remove the ammonia vapor. There was no time to address this issue.

Five, the ammonia vapor must be removed from the magnet and disposed. If it remains in the magnet pressure vessel, the pressure will rise to extremely high levels (up to 10,000 psi). In remote locations , the ammonia could be vented to the atmosphere. Burning the ammonia, releases too much heat (about equal to the thermal input to the MHD generator), and it requires a compressor or storage for the oxidizer. The best solution would be to condense it in water. Of course in this case, it could not be reused with copper.

In any case, the use of ammonia offers the potential of a major decrease in electric component sizes, if used with an efficient high power source, such as the present MHD generator. This would also allow the use of smaller components in power transfer systems.

3.6.2. Self-Excitation of the Non-Equilibrium MHD Generator:

As partially discussed in the previous Section, the design and operation of a self excited non-equilibrium MHD generator differs from the equilibrium conductivity generator using the seeded combustion gases as the working fluid. In the latter device, either Faraday connection, with a single pair of electrodes has been used , as in the PAMIR unit, or diagonal wall connection, also with a single electrode pair has been used (e.g.2,6). The former connection is feasible due to the very low and nearly constant Hall parameter (about 0.4),

while the latter is used when the Hall parameter exceeds 1, typically 2-4, but does not vary greatly along the generator axis.

Theoretically, the non-equilibrium generator, with its high Hall parameter, should be suitable for operation in the Hall connection mode, in which a single electrode load pair,located at the entrance and exit of the generator, is used. However,plasma instabilities lower the effective Hall parameter in linear generators to values of 1 to 2,making Hall or diagonal load connections impossible. While the suppression of these instabilities has been demonstrated with the use of fully ionized seed, no high power linear generator has operated to date in the Hall mode. [It should be noted that the disc generator, which is in effect a Hall device,has operated with non-equilibrium ionization, and suppression of plasma instabilities in the Hall mode. We have not investigated this device in the present study].

The present non-equilibrium generator operates at very high pressures, which results in relatively low Hall parameters. In all cases considered, the Hall parameter was set at a maximum of 4 at the generator exit, which results in an average value of 1-2 over the channel length. Although this should allow a diagonal connection,it may be difficult to implement because the Hall parameter increase sharply along the channel axis, typically by a factor of 3 to 4. Thus the diagonal electrode pitch would have to be increased in the downstream direction to operate the generator in the diagonal mode. This type of electrode construction is difficult to implement physically.

One major benefit of the use of helium is that the transverse load voltages in the Faraday connection are very high even at low B fields. For example in case #G-2, the downstream electrode load voltages range from 850 V. at X=.43 m. to 1020 V. at X=.6 m. This region consists of 9 electrode pairs, and produces 7.2 MW,required to power the NH_3 cooled magnet in Case #G2-A. Since the average Hall parameter in this region is only 1.55, increasing the electrode pitch from 0.1 to 0.2 would only lower the power output by 10%, and it would cut the number of electrode pairs in half. [We noted in the previous Section, that the need to ignite the non-equilibrium plasma, precludes the use of the upstream electrodes as the magnet power source.]

By dividing the magnet coils into 5 sections, one can connect each one of them to a separate electrode pair. We performed this analysis for Case G-2A.

For simplicity we used an electrode pitch of 0.2, the average voltage of the 5 electrodes of 935 V., and the average current of 1540 A/electrode. This results in an allowable coil resistance of 0.61 ohms, 122 winding turns for each of the 5 coils, a self inductance of 0.03 henries. We ignored the mutual inductance between the coils. In any case the L/R risetime of each coil is 0.05 seconds, or 1/10 the time we used in calculating the maximum allowable current with ammonia cooling.

The very low inductance of the magnet is due to the high power density output of the generator, which allows the use of a small magnet. This suggests interesting possibilities in the use of the generator and its magnet directly as a pulsed power source. This should be investigated.

3.7. Use of the CW MHD Generator to Power the Magnet for the Artec Explosive MHD Generator

One of the objectives of the present study was to explore the feasibility of using a cw MHD generator to power the magnet for an Artec type explosive MHD generator. Section 2.1.c discussed our estimate of the energy required to accomplish this with a capacitor storage system, which would be charged by the cw MHD generator. We estimated that to achieve 500 kJ gross explosive generator output/pulse, a minimum of 100 kJ must be stored in the magnet, which was double the value given in Ref.1. To this must be added the losses in the capacitor circuit which based on the experimental data reported in ref. 1 is about 75 kJ. Assuming this could be reduced by advanced capacitors and efficient placement of the circuit wires to 50 kJ, one would require 150 Kj per pulse. With 10 pulses/sec. the cw generator net output would be 150 kJ/0.1 sec.= 1.5 MW,or 15% of the net output of Case G-2A, in Table 13. Time constraints prevented us from analyzing such a small generator. In addition, we already have noted that since the present Artec generator's output pulse is 80 microseconds in duration, a pulse forming circuit is required to convert its output to the 10 microseconds specified for this project. Thus we recommend that a cw generator, in the power output range of Case G-2A be used directly with a pulse forming circuit, bypassing completely the explosive MHD generator.

Nevertheless,it is of interest to obtain a weight estimate of this capacitor driven configuration. Assuming that the capacitor technology results in weights in the 300-500 J/kg range (50), and taking the upper end of this range,

one obtains a weight of 300 kG for the present application. In addition, we assume that a 1.5 MW output cw MHD generator system weighs 330 kg,or twice the weight relative to the 1170 kg of the 10 MWe net output system of Case G-2A (See Section 3.8). One obtains a total weight for the magnet power supply of 630 kg. This is 33% of the total weight of the explosive MHD system (1) for the 0.5 MJ output case using a pulse forming network circuit,[See Table 1,Section 2.1, and Table 3, Section 2.4). It also compares very favorably with the magnet weight given in Ref.2 for the 50 kJ pulse system, which is also listed in Table 3. Thus the present non equilibrium generator is a very attractive device as a magnet power source for an Artec type explosive generator, operating as projected in Ref.1.

We did not have the time to analyze the circuit connections necessary to charge the capacitor system from the cw MHD generator, but it would have to be a constant current charging system.

We also examined the possibility of using a dc magnet powered by the cw generator for the entire 10 sec. operating time. Since a field of at least 5 Tesla is required by the Artec generator, we found,using the analysis of Ref.13, that this could not be achieved with a heat sink magnet. Using our ammonia cooled magnet concept, it was found that a current density of $3*10^8 A/m^2$ would be required to obtain the 5 Tesla field in a magnet within the tabulated dimension range given in Table 2.1 of Ref.13. The copper magnet coil would weigh only 70 kg. However, the power required for the magnet is estimated at 12.8 MW. This is near the net power output range of Case G-2A,(10.1 MW). However, the total system weight would be 1170 kg, including the cw MHD generator, or double the weight of the capacitor driven magnet. Nevertheless, it is still 66% of the weight given for the PFN explosive generator in Table 1.

It will be recalled from Section 2.1, that we concluded that self excitation of the Artec generator may be possible for gross power outputs up to 0.5 MJ. This is achieved by dividing the electrode and magnet regions into two separate sections. Thus this may be an alternative to the external magnet supply.

In conclusion, the concept of using the present cw MHD generator to power the magnet for the explosive generator appears to be feasible,both as a capacitor driven and cw driven magnet. However, the capacitor driven magnet is preferred both from a technology readiness point of view and from a weight point of view.

3.8. The Total Weight of the Metal Fuel Fired, Non-Equilibrium MHD Generator:

In addition to the weight of the magnet, the other components that have a major impact on weight are the combustor and the gas storage system.

3.8.1. Gas Storage System:

At first it appeared that the gas storage problem would be a major barrier to the implementation of the present concept because without liquid storage, the helium container would dwarf the rest of the system. However, in the process of investigating gas storage technology, we learned that noble gases are routinely supplied to NASA at 10,000 psi pressure, and 300°K, using composite fiber wound containers. Using carbon matrix fibers with aluminum filler, one can obtain 150,000 psi (680 atm) ultimate stress material having a density of 0.1 lb/ft^3. At 680 atm. & 300°K, the density of helium is 0.1 g/cc, compared to 0.147 g/cc, at 1 atm., and 4°K. Thus in terms of cost and present mission application, the high pressure storage method is preferred.

The analysis of the pressure vessel requires the use of non-isotropic stress theory. We contacted a fabricator of these vessels for NASA, but were unable to obtain any weight estimates from him. Therefore, we used simple isotropic thick pressure vessel theory to calculate the size and weight of the gas storage containers. For Case G-2, a 3'D sphere with a 1.25 " wall thickness and weighing 280 kg, is required to store a 10 second supply of helium.

The oxygen required for aluminum combustion requires a pressure vessel weighing 95 kg.

Combustor: We performed a transient wall heat transfer analysis to estimate the required materials and wall thickness for a combustor that would operate for 10 seconds in the present environment. For Case G-2, assuming combustion takes place at 4000°K, at Mach # of 0.1 in the combustor, and with 10 micron diameter Al particles, which require 1 ms combustion time (See Table 12, Section 3.3.), one obtains internal combustor dimensions of 16 cm D*40 cm.L. A 0.1 m. thick copper heat sink combustor wall was used, which results in a combustor weight of 280 kg.

Table 24 provides a summary of the weights of the major components and the fuel for the 10 second operation of the cw metal fuel fired combustor.

TABLE 24: SYSTEM WEIGHT FOR THE 10 MW MHD GENERATOR OUTPUT, CASE G-2

GAS STORAGE	-HELIUM CYLINDER	192 KG
-(COMPOSITES)	-OXYGEN CYLINDER	62 KG
FUEL WEIGHT	ALUMINUM	35 KG
OXIDIZER	OXYGEN	29 KG
NOBLE GAS	HELIUM	44 KG
COMBUSTOR-HEAT SINK COPPER		280 KG
MAGNET-COOLED-(INCLUDES 50% FOR SUPPORT)		400 KG
MAGNET COOLING FLUID		60 KG
TOTAL CW MHD WEIGHT-Ammonia Cooled Magnet		1102 KG
HEAT SINK MAGNET-(INCLUDES 50% SUPPORT)		4500 KG
TOTAL CW MHD WEIGHT -Heat Sink Magnet		5142 KG
WEIGHT OF AUXILIARY POWER SUPPLY & PULSE FORMING NETWORK-(FROM REF.1)		822 KG
TOTAL WEIGHT 0.5 MJ,10 PPS,10 SEC.		1924 KG-(NH_3 MAGNET) 5966 KG-(HEAT SINK MAGNET)
TOTAL WEIGHT FOR SAME OUTPUT-REF.1		1890 KG

The results clearly show the benefit of using the ammonia cooled magnet on the total system weight. We have not included the weight of the pulse forming circuit due to the lack of time. Even if the PFN circuit has the 65% efficiency assumed by Artec (1), the present generator supplies 10.1 MWe net power, compared to the 7.7 MWe net power required obtain ten pulses per second at 0.5 MJ per pulse. If we use the 822 kg weight estimate, (given in Ref.1 for the PFN in the Artec explosive system),for the present application, one obtains a total weight for the NH_3 cooled magnet system of 1992 kg, which is about the same as that given for the Artec self excited generator (1890 kg). However, the present system does not have the survivability problems of the explosive system.

3.9. Transient Heat Transfer to the Walls of the Combustor & Generator

One of the potential major problems to the long term operation (greater than several seconds) of this metal fuel fired, noble gas MHD system, is the maintenance of the integrity of the walls of the combustor, nozzle, and MHD channel under the intense radiative and convective heat transfer from the metal particles, and oxide particles, and the gas. In the present study, we performed a transient heat transfer analysis of the walls of the combustor and MHD generator to determine the length of time required to heat up the gas-solid interface to the melting point, and the time to heat the back surface of the wall above the initial room temperature.

3.9.1. Combustor Heat Transfer:

All the heat transfer to the walls of the combustor is due to radiation from the metal fuel and metal oxide combustion products. Assuming a 10 micron mean particle size, it is easily shown that at typical conditions used in the analyses, the radiation from the combustor gas stream is black body at the stagnation temperature. At $4000^{o}K$ (e.g. Case G-2, P_o=49atm.) the black body radiation to the wall is $4.6*10^{6}$ Btu/hr-ft^2 (1.45 kw/cm^2); and at $3000^{o}K$, (e.g. Case M-1, P_o=69 atm.), the radiation is $1.5*10^{6}$ BTU/hr-ft^2 (.47 kw/cm^2). We used a transient wall heat transfer analysis used for rocket combustion chambers, in which the "effective" wall heat transfer coefficient ,h in BTU/hr-ft^2, is obtained from (49)

$$h = (\xi * \sigma * T^4)/(T - T_{wo}) \qquad (3\text{-}23)$$

The transient heating rate of the combustor wall can best be approximated by assuming the wall to be either a one dimensional semi-infinite body, whose surface is exposed at t=0 seconds to a gas at a temperature T, or an infinite slab of finite thickness, one of whose side is exposed at t=0 sec. to a gas at temperature T, whose back surface is insulated. The former condition provides a first order estimate of the thickness of combustor wall required for heat sink operation at which the back wall temperature remains unaffected, while the second case provides a more accurate description of the conditions of present interest. In the analysis the maximum allowable surface-gas interface temperature is specified, and the time to reach this condition is calculated. One can then estimate to first order the overall temperature increase of the entire

combustor wall for the selected thickness, recognizing that the gas-solid interface may exceed the peak selected temperature for times greater than those obtained in the above analysis.

The transient wall heat transfer analysis is considerably simplified by published Tables (e.g. ref.49) of the heating of a semi-infinite solid under a wide range of boundary conditions.

In the analysis,we selected three materials, aluminum, copper, and tungsten, and computed the time vs temperature history at various locations in the semi-infinite solid, or semi-infinite slab of given thickness. The low melting point of aluminum results in too low a temperature, 1200°F,(922°K) to prevent the wall from melting during the 10 second time period of present interest. Tungsten is not suitable for a structural combustor wall and the results are of little interest. Copper can be used to below its melting point near 2000°F,(1367°K),with 3000°K gas temperatures for the full 10 seconds of operation. However, at 4000°K, the surface begin to melt after 5 seconds, as shown in the following Tables.

Table 25 shows the temperature at various depths from the surface of a semi-infinite solid at 10 seconds after startup. The "effective" film coefficient was 474 BTU/hr-ft^2 for the 4940°F (3000°K) case, and 952 BTU/hr-ft^2 for the 6740°F (4000°K) case. The results show that at a point 4 inches from the surface the temperature is unchanged,and this value was used to specify the combustor size and weight in Case G-2. However, at 6740°F combustion temperature, the copper-gas interface temperature exceeds the 2000°F limit,at which melting occurs after 5 seconds. However, at 1 inch depth,the copper temperature is well below this limit. Thus for 10 second operation at this temperature, some surface melting will occur.

Table 26 shows the more accurate boundary condition for the finite thickness combustor wall in that here the backside of the combustor is insulated. The Table shows the time required for the gas-copper surface temperature to reach the prescribed 2000°F limit. It also shows the backside temperature at this time. Again for the 6740°F case (i.e Case G-2), the gas-copper surface temperature limit of 2000°F is reached in only 3 seconds, compared to 5 seconds for the semi-infinite body in Table 25. However,the backside temperature is unchanged at 3 seconds. Using the 4 inch wall thickness,we calculated that

TABLE 25:TEMPERATURE IN A SEMI-INFINITE COPPER SLAB EXPOSED TO GAS AT t=0 sec.

DISTANCE FROM SURFACE (inches)	COPPER TEMP. (°F)	DISTANCE FROM SURFACE (inches)	COPPER TEMP. (°F)
A. GAS TEMP.=6740°F, t=5 sec.		B. GAS TEMP.=6740°F, t=10 sec.	
0	2011	0	2544
1	746	1	946
2	246	2	280
3	113	3	147
4	80	4	100
C. GAS TEMP.=4940°F, t=10 sec.		B. GAS TEMP.=4940°F, t=20 sec.	
0	1149	0	1489
1	615	1	979
2	274	2	566
3	90	3	323
4	80	4	225

TABLE 26:TIME FOR GAS-Cu INTERFACE TO REACH 2000°F, & BACK SURFACE TEMPERATURE AT THIS TIME, FOR A SEMI-INFINITE SLAB OF GIVEN THICKNESS,d.

	THICKNESS-d,in.	.25	0.5	1.	2	3	4
GASTEMP.							
4940°F;	TIME,sec.	4.	8.6	16.1	30.	39.4	46.1
	GAS-Cu TEMP,°F	2000	2000	2000	2000	2000	2000
	BACKSIDE TEMP,°F	1951	1936	1878	1489	1222	954
6740°F;	TIME,sec.	0.9	1.7	2.7	2.8	2.9	3.0
	GAS-Cu TEMP,°F	2000	2000	2000	2000	2000	2000
	BACKSIDE TEMP,°F	1345	1146	679	199	146	80

the entire radiative heat transfer from the 6740°F (4000°) combustion gases could be absorbed by the copper wall in 10 seconds with an average metal temperature increase of only 250°F. This confirmed that the 4 in. wall thickness could be used to estimate the weight of the combustor in Case G-2.

3.9.2. Heat Transfer to the MHD Generator Wall:

Since most of the oxide particles from the metal fuel combustion will be removed in the combustor, the bulk of the heat transfer to the walls of the MHD generator will be due to convection to all four walls of the diverging rectangular channel, as well as heating of the anode wall and cooling of the cathode wall due to the electrode voltage drops. Due to the low cesium seed concentrations, radiation from its excited states and the electrons will be relatively low, compared to the other heat transfer sources.

The convective heat transfer to the wall, q_v/unit area A, is given by (49)

$$q_v/A = h'*(T_r - T_w) \qquad (3\text{-}24)$$

where h', the convective heat transfer coefficient obtained from Reynolds analogy between friction and heat transfer. It is given by

$$h' = 0.5*C_f*\rho_g*c_g*U_g/(Pr)^{.67} \qquad (3\text{-}25)$$

and T_w is the wall temperature, and T_r is the recovery temperature

$$T_r = T_g*[1 + r*M^2(\gamma - 1)/\gamma] \qquad (3\text{-}26)$$

In the above equations, T_r is the static gas temperature; ρ_g the static gas density, c_g is the gas specific heat; U_g the local gas velocity; M is the local Mach number; Pr, the Prandtl number, equal to 0.7; r, the recovery factor, equal to about 0.88 (49); γ is the ratio of specific heat, equal to 1.67; and C_f is the wall friction factor. Based on our prior shock tunnel generator experiments (10), we deduced that C_f was 0.003 for a smooth wall channel and 0.008 for a channel in which the electrodes protruded into the gas stream beyond the boundary layer.

The electrode heating effect due to the local voltage drop is essentially equal to the ohmic dissipation at the electrodes. All our calculations were performed with a 100 to 200 V combined anode and cathode voltage drop. Due to the high current densities obtained in the analysis, this will result in an unrealistically high electrode heating effect. In all probability, at these high current densities, the voltage drops will decrease to the levels found in high

current arcs, namely about 10 V, and possibly less,due to the high thermionic emission capability of the electrodes. This still results in very high heating levels ,especially to the anode, where the cooling effect of electron emission that exists at the cathode is not available. In the present analysis,we concentrated only on the convective heating, and we did not analyze the effect of heating due to electrode losses, although we tabulated its values.

To simplify the analysis we considered the electrode wall of the channel to consist of a semi-infinite tungsten sheet of finite thickness, whose metal-gas interface temperature was limited to 3670°K (6146°F), or slightly below its melting point. This allows one to obtain not only the benefit of high temperature operation with tungsten, but also very high thermionic emissions, as discussed in Section 3.5. Boron nitride was selected for the two insulator walls of the channel due to its excellent shock resistance, and its peak operating temperature of 2770°K (4526°F). We should note that a major advantage of using helium-seeded with cesium in the generator is that it allows the use of tungsten and boron nitride, which cannot be used in a conventional combustion generators. The same transient heat transfer analysis used to analyze the combustor wall was used for the generator wall heat transfer analysis.

Cases #F-1 and #M-1 have been selected to illustrate the results at 3000 and 4000°K stagnation gas temperatures. The convective heat transfer calculations were performed at the entrance ,mid-point and exit of the MHD generator. The analysis was performed for tungsten and boron nitride sheets with thicknesses ranging from 0.25 to 2 inches. Tables 27 and 28 show the results of the analysis.There are several interesting points to be made:

-A major heat transfer problem occurs at the channel entrance region. Here the boron nitride wall is overheated in the 10 second operating time in the 4000°K case, but not in the 3000°K case. The calculations for the 4000°K case showed that for the 1 inch thick wall cases shown, the BN reaches the peak allowable temperature in 2.8 seconds for C_f=0.003, and in 0.3 seconds for C_f=0.008. Thus another type of wall construction is required at the entrance. One possibility is a "peg" wall (27) in which metal pegs ,parallel to the magnetic field, are embedded throughout the two insulator walls between the ceramic structure. This has been used successfully in high temperature combustion generators.

AD-A200 250 HIGH PULSED POWER SELF EXCITED MAGNETOHYDRODYNAMIC POWER GENERATION SYSTEMS(U) COAL TECH CORP MERION PA B ZAUDERER ET AL. 27 DEC 85 CT-85-10 AFOSR-TR-88-1002 2/2

UNCLASSIFIED F49620-85-C-0025 F/G 20/9 NL

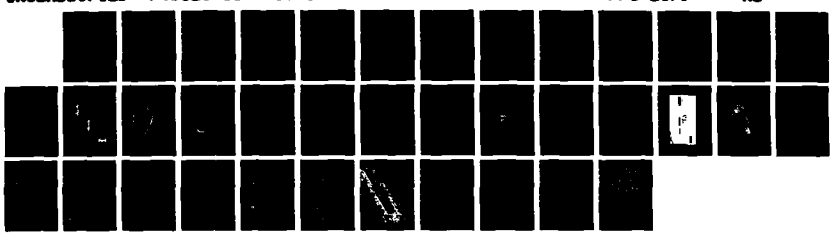

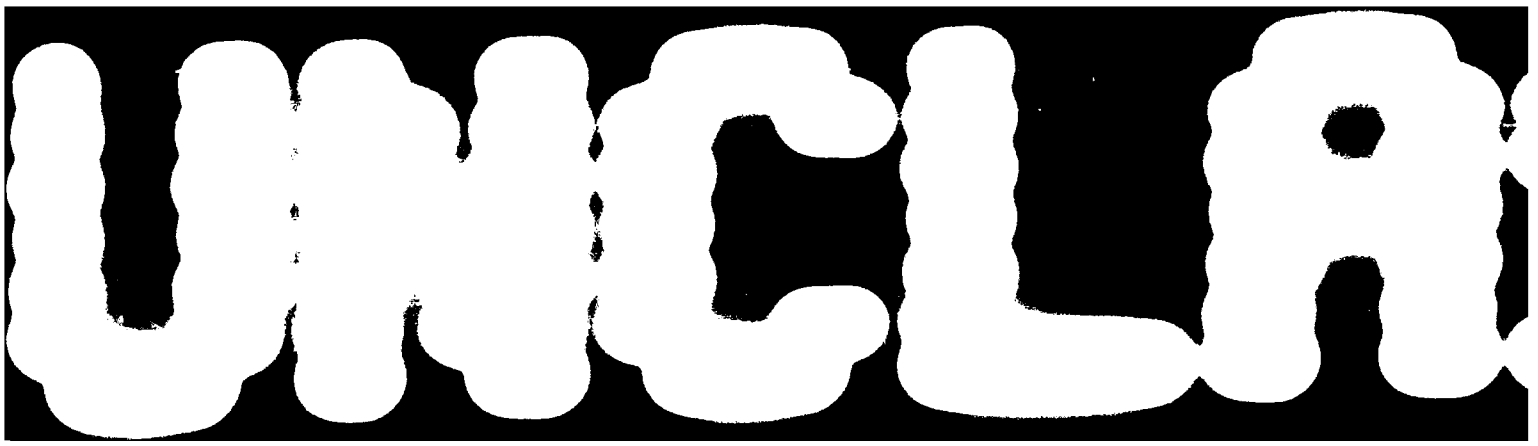
UNCLA

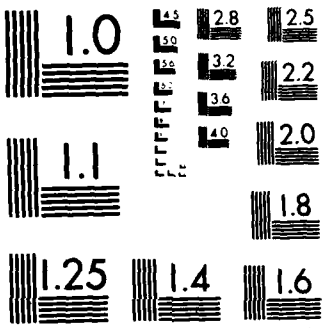
1.0
1.1
1.25
1.4
1.6
1.8
2.0
2.2
2.5
2.8
3.2
3.6
4.0
4.5
5.0
5.6

TABLE 27: CONVECTIVE HEATING OF THE MHD CHANNEL-CASE # F-1

-T_o=4000°K {6740°F}; P_o=72.4 atm.; A_{in}=25 cm^2; L=35 cm.; B=3 T.;

-Heat Input=43.6 MW; MHD Power=10.4 MW; Operating Time =10 sec.

-Tungsten Electrode Wall Thickness =2.5 cm.

-T_{wW}(max.)=3760°K; T_{wBN}(max.)=2770°K; Cathode & Anode Loss= 10 V. each.

X cm	T_g °K	M -	U_g m/s	h' watts/(cm^{2-o}K)	T_r °K	T_{wW} °K	T_{wBN} °K	q_{vW}/A w/cm^2	q_{el}/A w/cm^2	q_{vBN}/A w/cm^2
PART A: C_f=0.003										
0	1297	2.5	5220	0.86	3687	3043	>2770	553	2164	---
.2	1440	2.1	4520	0.30	3224	1879	2229	404	801	299
.35	1197	2.0	4077	0.14	2651	1029	1358	227	350	181
PART B: C_f=0.008										
0	1297	2.5	5220	2.28	3687	3517	>2770	388	2164	---
.2	1440	2.1	4520	0.81	3224	2638	2726	475	801	404
.35	1197	2.0	4077	0.39	2651	1710	1946	367	350	275

TABLE 28: CONVECTIVE HEATING OF THE MHD CHANNEL-CASE # M-1

-T_o=3000°K {4940°F}; P_o=69 atm.; A_{in}=50 cm^2; L=60 cm.; B=4 T.;

-Heat Input=73. MW; MHD Power=19.8 MW; Operating Time =10 sec.

-Tungsten Electrode Wall Thickness =2.5 cm.

-T_{wW}(max.)=3760°K; T_{wBN}(max.)=2770°K; Cathode & Anode Loss= 10 V. each.

X cm	T_g °K	M -	U_g m/s	h' watts/(cm^{2-o}K)	T_r °K	T_{wW} °K	T_{wBN} °K	q_{vW}/A w/cm^2	q_{el}/A w/cm^2	q_{vBN}/A w/cm^2
PART A: C_f=0.003										
0	973	2.5	4570	0.93	2765	2346	2420	390	900	320
.3	1069	2.1	4036	0.38	2458	1573	1832	336	400	237
.6	860	2.1	3564	0.16	1946	860	1073	174	140	140
PART B: C_f=0.008										
0	973	2.5	4570	2.48	2765	2642	2642	305	900	305
.3	1069	2.1	4036	1.01	2458	2113	2199	346	400	261
.6	860	2.1	3564	0.41	1946	1353	1501	245	140	184

-At 3000°K stagnation temperature, the recovery temperature is 2738°K. which is below the peak operating temperature of BN of 2770°K, so that continuous operation of the channel is possible.

-The tungsten does not reach the peak allowable operating temperature in most of the channel, and even at the entrance,this does not occur until late in the operating time of 10 seconds. Thus to obtain high temperature emission with the tungsten at the channel entrance, the tungsten electrode thickness must be reduced. It will be necessary to increase the thickness in the downstream direction to obtain the optimum balance between electrode heating for peak thermionic emission and remain within the allowable operating temperature of tungsten.

-At 3000°K it may be desirable to deliberately increase the surface roughness to heatup the electrode, as can be seen by comparing the results from the two friction factors.Alternatively, one can balance the effect of thermionic emission from bare tungsten at high temperature at the upstream end of the generator, with cesiated tungsten at lower temperature at the downstream end of the generator.

-The additional heating, primarily at the anode, due to electrode voltage loses, is equal to,{or much greater at the channel entrance}, to the convective heat transfer. The inclusion of this effect on the electrode wall heat transfer will require more detailed analysis.

In general,one can conclude that with the exception of the insulator wall at the channel entrance, the wall heat transfer inside the channel appears to be amendable to solution, compared to the combustor wall heat transfer. We should note that there are several concepts that can be used, such as active wall cooling, to allow generator operation in the power output density range represented by the two examples in this sub-section.

4.Research Needs to Establish the Technical Feasibility of the Metal Fuel Fired Noble Gas MHD Generator:

The research and development requirements to implement this new MHD concept are summarized in Table 29. This report has shown that to utilize this new MHD technology it is necessary to operate the system at MHD power densities,combustor heat release rates, magnet cooling rates, and wall heat transfer rates that are at the upper limits of current technology. Therefore, a number of technical issues must be addressed analytically,before an experimental verification program can be undertaken. They are:

COMBUSTOR: The method for small metal fuel particle injection, fuel combustion, fuel mixing with the noble gas, and metal oxide separation from the noble gas prior to the combustor exit,must be analyzed in much more detail than was possible to-date. Also, the combustor walls are subject to extremely high heat transfer rates, which for the present operating times are at the upper limit of heat sink operation. Existing and new concepts must be evaluated for the injection, cooling, and metal oxide-noble gas separation,and reduced to a practical engineering design.

MHD GENERATOR: The problem of generator performance; in the presence of residual small metal oxide particles; under conditions where plasma instabilities are suppressed; in the presence of high electrode emission levels; and high wall heat transfer rates, all of which are present at maximum performance must be analyzed and reduced to a practical engineering design. There are concepts based on prior art that can be used to accomplish these objectives.

MAGNET: The major technical issue is the whether a practical design based on the present very light weight, actively cooled room temperature magnet can be developed. Based on existing heat transfer data, the magnet designs analyzed in the present study are feasible. However, the key issue is feasibility of continuously cooling the conductor coils with boiling heat transfer,without transition to a vapor phase between the conductor and the liquid. The benefit of such a lightweight room temperature magnet is considerable. In fact this concept could be applied to other power transformer devices. Finally, the problem of protecting the copper conductor in the presence of ammonia by means of coatings must be solved, if this approach is to be used for long duration operation.

GAS STORAGE: This technology is state of the art. However, it is necessary to fully explore the technical issues involved. We should also note that at the higher power levels (100 MW output over 10's seconds), the gas usage starts to become a major consideration in the operation of this system.

POWER CONDITIONING: Finally, the issues involved in adapting this generator to pulse shaping circuits must be addressed. In this area, a more general approach than the present 10 microsecond pulse application is of interest, because this generator system can be used in a wide range of pulsed power applications, (e.g. rail guns, continuous nuclear space power systems).

TABLE 29: RESEARCH NEEDS TO ESTABLISH THE TECHNICAL FEASIBILITY OF THE METAL FUEL FIRED, NOBLE GAS MHD GENERATOR AS A PULSED POWER SOURCE.

(a) DETAILED ANALYSIS & CONCEPTUAL DESIGN OF A METAL FUEL FIRED, HELIUM COMBUSTOR, WITH EMPHASIS ON:

- -Fuel Particle Injection
- -Particle Combustion
- -Oxide Removal in Combustor
- -Pulsed Combustor Operation
- -Active Wall Cooling, with boiling, or heat pipe, or liquid oxide layer

(b) ANALYSIS OF THE NOBLE GAS MHD GENERATOR OVER A WIDE RANGE OF POWER LEVELS, WITH EMPHASIS ON:

- -Use of more rigorous MHD code
- -Focus on electrode emission,
- -Focus on wall cooling
- -Focus on self excitation
- -Focus on power output & pulse shaping

(c) ANALYSIS OF ACTIVELY COOLED, LIGHT WEIGHT 300^{0}K MAGNET, WITH EMPHASIS ON

- -Continuous active cooling inside coils and heat rejection in 2 phase flow

(d) ANALYSIS OF COMPOSITE STRUCTURES FOR GAS STORAGE

(e) ANALYSIS OF SOLID SLUG MHD POWER CONVERSION USING LIGHT WEIGHT COMPOSITES, AND INTERNAL COMBUSTION TO ACCELERATE SLUG, AND SHARPLY RAISE ITS BUCKLING STRENGTH

THE PRIMARY EMPHASIS SHOULD BE ON ITEM (a)

References

1.S.P.Gill,et.al.,"Preliminary Design of a 50 Gigawatt Power Supply",Artec Associates,Hayward,CA. Air Force Weapons Laboratory-SBIR Program Phase 1 Final Report-FR-190,April 1984.

2.D.W.Swallom,"MHD Generator Field Use Concepts for Rep-Pulsed Electric Discharge Lasers", Report-AD-B082569,Jun.1983.

3.C.D.Barngerter,et.al.,"Explosively Driven MHD Power Generation", in Proc. 6th Int.MHD Symposium,NTIS Report-CONF-750601-P4,June 1975,Vol.IV,p.155

4.C.D.Barngerter,et.al."Explosive MHD Program",NTIS-AD-762934,May 1973

5.J.Teno,et.al.,"Dev.of Explosively Driven MHD Generator",NTIS-AD-784903,June 1974

6.C.D.Maxwell,et.al,"Initial Tests of a Lightweight,Self excited MHD Generator", in Proc.23rd. Symp.End.Asp.of MHD,Somerset,PA,June 25,1985,p.147

7.E.Velikhov,"Utilization of a Pulse Type MHD Generator for Geophysical Research & Earthquake Prediction",loc.cit.Ref.3,Vol.V.p.211.

8.S.P.Gill,et.al.,"Principles of Efficiency in High Power MHD Experiments".Artec Associates,Hayward,CA,Final Report FR-165,Office of Naval Research Contract N00014-81-C-0045,Jan.1984

9.D.W.Baum,et.al.;"High Power Pulsed Plasma MHD Experiments",Artec Associates, Hayward,CA,Annual Office of Naval Research Contract Number N00014-81-C-0045,(AD-A120526),Sep.1982

10.C.H.Marston,B.Zauderer,E.Tate,"Large Enthalpy Extraction Results in a Nonequilibrium MHD Generator",loc.cit. Ref.3,Vol.3,p.89

11.H.Knoepfel,Pulsed High Magnetic Fields,(North Holland,Amsterdam,1970)

12.D.A.Oliver,et.al,"High Magnetic Reynolds Number & Strong Interactions Phenomena in MHD Channel Flows", in Proc.7th Int.MHD Symposium, MIT,Cambridge,MA, June 1980,Vol.IIp.565

13.R.J.Thome & J.M.Tarrh,MHD & Fusion Magnets,John Wiley,NY,1982),Ch.2.

14.F.E.Terman,Radio Engineer's Handbook,(McGraw-Hill,NY,1943),Section 2

15.J.Teno,loc.cit.Ref.5

16.S.Glasstone,Principles of Nuclear Reactor Engineering,(Van Nostrand,Princeton,1955),Ch.8

17.W.F.DeMario,"Aerospace Composites",in Aerospace America,V.24,p.36,Oct.1985

18.B.A.Bennett,et.al.,"Carbon-Fiber Composites",in Mechanical Engineering,V.107,p.34,1985

19.A.Kamrukov,et.al.;"A Plasma Source w. an Explosive MHD Generator", Report No.FSTC-HT-766-84,Aug.84

20. E.I.Asinovsky,et.al.,"Inv.of Processes Determining the Efficiency of Energy Conversion in a Linear Explosive MHD Generator",in Proc.7th Int. MHD Symposium,MIT,Cambridge,MA,Vol.2,p.605,June 1980

21.M.S.Jones,et.al.,"Parametric Studies of of Explosive Driven MHD Generators", Proc.2nd Int. MHD Symp, (OECD,Paris,France),July 1964.

22.M.S.Jones,et.al.,"Explosive Driven MHD Generator",Conf.on MGauss Field Generation by Explosive Devices,Frascati,Italy,Sept.1965

23.E.I.Asinovski,et.al."Motion of a Plasma Driven By a Non-Conducting Piston in a Magnetic Field",in loc.cit.Ref.16,p.53

24.A.Orlov,"Signals from the Earth's Depths;MHD Generator Experiments for Earthquake Predictions",FSTC-HT-83-80,Sep.1980

25.V.V.Vengerskiy,et.al.,"A Solid Fuel MHD Generator with a 100 second Pulse Duration",Report FSTC-HT-0771-83,Oct.1983 (AD-B082 848)

26.E.Velikhov,Comments in Proc.6th Int.MHD Symp.,(NTIS Doc.No.CONF-750601-P6),Washington,D.C. June 1975, Vol.VI.p.269.

27.R.J.Rosa,MHD Energy Conversion,(McGraw-Hill,NY,1968)

28.B.Zauderer,"Shock Tube Studies of Magnetically Induced Ionization",Phys. Fluids,Vol7,pp147-9,(1964)
29.D.W.Swallom,et.al.,"High Power MHD System",AFAPL-TR-78-51,Vol.1,July 1978.
30.J.H.Blom,"Rapporteur Report",in loc.cit.Ref.5,Vol.VI,p.104
31.H.Yamasaki,et.al.,"Closed Cycle MHD Disc Exp.at Tokyo Inst.Tech.", in loc. cit.Ref.6,p.430
32.M.Zlatanovic,et.al.,"Perform.of a Closed Cycle MHD Generator w.Molecular Impurities",in Proc.17th Symp.Eng.Aspects of MHD,Stanford U.,Mar.1978,p.H.2
33.B.Zauderer,et.al."Design of a 50 MWT Closed MHD Blowdown Experiment",EPRI Doc.No.233,Sept.1975
34.J.C.Corman,et.al.,"Energy Conversion Alternatives Study,ECAS-GE Phase 1 Rpt.",NASA CR-134948,Feb.1976
35.C.H.Marston,et.al,"Parametric Analysis of Closed Cycle MHD Power Plants", DOE/NASA/0135-1,NASA CR-165450,Sept.1981
36.B.Zauderer,"Inv.of a Non-Equilibrium MHD Generator"US-ONR Annual Rpt.,Contr. NOOO14-70-C-0321,July,197
37.C.S.Cook,et.al.,"Argon Contamination in Ceramic Heat exchangers for Closed Cycle MHD",in Proc.16th Symp.Emg,Aspects of MHD,Pittsburgh,PA,May 1977,p.II.4
38.J.Teno,et.al."Boundary Layers in MHD Generators",in Proc.10th Symp.Eng.Aspects of MHD,MIT,Cambridge,MA,Mar.1969,p.15
39.B.Zauderer,"Optimization of a Linear Non-Equilibr.MHD Generator",GE-TIS No. 70SD261,June 1970
40.I.Glassman,"Combustion in Metals",in Prog.in Aero & Astronautics,(AIAA,NY, 1960),Vol.1,p.253
41.H.Hurwitz,et.al.,"Influence of Tensor Conductivity on Current Distribution in a MHD Generator",J.Appl.Phys. Vol.32,p.205,(1961)
42.J.P.Reilly,"Open & Short Circuit Performance w. a Non-Equilibrium MHD Generator, Using HOT & Cold El;ectrodes",Proc.10th Symp.Eng.Aspects of MHD, MIT,Cambridge,Mar.26,1969,p.158
43.T.Nakamura,"Stability of Non-Equilibrium Helium-Cesium Plasma in the Regime of Fully Ionized Seed",in Proc.13th Symp.Eng.As pects of MHD,Stanford U.,Mar.26,1973,p.VI.4
44.C.H.Marston,et.al,"Coal Fired,Closed Cycle MHD Retrofit Study",Southern Cal. Edison Co. Report No.81-RD-32,May 15,1981
45.A.H.Shapiro,The Dynamics & Thermo.of Compressible Fluid Flow,(Ronald Press,NY,1953),Vol.1,Ch.8
46.G.W.Sutton & A.Sherman,Engineering MHD,(McGraw Hill,NY,1965),p.247
47.A.C.J.Mattsson & T.R.Brogan,"Self-excited MHD Generators",in Electricity from MHD,(IAEA,Vienna,1964),Vol.3,p.665
48.R.C.Weast,Handbook of Physics & Chemistry,(Chemical Rubber Co,Cleveland,1966-7),47th Ed.
49.W.M.Rohsenow & H.Y.Choi,Heat,Mass & Momentum Transfer,(Prentice-Hall,Englewood Cliffs,NJ,1961),Ch.9
50.M.F.Rose,"Technique & Applications of Pulsed Power Technology",in Proc.16th IECEC Conference,Atlanta ,GA ,Aug.9,1981,(ASME,NY,1981),p.146
51.V.M.Gremyachkin, "Theory of Ignition of Metallic Particles," Translation from Fizika Goreniya i Vzryva, Vol. 19, No. 3, pp.9-14, 1983.
52. D.R. Stull and H. Prophet, Project Directors,JANNAF Thermochemical Tables, 2nd ed., NSRDS-NBS 37, June,1971.
53. Fassell, M. et al. "The Experimental Nature of the Combustion of Metallic Powders", Proceedings of ARS Solid Propellant Rocket Conference, ibid., 1960.
54.T.A.Brzustowski, and I.Glassman, "Vapor-Phase Diffusion Flames in the Combustion of Magnesium and Aluminum: I. Analytical Developments", Prog. in Aeronautics and Astronautics, Heterogeneous Combustion, Vol. 15, 1964.

55. E.W.Price,"Combustion of Metalized Propellants", Prog. Aeronautics and Astronautics, Solid Propellants, Vol.92,1982.
56.A.V.Grosse,and J.B.Conway, "Combustion of Metals in Oxygen", Industrial and Engineering Chemistry, Vol. 500, No. 4, April, 1958.
56.M.E.Derevyaga, "Effect of Pressure on Magnesium Combustion", Translation from Fizika Goreniya i Vzryva, Vol.19, No. 1, pp.34-39,1983.
57.North American Combustion Handbook, nd. ed., North American Mfg. Co., Cleveland, Oh., 1978.
58. Kudryavtsev, V.M. et al., "High=Pressure Combustion of Metals (Three-Zone Model)", Translated from Fizika Goreniya i Vzryva, Vol.15, No.6, pp.50=57, 1979.
59.J.L.Prentice, "Combustion of Pulse=Heated Single Particles of Aluminum and Beryllium", Combustion Science and Technology, Vol. 1, pp. 385-398, 1970.
60. Chemical Engineers' Handbook, R.H. Perry and C.H. Chilton, eds., 5th ed., McGraw-Hill Book Co.,N.Y. 1973.
61. I.Glass, "Combustion", Academic Press, N.Y., 1977

5. PUBLICATIONS

Due to the fact that we are filing one, possibly two,patents on work related to this project, we will not publish any results until these patents are filed. However, the results are of considerable importance to the pulsed power MHD field, and we plan to present and publish one or two papers at one or more of the following Symposia.

1. 24th Symposium on Engieering Aspects of MHD,Butte, MT,June 1986,

2. 9th International Conference on MHD Power Generation, Tsukuba,Ibaraka, Japan, Nov.,1986

3. 21st Intersociety Energy Conversion Conference,San Diego,CA ,Aug.1986

The tentative titles for the papers are:

1.AN INNOVATIVE ULTRA-HIGH POWER,SELF EXCITED MAGNETOHYDRODYNAMIC POWER GENERATOR SYSTEM, USING CHEMICAL FUELS TO DIRECTLY HEAT THE NOBLE GAS GENERATOR WORKING FLUID.

2.A HIGH POWER DENSITY,LIGHTWEIGHT MAGNET FOR MHD AND PULSED POWER APPLICATIONS

The authors will be B.Zauderer, E.Fleming, C.H.Marston

6. PROFESSIONAL PERSONNEL

The following individuals contributed to the project:

Dr.Bert Zauderer, Principal Investigator, President ,Coal Tech Corp.
M.S.,Sc.D. Mechanical Engineering,MIT,Cambridge, 1962
Thesis:" MHD Containment in Partially Ionized Gases"

Dr.E.Fleming,Research Engineer, Consultant-Coal Tech Corp.
Ph.D.,Physical Chemistry,Boston College,1975

Mr.J.Wang,Graduate Student,Mech.Eng.,Villanova U.,Consultant-Coal Tech

7. INTERACTIONS (Coupling Activities)

1. In the course of our work on this Project, we responded in July 1985, with a white paper to a requirement by the Air Force Space Technology Center, Kirtland AFB for a multi-megawatt power system for use in the SDI mission. The title of the paper was "AN INNOVATIVE MHD POWER GENERATION SYSTEM". This response was funded with Coal Tech resources, and it was motivated by our invention on the use of a metal fuel combustor for directly heating a noble gas, MHD generator working fluid. This invention in turn was an outgrowth of Coal Tech's work on the development of a cyclone combustor, as well as the prior experience of the PI in noble gas non-equilibrium MHD generator research. This invention was successfully applied to the present project,as described in this Report.

Our application of this new MHD concept to power levels in the 100's to 10,000's of MW MHD output indicate that it has the potential to far exceed the performance of other MHD concepts,and to exceed the performance of highly advanced gas turbine systems.

The preliminary results of the study have also been submitted to the SDI Office.

2. The present work was performed with the use two novel concepts which were invented this year,by B.Zauderer with Coal Tech resources. One was the metal fuel fired, non-equilbrium MHD generator, for which Coal Tech is in the process of filing for a patent application. The other invention is the ammonia cooled, high power,light weight, room temperature magnet, for which Coal Tech plans to file for a patent application as soon as certain aspects related to the design and operation of the magnet are clarified.

3. Dr.Zauderer is an officer of the Steering Committee that organizes the Annual Symposia on Engineering Apsects for MHD. During the 23rd Meeting held in Hidden Valley,PA in June 1985, Dr.Zauderer discussed those aspects of the present project related to the prior art on combustion and explosive MHD generators,with several researchers that were major contributors to the prior work. The purpose of these discussions was to clarify certain aspects related to this prior art. One result of these discussions was that it re-enforced our conviction that it would be extremely difficult to improve on the reported performance in high power combustion MHD generators and on explosive MHD generators.

This was an important factor in our decision to change our original approach which was to use these systems, and instead to replace them with the novel metal fuel, noble gas MHD system,to meet the present project objectives.

4. The work on the present project has convinced us that the metal fuel fired, noble or inert gas MHD generators potentially represents a major breakthrough in the field of high power generation. As such it has applications to several important DOD missions in power and propulsion for flight, terrestrial, and seaborne missions. It is our intention to further explore these applications and to propose reseach activities focussed on those areas holding the highest payoff potential. At present it appears that the SDI mission is the prime application for this concept.

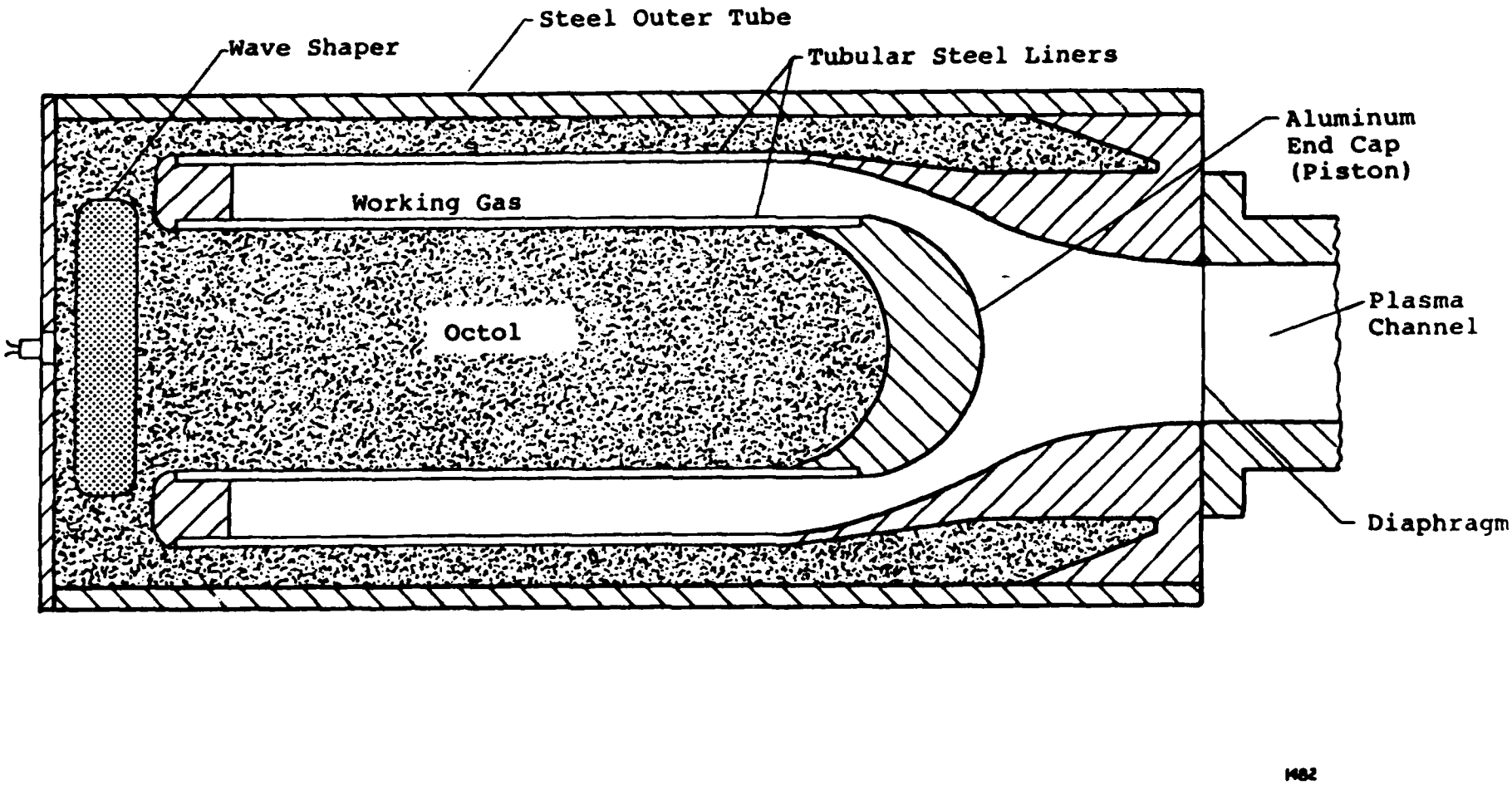

FIGURE 1: SCHEMATIC OF ARTEC'S EXPLOSIVELY DRIVEN PLASMA SOURCE GENERATOR
(From.Ref.1)

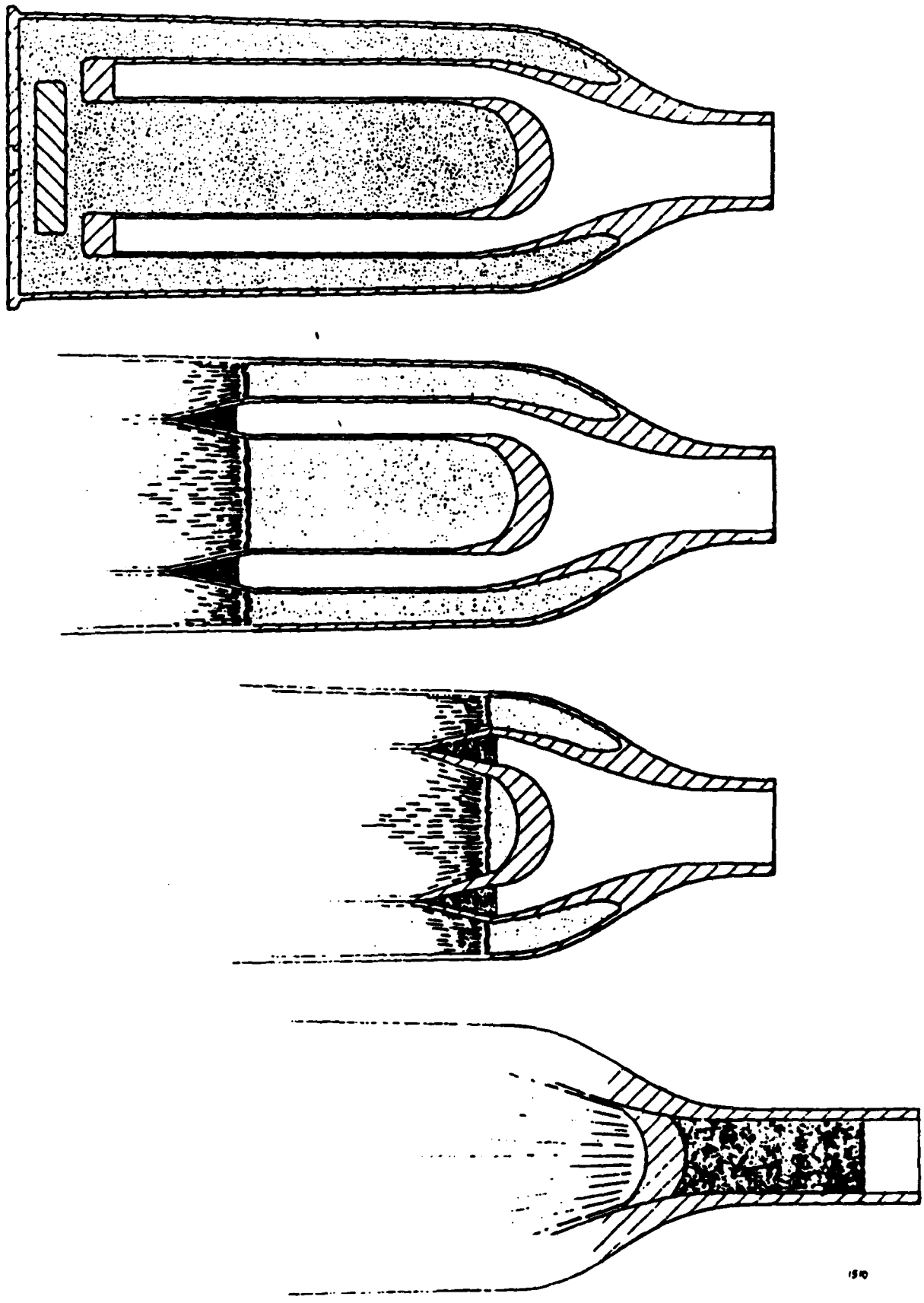

FIGURE 2: SCHEMATIC SHOWING SEQUENCE OF OPERATION OF ARTEC'S PLASMA SOURCE GENERATOR-(From. Ref.1)

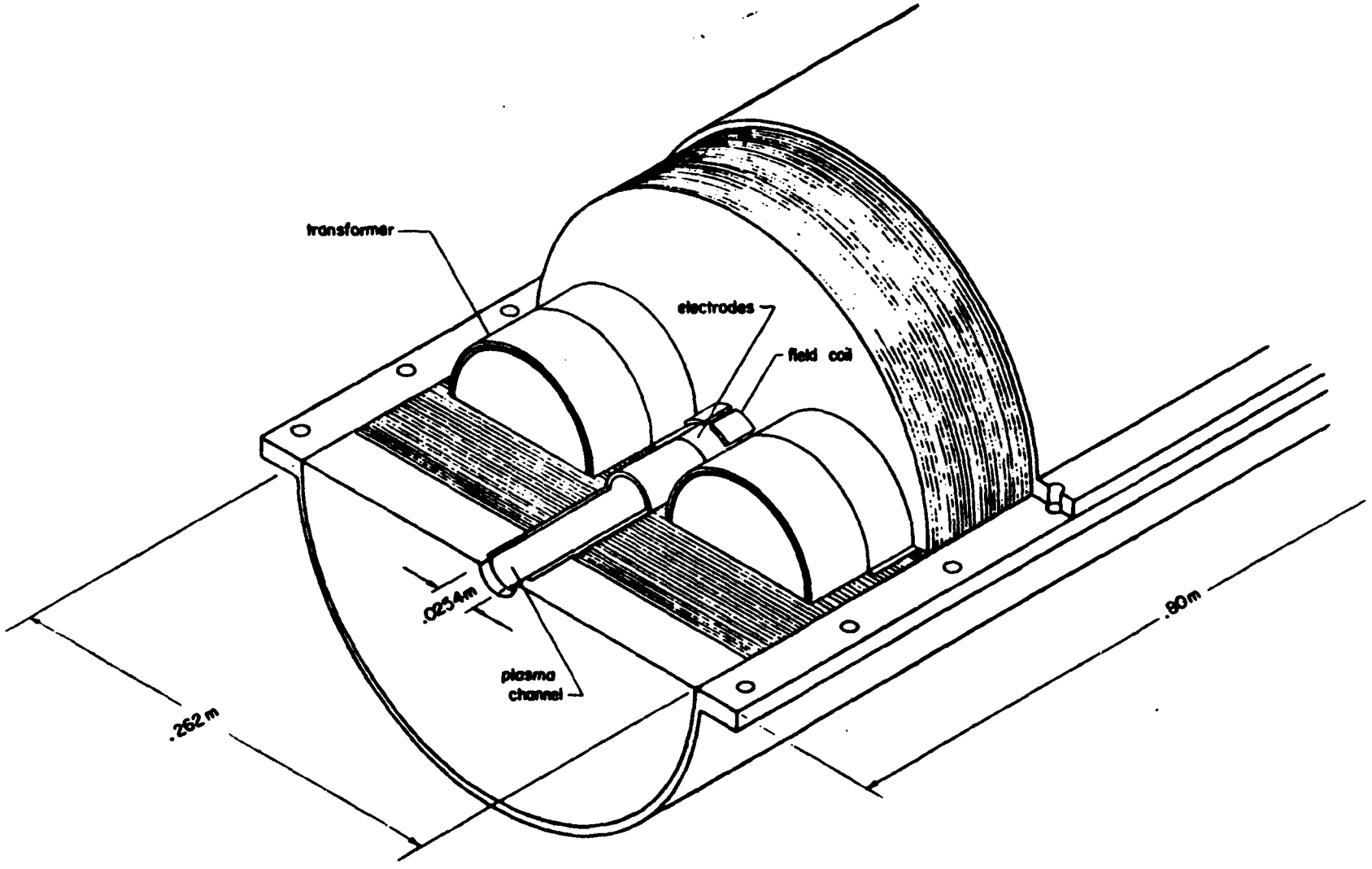

FIGURE 3: SCHEMATIC OF ARTEC'S DESIGN CONCEPT OF A REPETITIVELY PULSED DC-MHD GENERATOR,WITH BUILT IN PULSE TRANSFORMER-(From Ref.1)

MHD CHANNEL ASSEMBLY

ARTEC ASSOCIATES INCORPORATED

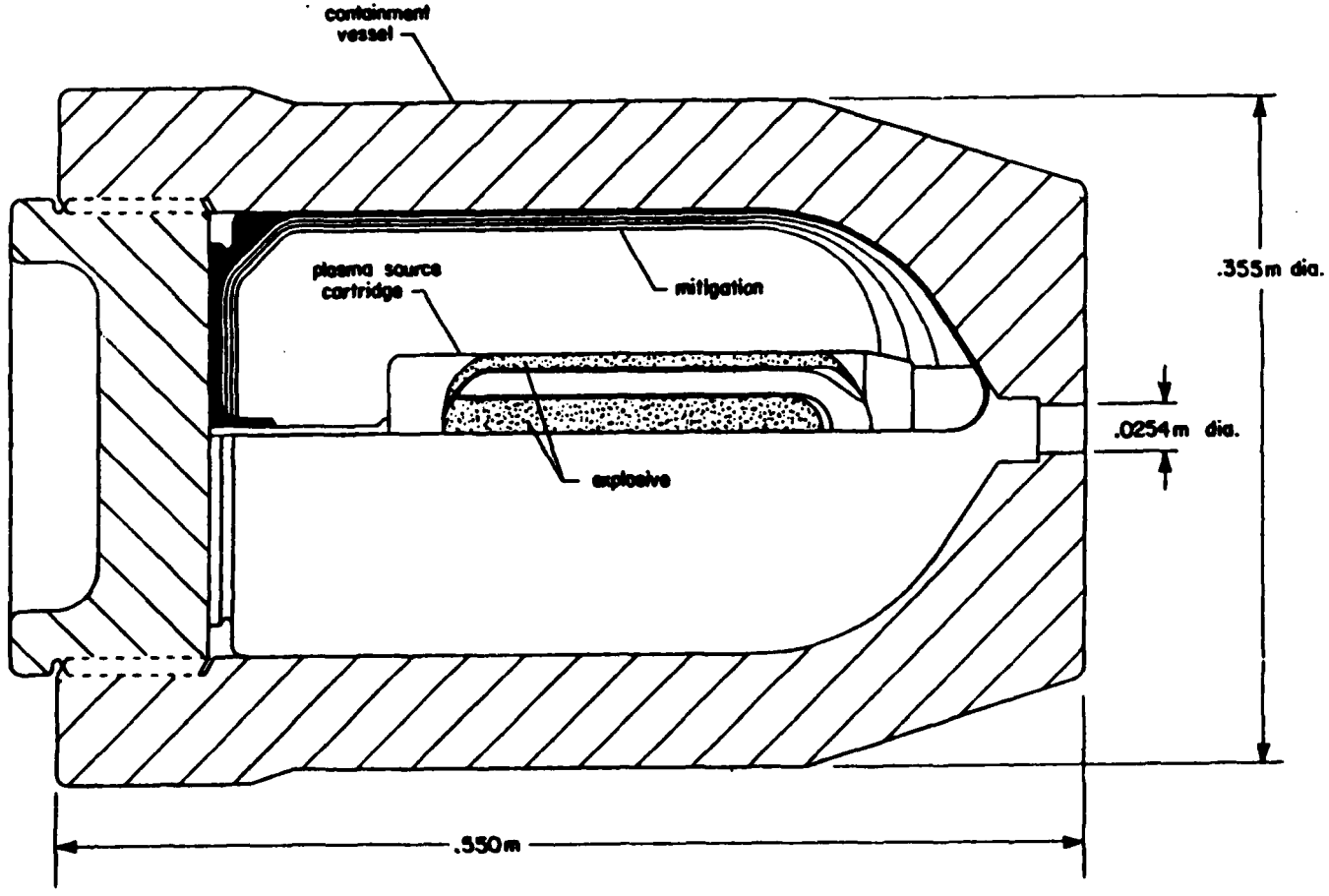

FIGURE 4: SCHEMATIC OF ARTEC'S DESIGN CONCEPT FOR A REPETITIVELY FIRED EXPLOSIVE, BREECH LOAD ASSEMBLY AND PLASMA SOURCE CARTRIDGE-(From Ref.1)

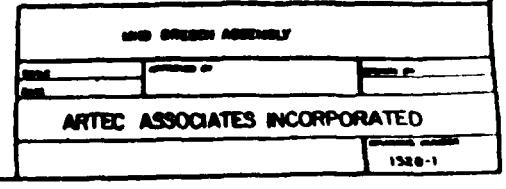

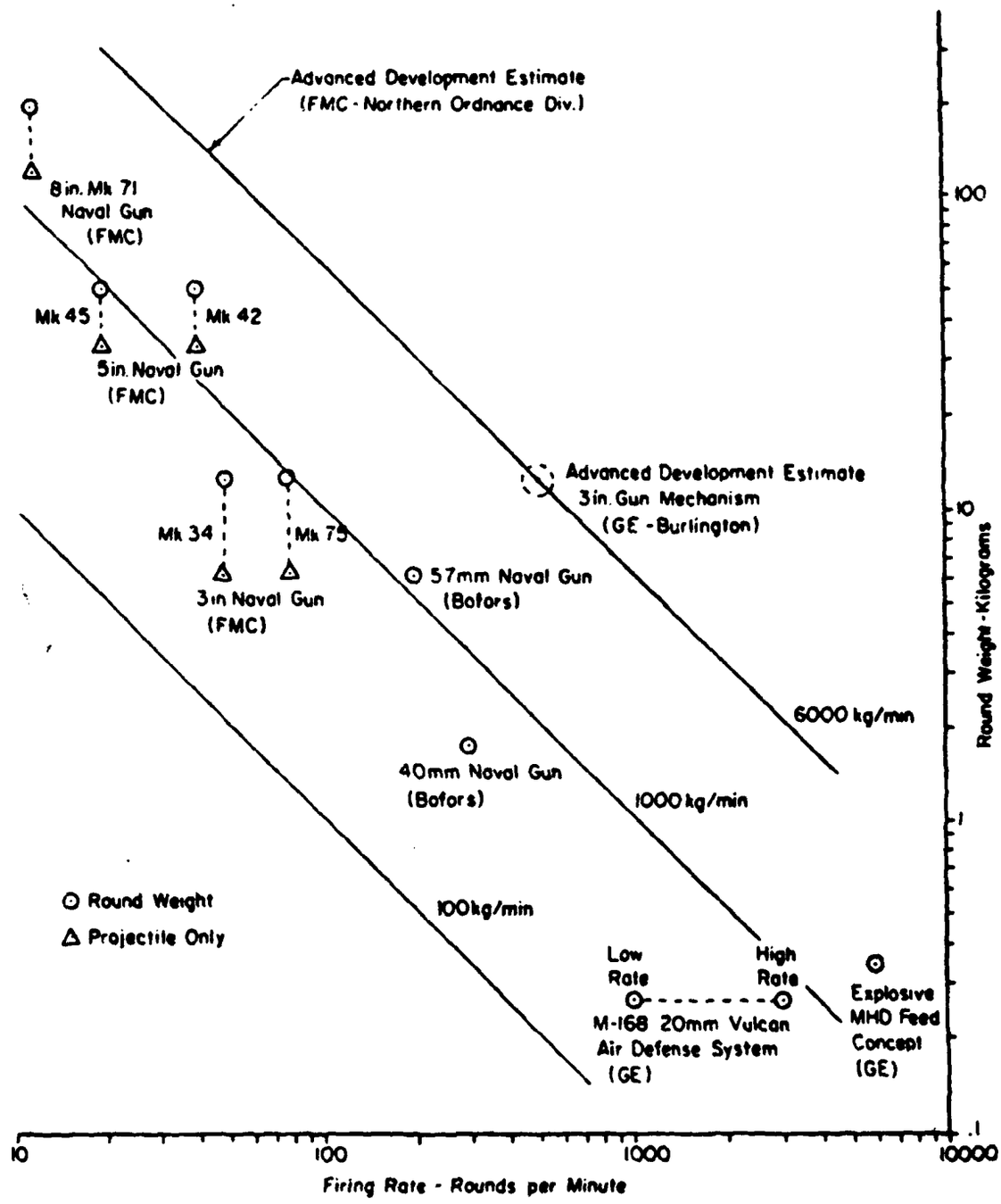

FIGURE 5: RELATIONSHIP OF ARTEC/GE'S CONCEPT OF A REPETITIVELY FIRED EXPLOSIVE PLASMA SOURCE GENERATOR COMPARED TO OTHER RAPID FIRE GUN SYSTEMS-(From Ref.1)

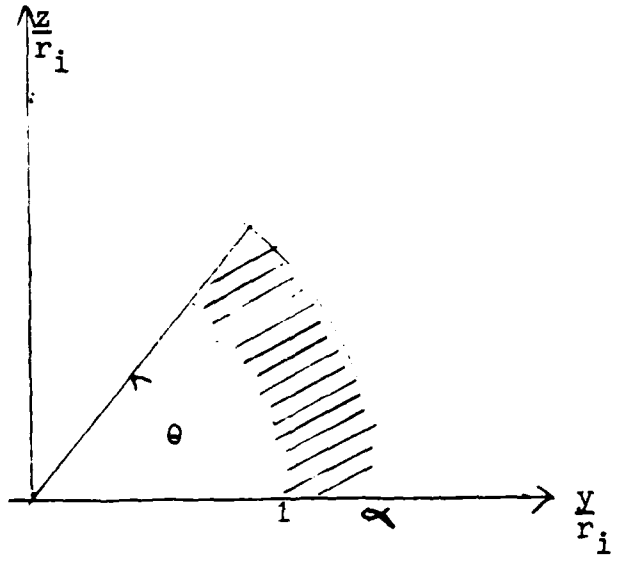

FIGURE 5 A:Normalized Coordinates for a Saddle Coil with Circular Winding Cross-section. Only the first quadrant of the coil is shown.
r_i is the inner radius of the coil
r_o is the outer radius of the coil.
$\alpha = r_o/r_i$

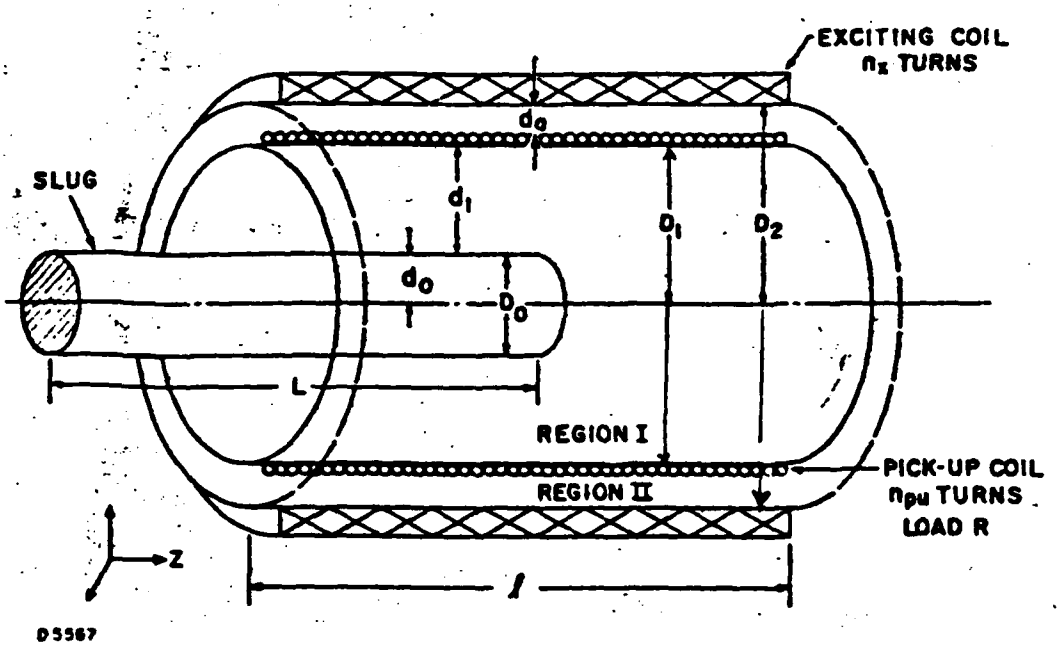

FIGURE 5B. SCHEMATIC OF THE APPARATUS FOR ENERGY EXTRACTION WITH A METAL SLUG THAT IS INDUCTIVELY COUPLED TO A SOLENOID-[REF.5]

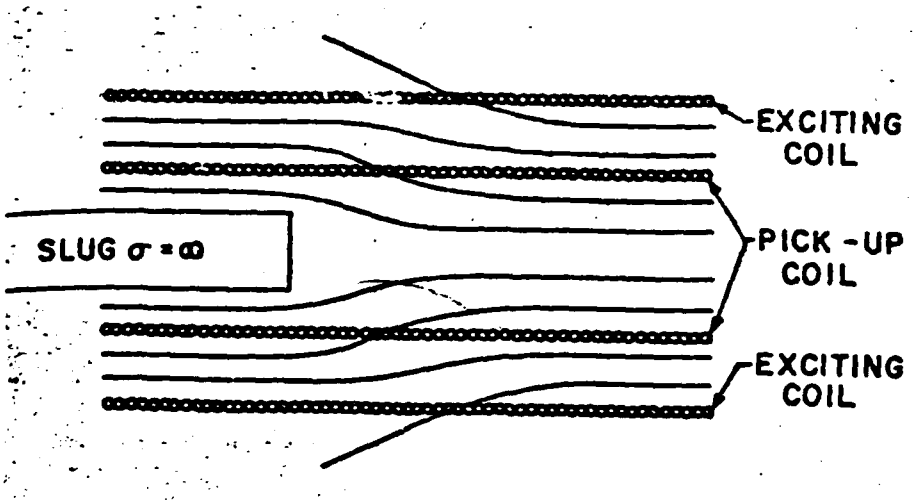

FIGURE 5C. SPATIAL POSITION OF THE MAGNETIC FIELD LINES AS THE METAL SLUG ENTERS THE SOLENOID -[REF.5]

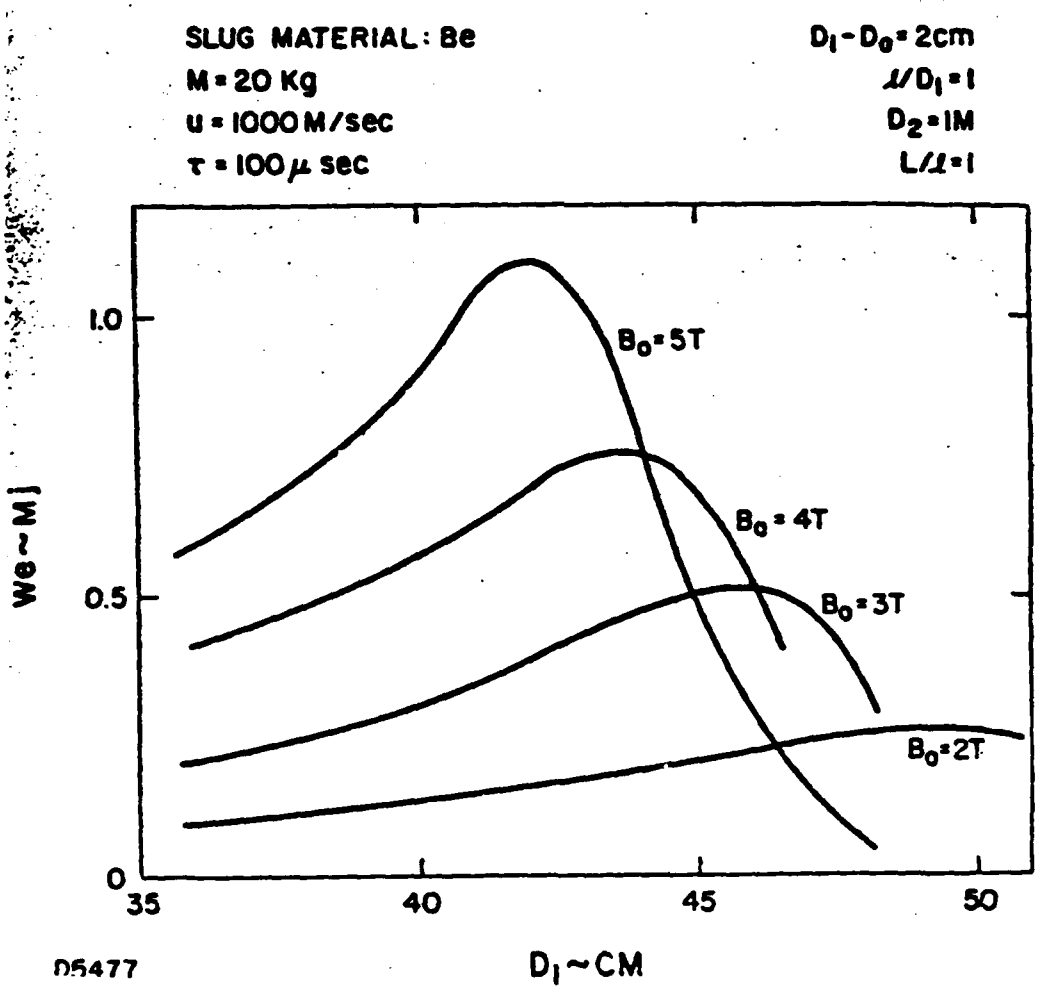

FIGURE 5D. COMPUTED ELECTRICAL ENERGY EXTRACTION AS A FUNCTION OF PICKUP COIL, LOCATED INSIDE THE APPLIED FIELD, SOLENOID.-[REF.5]

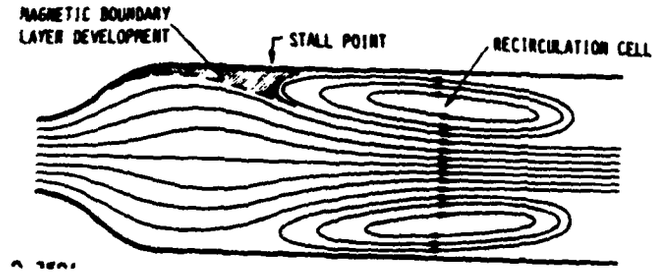

FIGURE 6: ESTIMATED PLASMA FLOW PATTERNS IN A LINEAR DC-MHD GENERATOR OPERATING AT HIGH MAGNETIC REYNOLDS NUMBERS- The estimated velocity streamlines show that the plasma flow will choke (i.e. stall) as it enters the inter electrode region of the generator-(From Ref12)

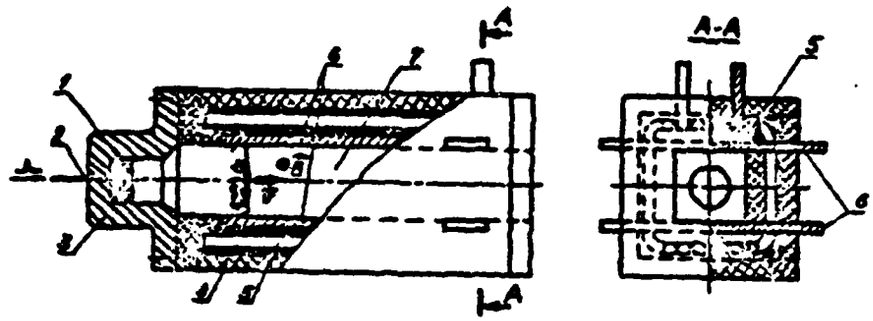

FIGURE 7: SCHEMATIC OF A LINEAR,EXPLOSIVE CHARGE DRIVEN,MHD GENERATOR SYSTEM
1 - ES charge; 2 - electric detonator; 3 - retaining explosion chamber;
4 - generator housing; 5 - saddle-shaped magnetic system; 6 - electrodes;
7 - MHD channel.
(From Ref20)

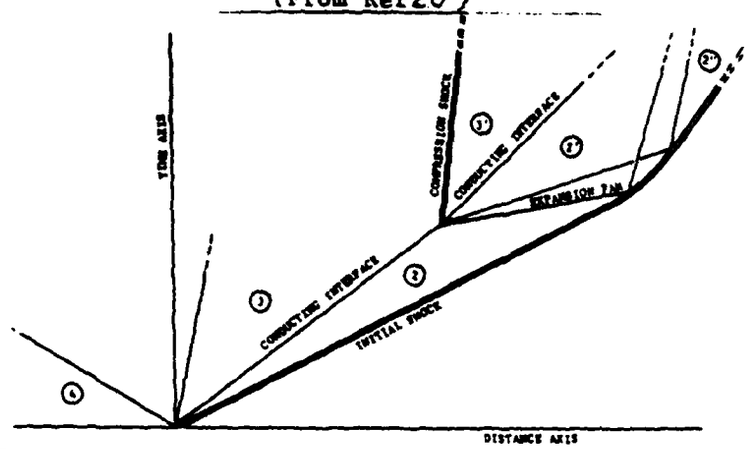

FIGURE 8: SCHEMATIC OF THE DISTANCE-TIME WAVE PATTERN GENERATED BY A LINEAR, EXPLOSIVE DETONATION SHOCK,ENTERING A MHD GENERATOR DUCT AT THE SPATIAL INTERFACE BETWEEN ZONES 3 AND 3'-The detonation gases are in regions 3,3',and 4, while the driven gas-(e.g.air) is in region 2,2',2"-(From Ref.3)

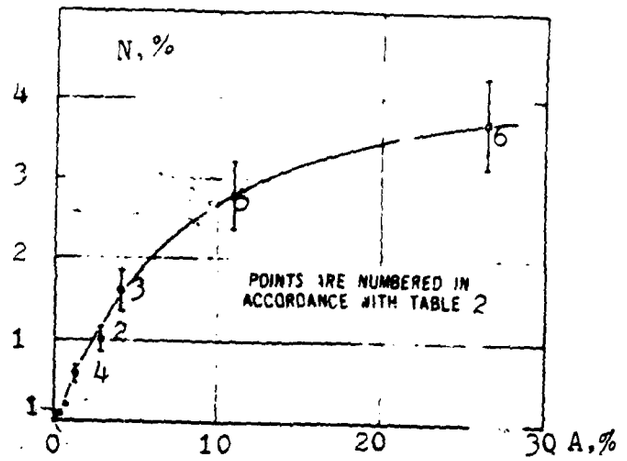

FIGURE 9: OVERALL EXPLOSIVE TO ELECTRIC OUTPUT CONVERSION EFFICIENCY (N,%) VERSUS THE RATIO OF MAGNETIC FIELD ENERGY TO EXPLOSIVE ENERGY-(A,%),FOR THE LINEAR EXPLOSIVE MHD GENERATOR EXPERIMENTS LISTED IN TABLE 2

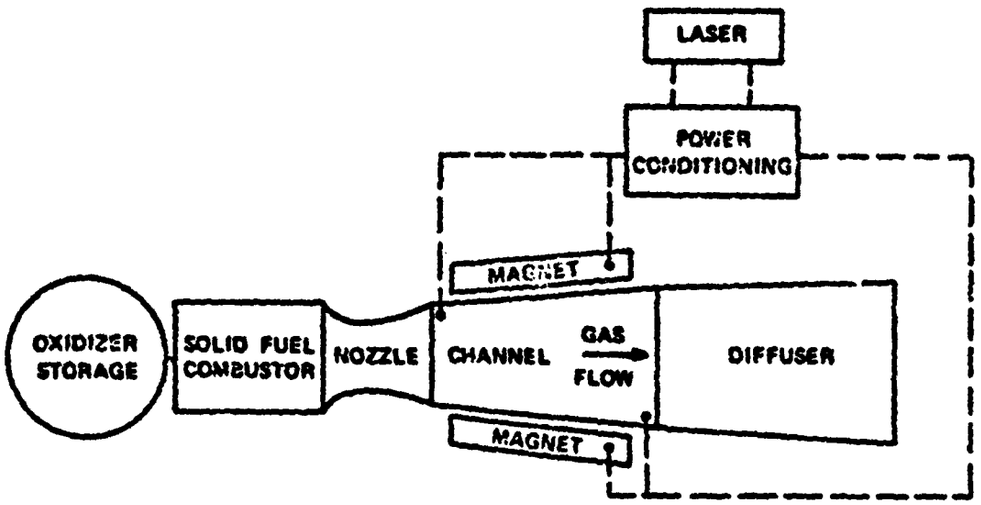

FIGURE 10: SCHEMATIC OF A CW-DC-MHD GENERATOR FIRED WITH A SOLID ROCKET FUEL (From.Ref.2)

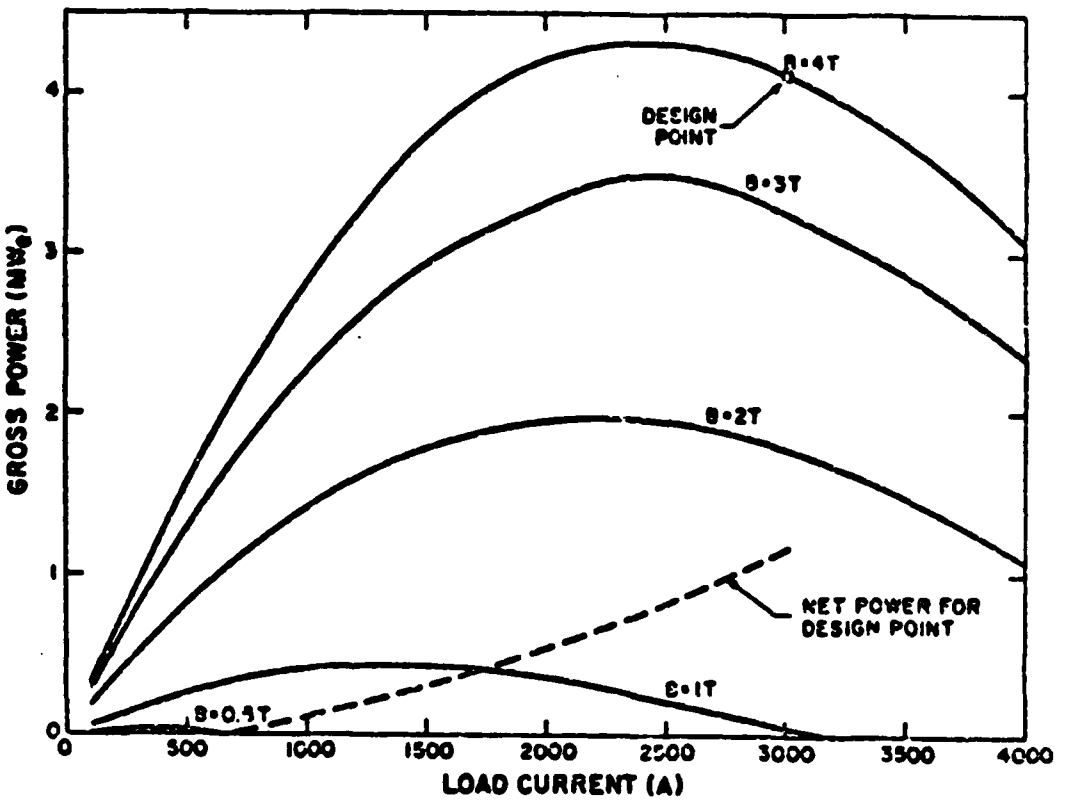

FIGURE 11: CALCULATED CW-DC-MHD GENERATOR GROSS AND NET (AFTER SUBTRACTING MAGNET SELF EXCITATION POWER) POWER OUTPUT -Design point is at 1 MWe net output power-(From.Ref. 2

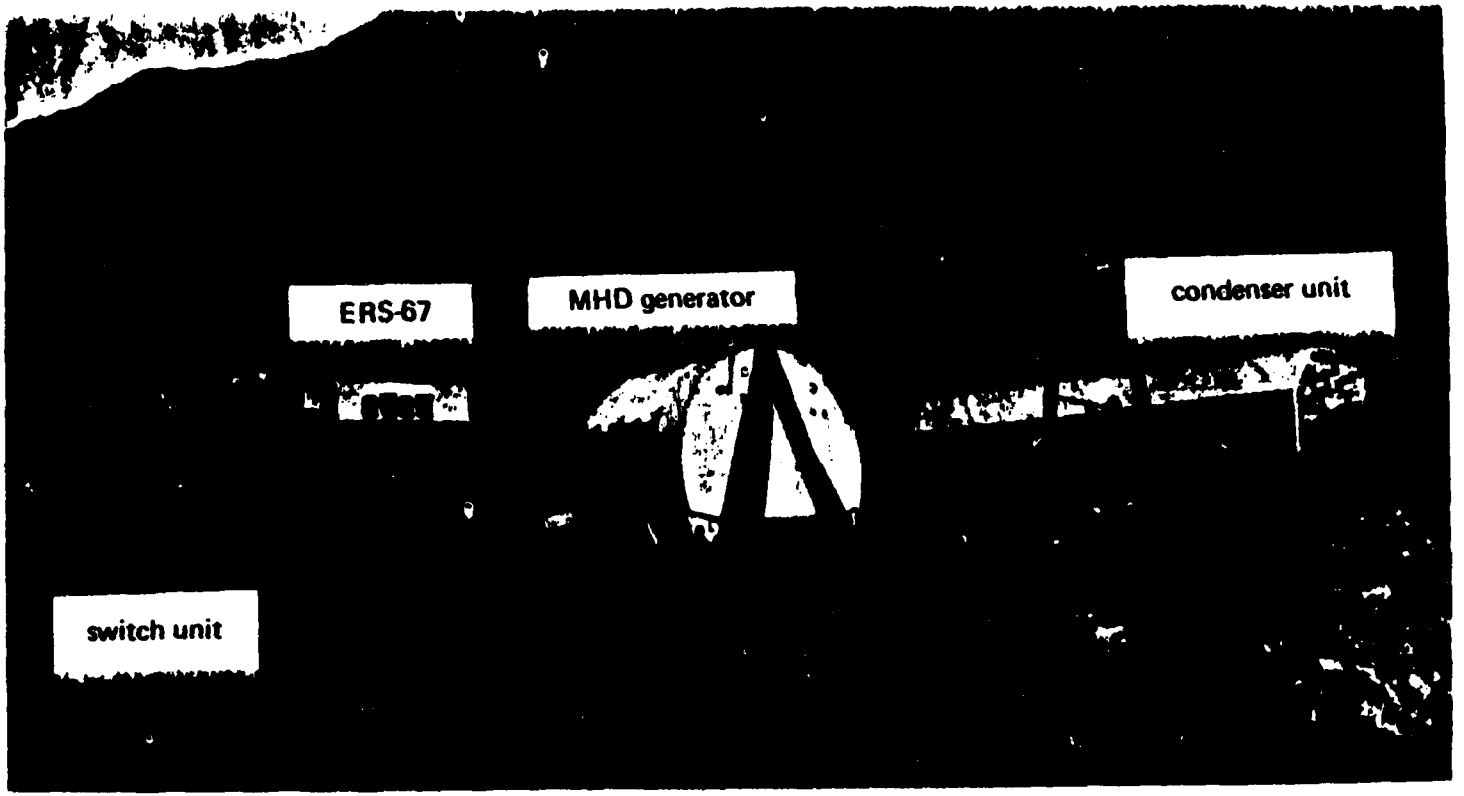

FIGURE 12: PHOTOGRAPH OF THE FIELD INSTALLATION OF THE RUSSIAN "PAMIR" TYPE, 15 MWe OUTPUT, SOLID FUEL FIRED,SELF EXCITED MHD GENERATOR-(From.Ref. 7)

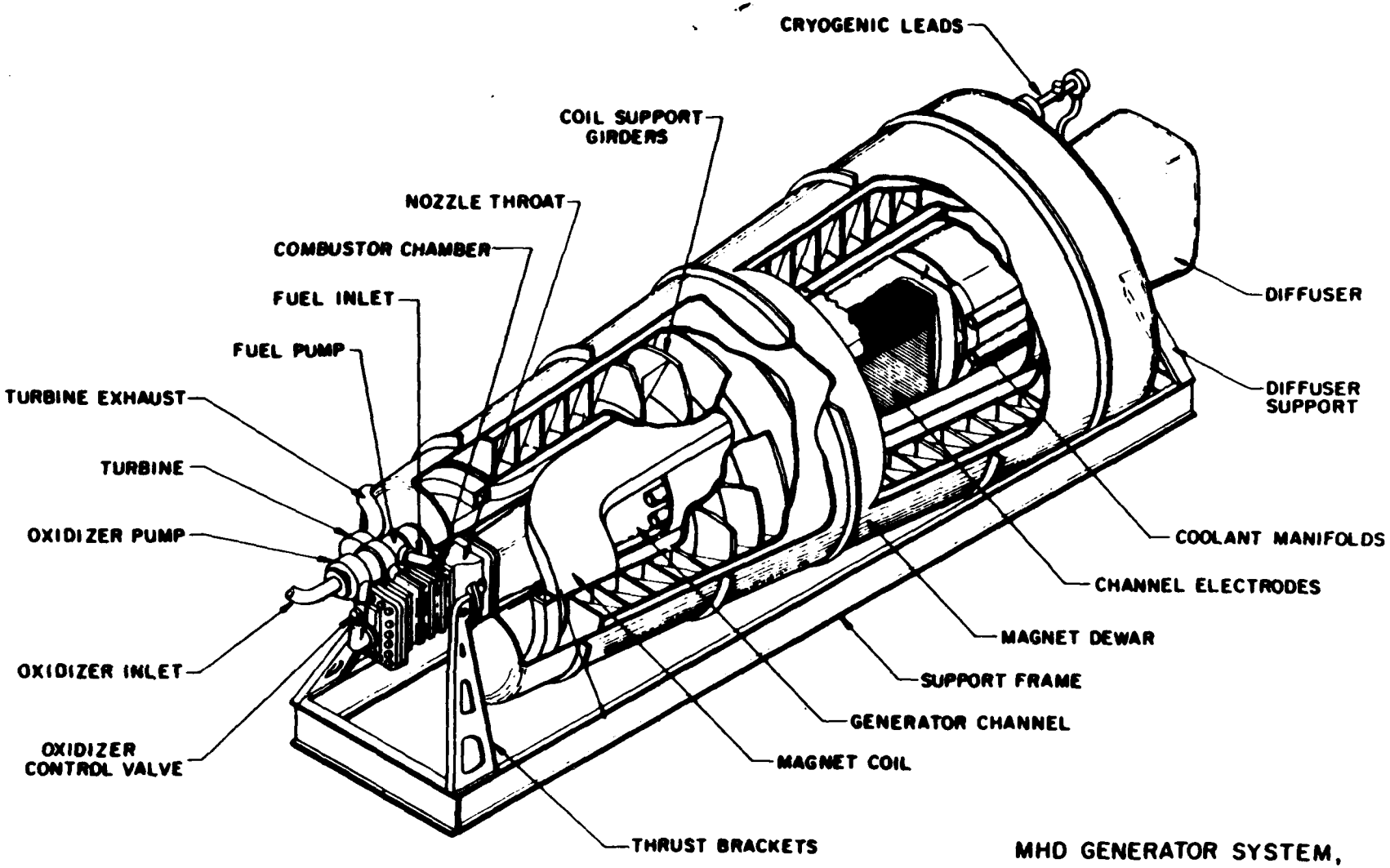

FIGURE 13: SCHEMATIC OF THE DESIGN OF A LIGHTWEIGHT, MULTI-MINUTE OPERATING, MHD GENERATOR, FIRED WITH A HIGH ENERGY LIQUID OR SOLID FUEL, AND USING A SUPERCONDUCTING MAGNET-(From.Ref.29)

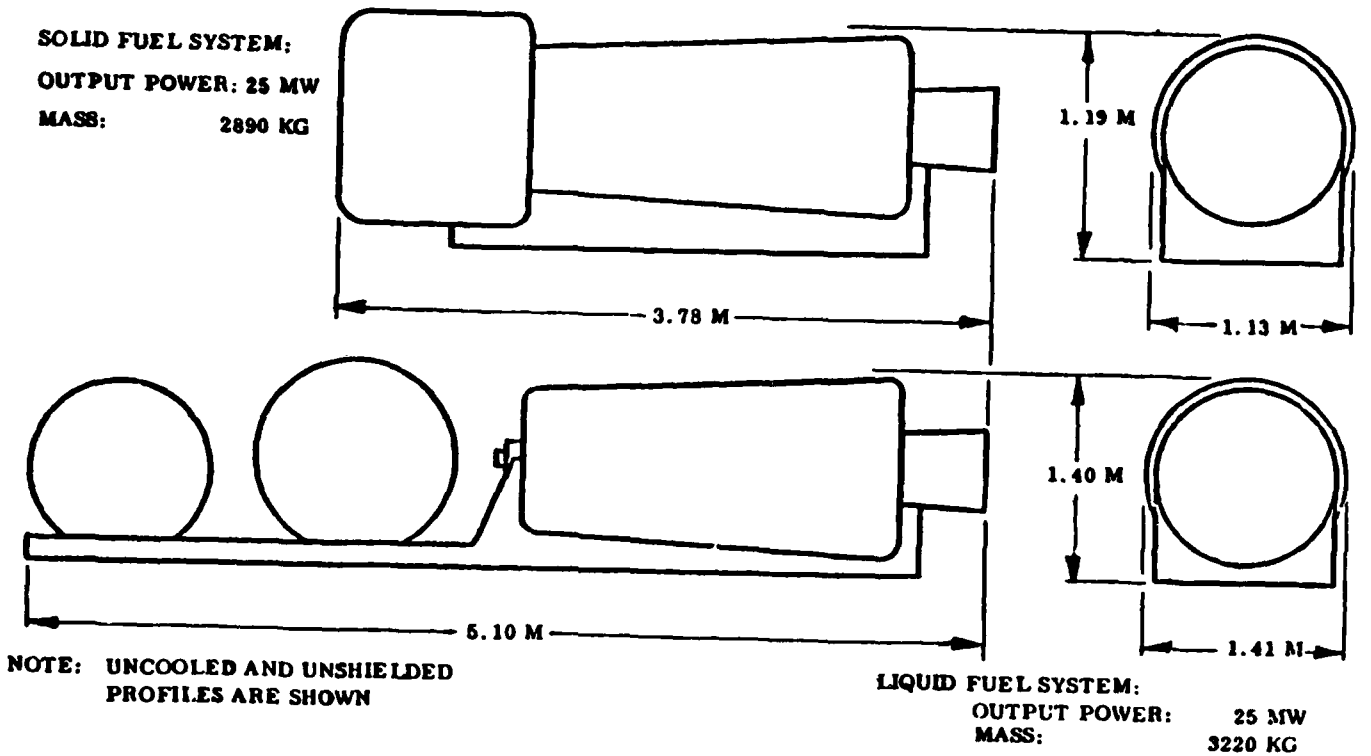

FIGURE 14: SCHEMATIC OF THE OVERALL SYSTEM DIMENSIONS OF THE GENERATOR SYSTEM SHOWN IN FIGURE 13, FOR 25 MWe NET POWER OUTPUT-(From.Ref.29)

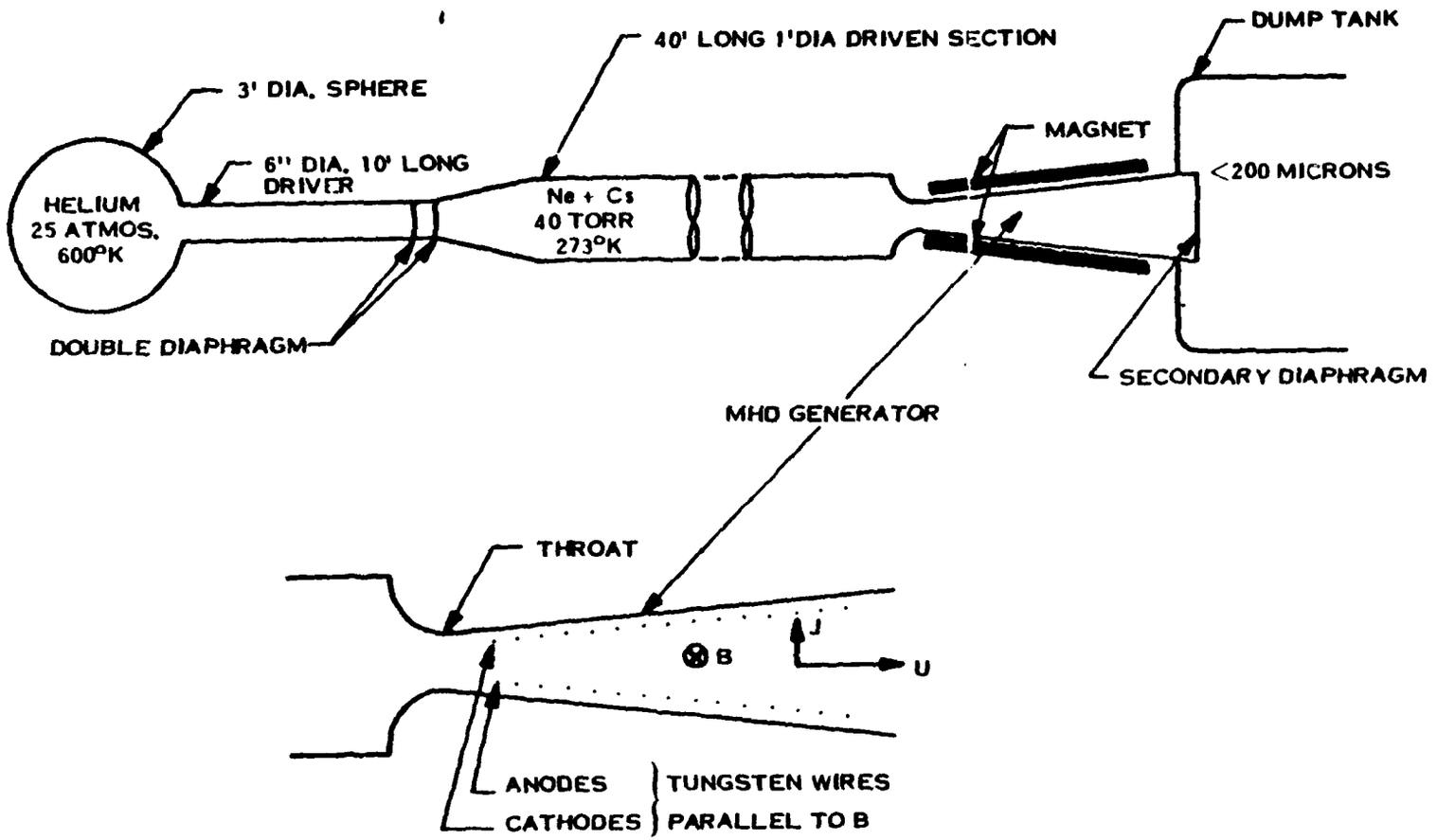

FIGURE 15 Schematic of the ONR Shock Tunnel Facility
(From Ref. 10)

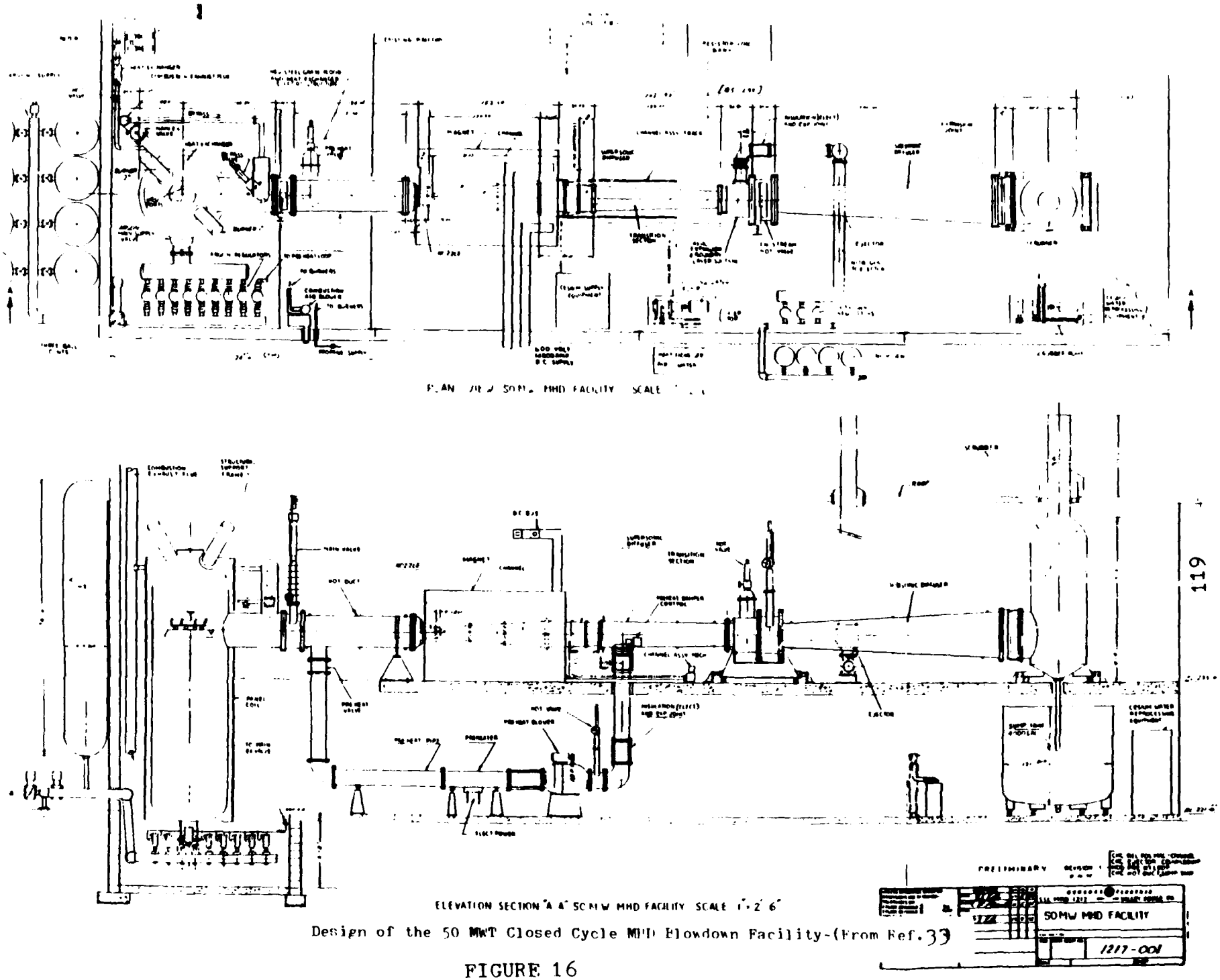

Design of the 50 MWT Closed Cycle MHD Blowdown Facility-(From Ref. 33)

FIGURE 16

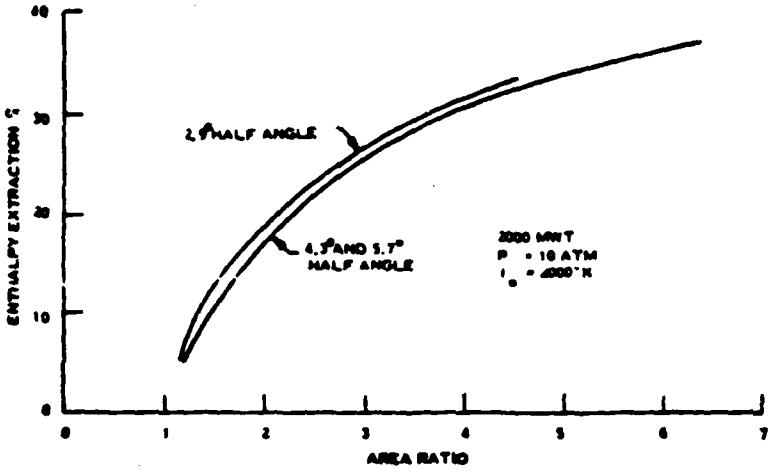

FIGURE 17 **Enthalpy Extraction as a Function of Area Ratio in a 2000 MWT Channel**

(From Ref.10)

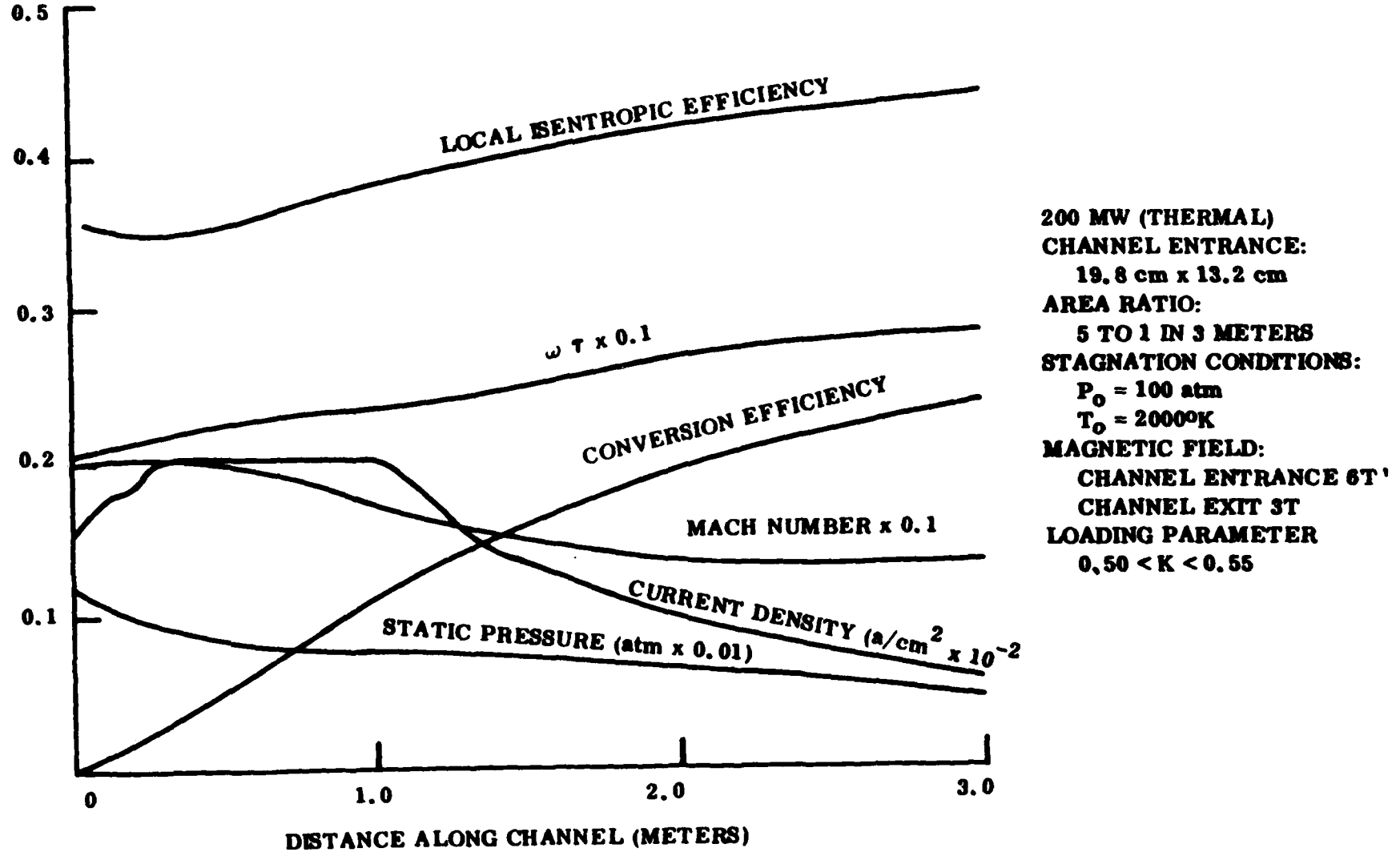

Figure 18 Computed performance of an MHD channel using argon and cesium at 2000°K and 100 atm. (From Ref.36)

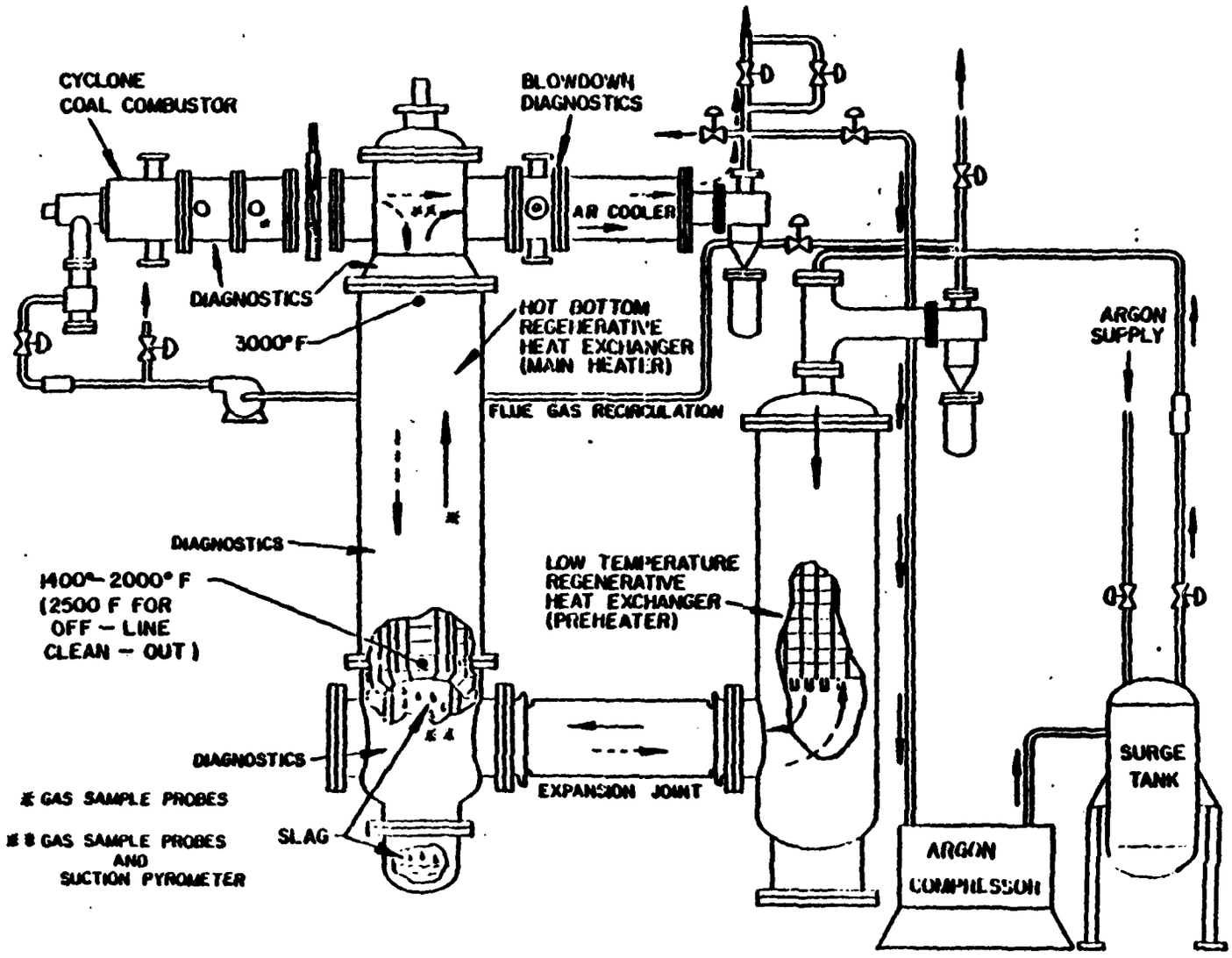

Figure 19

Closed Cycle MHD Combustor/Heat Exchanger Test Facility
Combustor & Heat Exchanger Rated at 1 MMBTU/hr-(From Ref. 37)

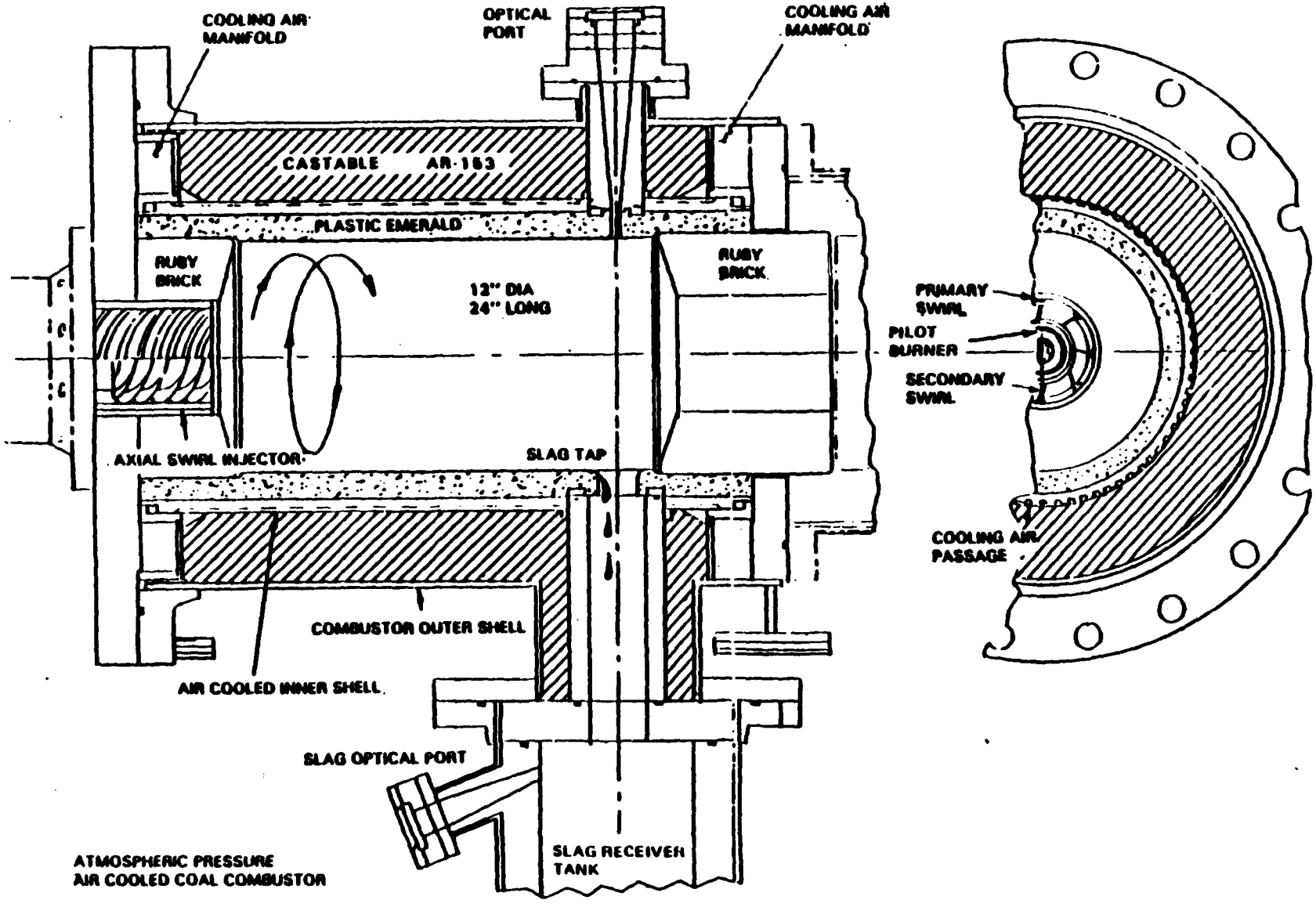

Figure 10: Schematic of 1 MMBTU/hr Air Cooled Cyclone Coal Combustor-(Ref. 17)

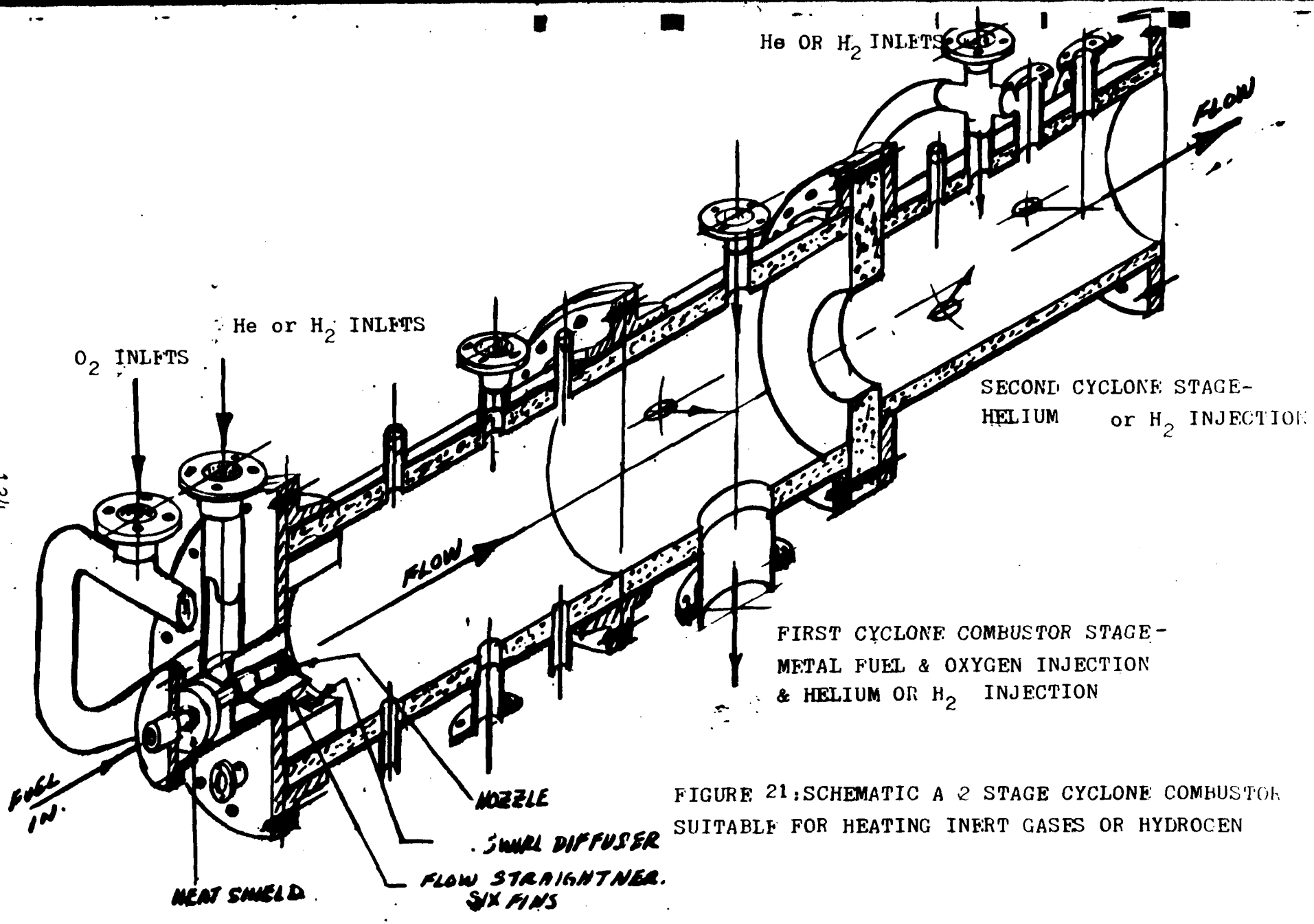

FIGURE 21: SCHEMATIC A 2 STAGE CYCLONE COMBUSTOR SUITABLE FOR HEATING INERT GASES OR HYDROGEN

COAL-TECH. CORP.
9-20-85
SK - BY Y.A.T.'L.

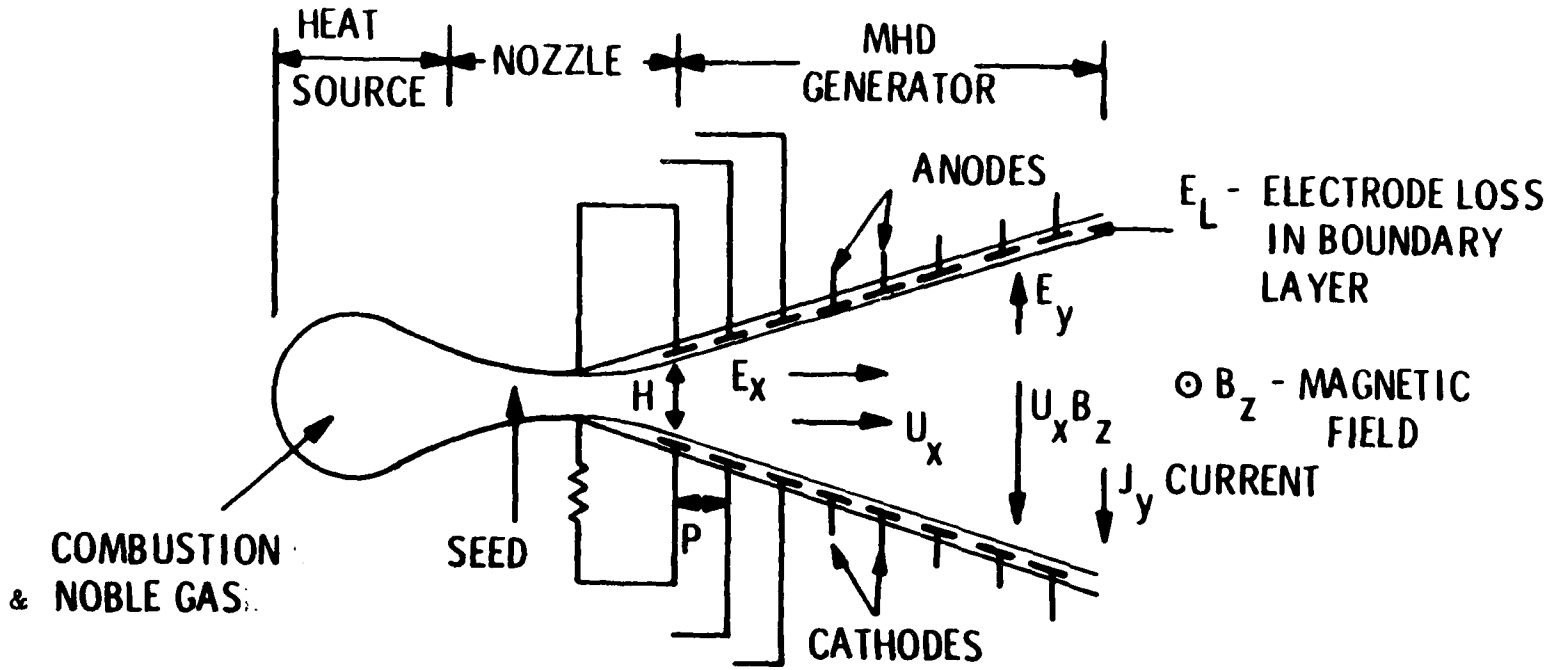

$$\text{HALL FIELD} = E_x \leq (\omega_e \tau_e)\ (U_x B_z - E_y - E_L)$$

$$\text{POWER DENSITY} = J_y \cdot E_y = \sigma_E U_x^2 B_z^2 K(1-K)$$

$$\text{ISENTROPIC GENERATOR EFFICIENCY} \leq K$$

U_x = GAS VELOCITY

σ_E = EFFECTIVE CONDUCTIVITY

$\beta = \omega_e \tau_e$ = HALL PARAMETER

$K = (E_y + E_L)/U_x B_z$ = LOAD FACTOR

Figure 12: Schematic Diagram of Faraday Mode MHD Generator Showing Orientation of Magnetic and Electric Fields and Separately Loaded Electrodes.

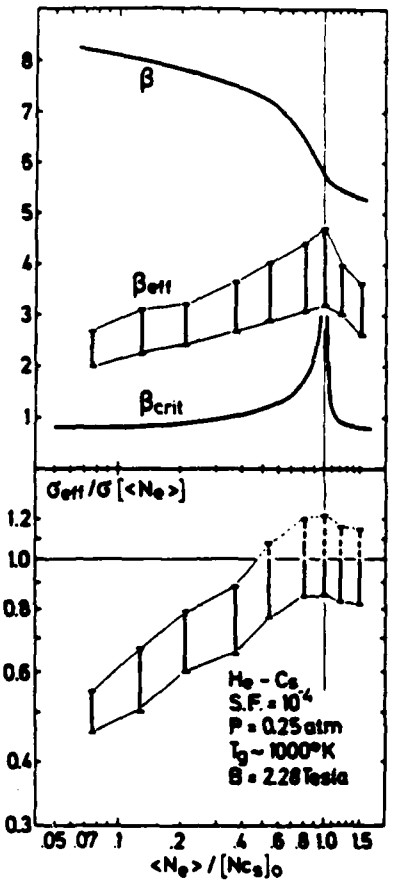

FIGURE 23: Effective Hall Parameter & Conductivity vs Degree of Ionization of the Seed-(From Ref.43)

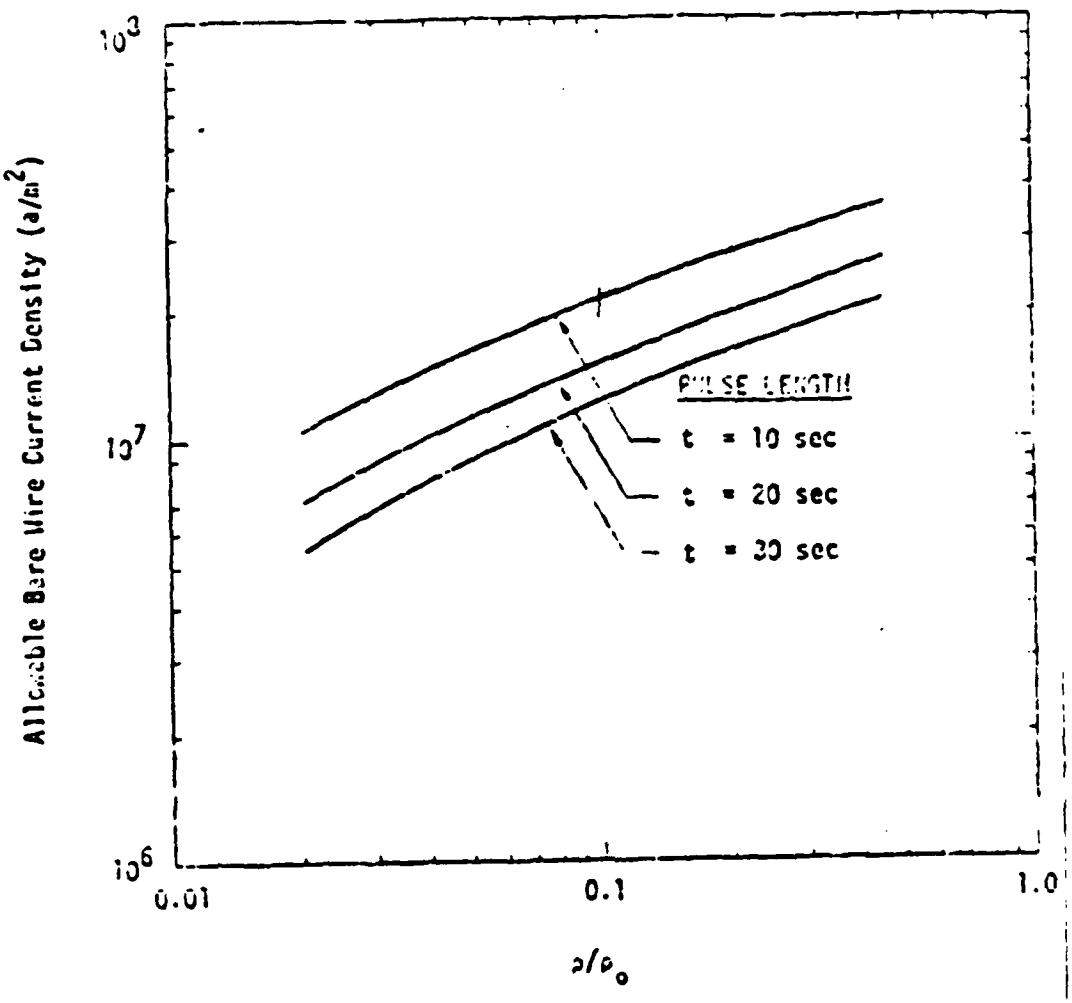

FIGURE 24: Change in Conductor Resistance vs Current Density for a Pulsed Heat Sink Coil. Initial Coil Temperature-77°K-(From.Ref.4)